Genetic and Molecular Studies of Early Embryogenesis in *Drosophila*

Thomas Kidd
Magdalen College
Oxford

Submitted to the University of Oxford
for the degree of Doctor of Philosophy
July 1994

Imperial Cancer Research Fund, Developmental Biology Unit,
Department of Zoology, University of Oxford

Genetic and Molecular Studies of
Early Embryogenesis in *Drosophila*

Thomas Kidd

ABSTRACT

The *Drosophila* embryo is patterned by a complex interplay of zygotically expressed genes and maternally supplied components, a large number of which have been identified. However, many maternal components are encoded by essential zygotic genes whose maternal effects are not amenable to conventional genetic analysis. Investigation of such genes requires the generation of homozygous mutant germ cells in chimeric females, and analysis of their embryos. The recent development of techniques which allow the efficient generation of germline clones has made the screening of zygotic lethal mutations for maternal effects more feasible. I have generated a collection of X-linked zygotic lethal mutations and used FLP recombinase catalysed mitotic recombination to look for maternal effects affecting segmentation.

Two mutations have been recovered which have maternal effect phenotypes similar to those of the pair-rule segmentation genes. The *leprechaun* mutation affects oogenesis, so fertile females are very rare, preventing straightforward phenotypic analysis of the segmentation phenotype. Attempts to generate a rescuing duplication are described.

The second mutation, *stunted (sun)*, initially gave rise to a segmentation cuticle phenotype. Subsequent attempts to reproduce the phenotype were unsuccessful as it was masked by a severe reduction in the amount of cuticle secreted, a phenotype characteristic of the neurogenic genes. Detailed analysis revealed that the primary lesion affects neither segmentation or neurogenesis. Rather, *sun*$^{+}$ is required for cellularisation of the syncytial blastoderm and for the localisation of actin to 'caps' above the syncytial nuclei. Cloning of a candidate gene for *stunted* revealed a predicted protein product limited homology to cyclins.

In addition to searching for novel segmentation genes, potential protein-protein interactions of the segmentation gene *hairy's* protein product were also investigated, and a model is presented for its mode of action as a transcriptional repressor.

'I emerged at last, stumbled a few steps in the mud and then I saw it: an ethereal mountain emerging from a tossing sea of clouds framed between two dark barracks - a massive blue-black tooth of sheer rock inlaid with azure glaciers, austere yet floating fairy-like on the near horizon.'

Felice Benuzzi

'No picnic on Mount Kenya'.

'My limbs seemed to thud against their joints, and I looked up to warn Tom to stay at the belay, only to see him on the rope silhouetted against the darkening sky. "Did you just get struck by lightning too?" he asked on reaching the ledge.'

Paul Glossop

Alpine Report 1991

Acknowledgements

None of the work in this thesis would have been possible without the support and advice of my supervisor, David Ish-Horowicz, and I am correspondingly grateful. I also benefited from the presence of all the members of the ICRF Developmental Biology Unit.

Within the Developmental Genetics Laboratory, Sheena Pinchin gave me a solid start in the world of fly genetics and much subsequent advice. Mark Wainwright perhaps best understood my sense of humour. Domingos Henrique provided national pride and expert help in cloning. I had stimulating discussions on genetics and segmentation with Masayuki Seki and Gerardo Jimenez. Helen Francis-Lang suggested the name *stunted*, and recognised the *stunted* maternal effect phenotype as similar to that of the *nullo* mutant. Ze'ev Paroush encouraged me in all areas and made a very real contribution to the writing of this thesis.

I would also like to thank others who worked in the fly room, Phil Ingham, Marcel van den Heuvel and Michael Fietz for company, advice and discussions.

Harv Isaacs, Betsy Pownell, Jihwan Song, Anna Myat, Patrick Blader, Abigail Tucker, Suresh Jesusthan, Catherine Haddon, Jonny Pierce provided a more social side to things.

Outside of science, Ilan Davis, Jonathan Wilkinson, Andrew Berry, Gill Cooper and Anthony Underwood were responsible for social relaxation.

I would like to thank all those people who I climbed with during my stay in Oxford, members of both the OUMC and UCLMC, especially Paul Glossop, Simon Cooke, Lisa Mellor, Felix Ng, Richard Adams, Paul Morris, Ian Lewis, Rick Thomas, Stuart Leitch, Jim Hart and Robin Fieldhouse.

Finally, an extra special thanks to Lucy Regan.

TABLE OF CONTENTS

LIST OF FIGURES

LIST OF TABLES

Chapter 1. Introduction

1.1 Introduction

Early embryogenesis of the fruit fly *Drosophila melanogaster* consists of many concurrent processes, from patterning of the embryonic axes to changes in cell morphology and movement. Genetic analysis has identified many genes that regulate early embryogenesis. These genes encode proteins required for a wide variety of processes, including mitosis, morphogenesis, establishment of segmentation and neurogenesis. The work presented in this thesis touches on all of these areas, so an overview of each is presented.

1.2 Early morphogenesis

At fertilisation, the *Drosophila* egg consists of a regular distribution of yolk grains and cytoplasm, with the diploid zygotic nucleus near the anterior of the egg. The first thirteen nuclear divisions are rapid, synchronous, and occur without cytokinesis (figure 1.1). During the first four cycles of nuclear division, the nuclei are arranged roughly in a sphere near the anterior of the embryo, each with its own island of clear cytoplasm (energid). During cycles 4-6, the nuclei undergo axial expansion, moving towards the poles of the embryo to form a hollow ellipsoid arrangement. The nuclei then migrate out to the cortex, and occupy an area of clear periplasm which lies underneath the embyronic plasma membrane. The nuclei which reach the posterior pole are enclosed by cell membranes and form the pole cells, the future germline. Some nuclei fall back into the yolk, and remain there to form the yolk nuclei. As the majority of nuclei all share a common cytoplasm, the embryo at this stage is called a syncytial blastoderm.

Cortical migration is finished by cycle 10, and a further three nuclear divisions take place, with the area of clear periplasm increasing in thickness. As the nuclei reach the cortex, they appear to push into the

Figure 1.1 Nuclear behaviour in the early embryonic stages of Drosophila

The figure illustrates the behaviour of nuclei (black dots) from fertilisation until the end of cellularisation in the Drosophila embryo. Yolk grains are represented by stippling; each nucleus is surrounded by its own island of clear cytoplasm (energid). The cytoplasm beneath the plasma membrane (periplasm) is also yolk free. During cycles 4-6, the nuclei change from a spherical arrangement to that of a hollow ellipsoid as they move towards the poles of the embryo (axial expansion). The nuclei migrate out to the cortex in cycles 7-10 and occupy the periplasm. The nuclei which reach the posterior pole are enclosed by cell membranes and form the pole cells during cycle 10. The pole cells are no longer in mitotic synchrony with syncytial nuclei. Nuclei which fall back into the yolk form the yolk nuclei and cease dividing in cycles 8-10, becoming polyploid. During cycles 10-13 the syncytial nuclei in the periplasm continue to divide synchronously. As the majority of nuclei all share a common cytoplasm, the embryo at this stage is called a syncytial blastoderm. At the beginning of cycle 14, membrane furrows invaginate between the nuclei to simultaneously form separate cells over the entire surface of the embryo. After the completion of cellularisation, the embryo begins to gastrulate, beginning with the formation of the cephalic furrow at the anterior of the embryo and infolding of the posterior midgut furrow (figure from Foe and Alberts, 1983).

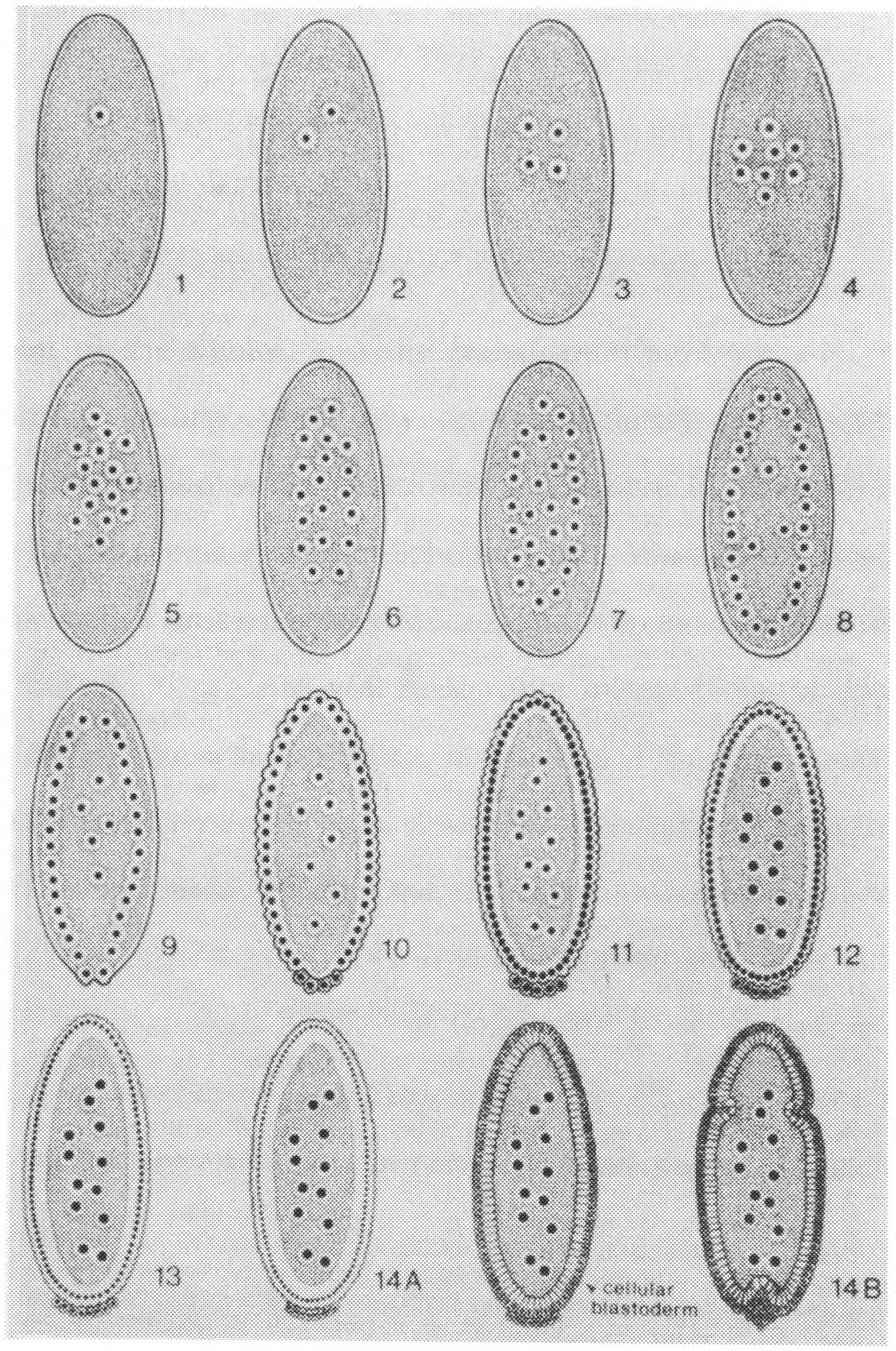
1
2
3
4
5
6
7
8
9
10
11
12
13
14A
cellular blastoderm
14B

plasma membrane, so that the plasma membrane resembles a series of hemispheres, each of which contains a nucleus. These cytoplasmic buds flatten during mitosis and breakdown completely by telophase, reforming during the next interphase. During prophase and metaphase, the sides of the buds protruding either side of the mitotic spindle resemble cleavage furrows, and so are sometimes called pseudocleavage furrows. They do not actually separate the nucleus from the rest of the egg cytoplasm and the embyro remains a syncytium.

1.3 The role of the cytoskeleton during early morphogenesis

Migration of the nuclei, and the transformation from a syncytium to a multicellular embryo must rely on cytoskeleton components. Different roles for microtubules and microfilaments have been identified in these early events (reviewed in (Schejter and Wieschaus, 1993b)). Axial expansion relies on actin based microfilaments, as indicated by sensitivity to cytochalasin B, a drug which disrupts microfilaments (Hatanaka and Okada, 1991). Cortical migration is unaffected by cytochalasin B, but is inhibited by colcemid, which disrupts microtubules. Microtubules are found to be distributed in long astral arrays that interconnect neighbouring nuclei during cortical migration. This observation led Baker et al. (Baker et al., 1993) to propose a model in which the force necessary for cortical migration is supplied by a microtubule motor acting between anti-parallel microtubules, generating an outward force and pushing nuclei away from each other.

During early morphogenesis, the cytoskeleton undergoes dynamic changes in response to cell cycle cues. The microtubule network reorganises into spindles for each mitosis, and each time, cortical migration is interrupted until the long astral arrays interconnecting each nucleus are reformed. When the nuclei reach the actin rich cortex, the actin concentrates above

each nucleus in 'caps'. The actin cytoskeleton also responds to cell cycle cues (figure 1.2). As the nuclei enter metaphase and spindles form, the actin redistributes to the sides of the cytoplasmic buds, at the pseudocleavage furrows. At the end of mitosis, actin relocalises into caps above each nucleus (Warn et al., 1984; Karr and Alberts, 1986; Kellogg et al., 1988).

The concentration of actin at the plasma membrane has been suggested to have two functions: (i) to prevent microtubules from pushing against the plasma membrane, allowing the nuclei to arrive in the periplasm, and (ii) to anchor the nuclei at the plasma membrane. Continued microtubule-dependent force pushes the nuclei into the cytoplasmic buds, and maintains the nuclei equidistant to each other. At the same time the yolk is compressed, leading to increased thickness of the clear periplasm (Foe et al., 1993).

The cytoskeletal rearrangements that form the syncytial embryo appear to be controlled by the same basic biochemical mechanism which drives the cycles of DNA replication and chromosome segregation. The mechanism has been termed the mitotic oscillator, and it appears to act through the centrosomes. Centrosomes not only act as spindle poles during mitosis, but nucleate the microtubule arrays that move and position the nuclei. Even in the absence of nuclei, centrosomes are able to replicate and migrate to the cortex, where they form cytoplasmic buds and organise nearly normal cyclical changes in the microtubule and microfilament networks (Raff and Glover, 1989; Yasuda et al., 1991).

1.4 Genetic analysis of early morphogenesis

The advantage of *Drosophila* as an experimental organism is the ability to utilise a genetic approach to dissect biological processes. Early morphogenesis relies entirely on gene products laid down in the egg by the

Figure 1.2 Mitosis in the syncytial blastoderm

The figure illustrates cytoskeletal rearrangements and cytoplasmic bud formation during mitotic cycle 10. Yolk grains are represented by large light grey filled circles, the nucleus by a large dark grey filled circle centrosomes by small light grey circles, actin by small black lines and microtubules by large thick black lines; the latter when dotted represent microtubules disintegrating. All events occur in the periplasm beneath the plasma membrane which is represented by a thick black line. During early interphase, actin is present in a cap between the nucleus and the plasma membrane; microtubules protrude into the yolk grains. The centrosomes which have already duplicated, begin to move apart until, during prophase they are diametrically opposite sides of the nucleus. The plasma membrane and cytoplasm around the nucleus form a dome, the cytoplasmic bud. Actin concentrates around the sides of the bud. Chromatin condenses, and during early metaphase, the nuclear envelope breaks down completely near the centrosomes. Long astral microtubules completely break down, and the mitotic spindle forms with the chromosomes arrayed on the equator. Actin is concentrated on the sides of the 'pseudocleavage furrows', next to the centrosomes. By telophase, the cytoplasmic bud has collapsed. Actin is reorganised into caps above each centrosome pair, and also at the site of the spindle equator. The centrosomes rotate 90° so that once more they separate the nucleus and the plasma membrane. Astral microtubules begin to elongate and penetrate the yolk grains (adapted from Foe et al., 1993).

Sectional views

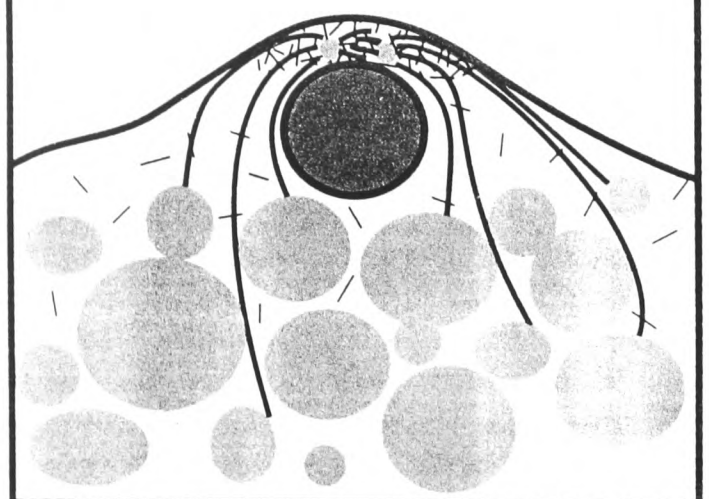

Top views

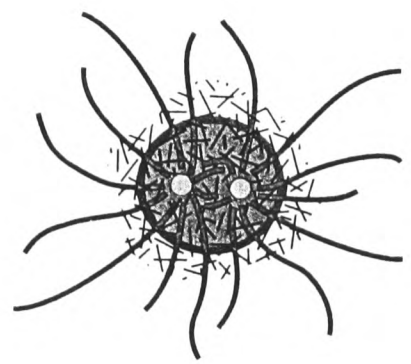

Early Interphase

Sectional views

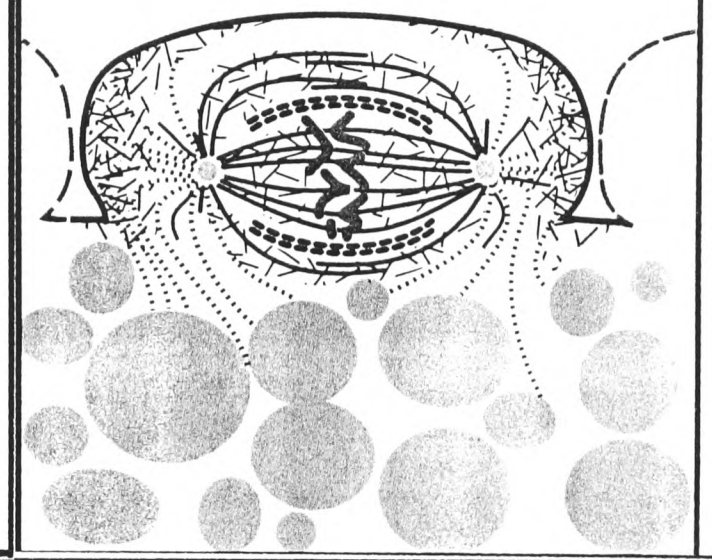

Top views

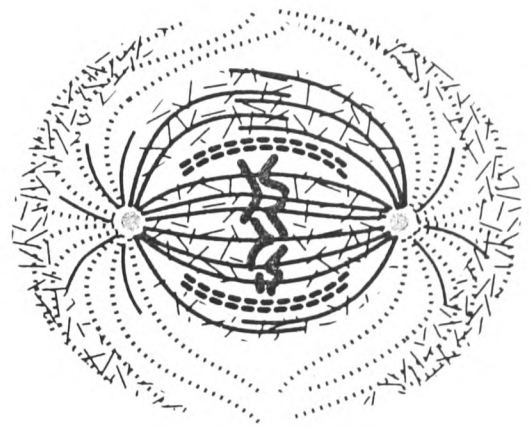

Early Metaphase

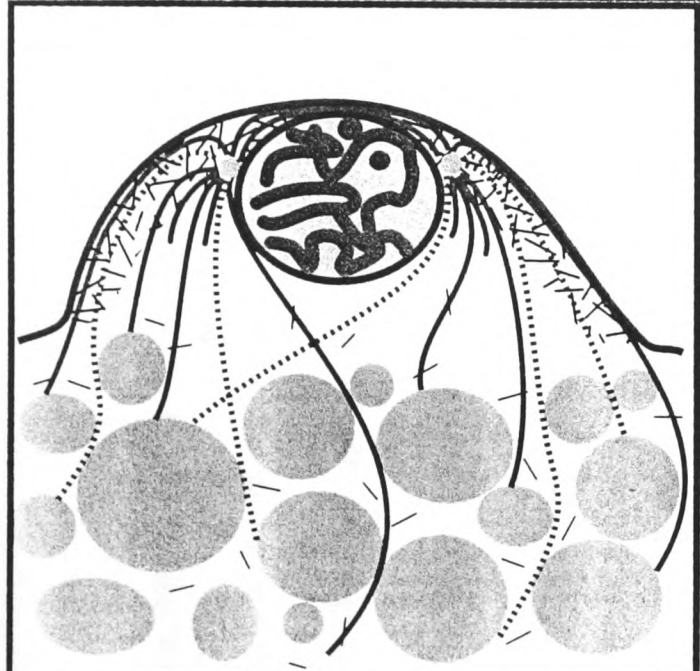

Prophase

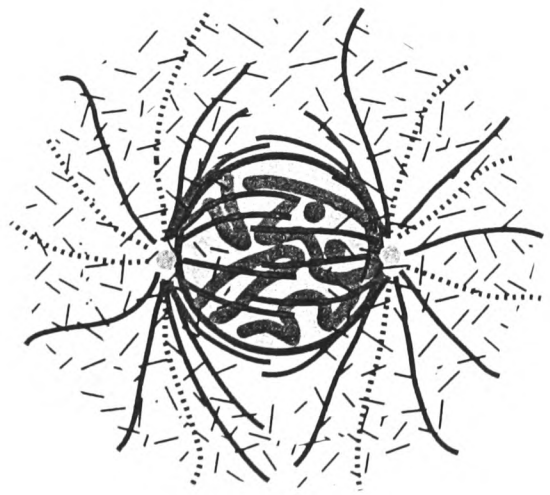

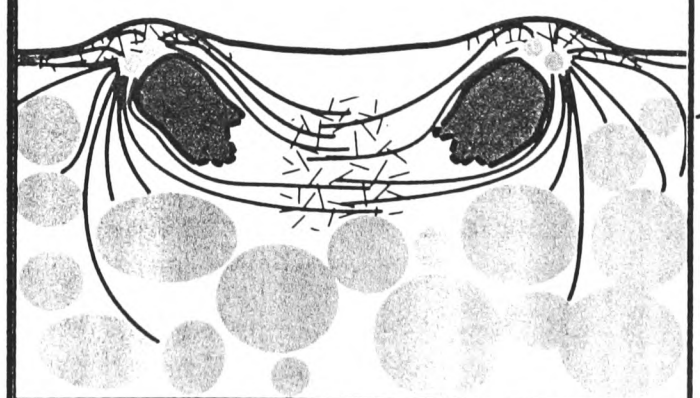

Telophase

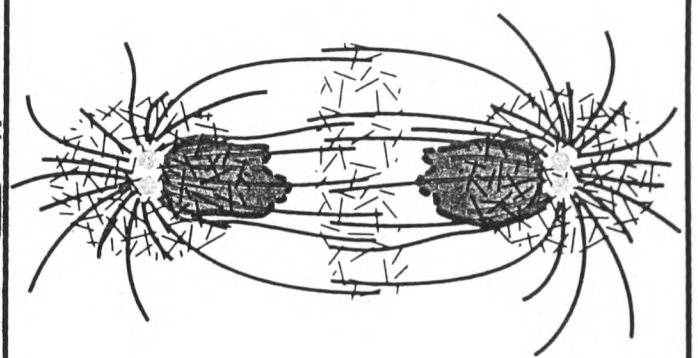

mother. This is demonstrated by injection of transcriptional inhibitors, such as α-amanitin, which has no effect on either axial expansion or cortical migration (Edgar et al., 1986a).

A large number of maternal effect mutations are thought to have specific roles in the embryonic cell cycle of *Drosophila* (catalogued in Foe et al., 1993). Obviously, arrest of early cell cycles prevents morphogenesis, although in embryos mutant for *plutonium* or *pan gnu,* which initiate DNA synthesis without fertilisation, centrosomes continue to replicate and migrate in the absence of nuclei (Freeman et al., 1986; Shamanski and Orr, 1991). As early morphogenesis responds to cell cycle cues, and the microtubule network is required for proper cell cycles, mutations can affect both morphogenesis and mitosis simultaneously. Mutations with phenotypic effects limited to morphogenesis are rare. Three examples are *gs(1)N26, gs(1)N441* and *paralog,* all of which lead to absent or abnormal axial expansion with normal cortical migration (Hatanaka and Okada, 1991).

1.5 Cellularisation

During nuclear cycle 14, the syncytial blastoderm is transformed into the cellular blastoderm by invaginating membrane furrows which move down between the nuclei perpendicular to the plasma membrane, and ultimately enclose the nuclei (figure 1.3). Invagination is initially slow, but enters a second phase in which the membrane furrows advance more quickly. During cellularisation, the nuclei elongate while still retaining a distinct polarity as marked by the position of nucleoli and centrosomes. As the furrows pass by the nuclei, the leading edges thicken and start to fuse to enclose the nuclei at the same time as the yolk is reached. The partitioning of each nucleus into a single cell is complete by the end of cycle 14, and

Figure 1.3 Cellularisation in the syncytial blastoderm

During the interphase of cycle 14, the syncytial blastoderm is converted into the cellular blastoderm. The figure illustrates cellularisation and the cytoskeletal rearrangements that occur during the process. Actin, microtubules, nuclei, centrosomes and yolk particles are represented as in figure 1.2. The start of cellularisation is marked by the formation of furrow canals between the nuclei. Myosin co-localises with actin in the furrow canals to form a contractile ring. Astral microtubules elongate rapidly, and reach the yolk particles by the start of the slow phase of membrane extension. The nuclei which have swollen and elongated, appear to be pinched by the actin-myosin contractile ring localised the leading edge of the inward moving furrow. When viewed from the surface, actin and myosin form a highly regular hexagonal network. As the furrow passes the nuclei, the hexagons change to rings that become smaller, and the inward movement of the furrow increases. The rings are of a small diameter by the time they reach the yolk particles, and they remain to transiently form a 'yolk stalk' (adapted from Foe et al., 1993).

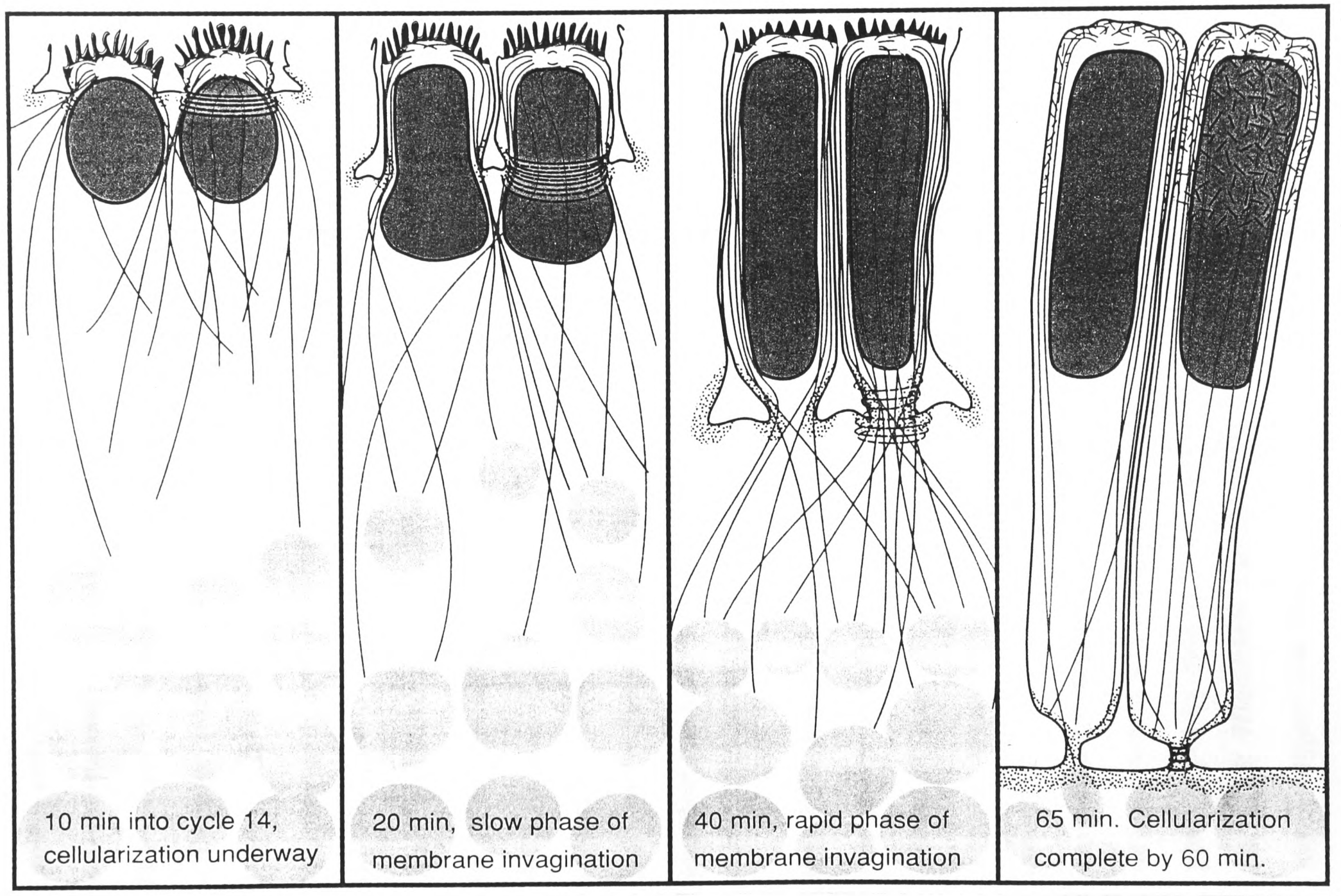

10 min into cycle 14, cellularization underway

20 min, slow phase of membrane invagination

40 min, rapid phase of membrane invagination

65 min. Cellularization complete by 60 min.

transforms the embryo from a syncytial blastoderm into a cellular blastoderm.

During cellularisation, the invagination of membranes between the nuclei is accompanied by a dramatic restructuring of the cytoskeleton (figure 1.3). The microtubule network rearranges into 'baskets' around each nucleus, with long astral arrays extending to the yolk surface. Actin begins to concentrate at the leading edge of the membrane furrows. Myosin co-localises with actin to form a hexagonal network which probably provides the contractile force for cellularisation (Simpson and Wieschaus, 1990; Warn and Robert-Nicoud, 1990; Young et al., 1991). During the rapid phase of membrane extension, the actin-myosin hexagons change to rings which decrease in diameter as they get nearer to the yolk. The contractile rings constrict fully as they near the yolk layer, but do not completely pinch off the newly formed cell from the yolk layer, until after the onset of germband extension.

1.6 Zygotically expressed genes required for cellularisation

Cellularisation is completely blocked by injection of transcriptional inhibitors. This raises the question of how many zygotically expressed genes are required for this process. Embryos lacking large cytologically defined regions of chromosomes were generated from stocks bearing compound chromosomes or Y chromosome translocations, and were examined for defects in cellularisation (see figure 1.4). Such experiments defined seven autosomal and one X-linked region which display discrete phenotypes by mid cycle 14, consistent with single gene defects (Merrill et al., 1988; Wieschaus and Sweeton, 1988). The small number of zygotic genes suggest that they act on structures already provided maternally. The zygotic gene products may be required to co-ordinate various phases of cellularisation at the correct times.

A

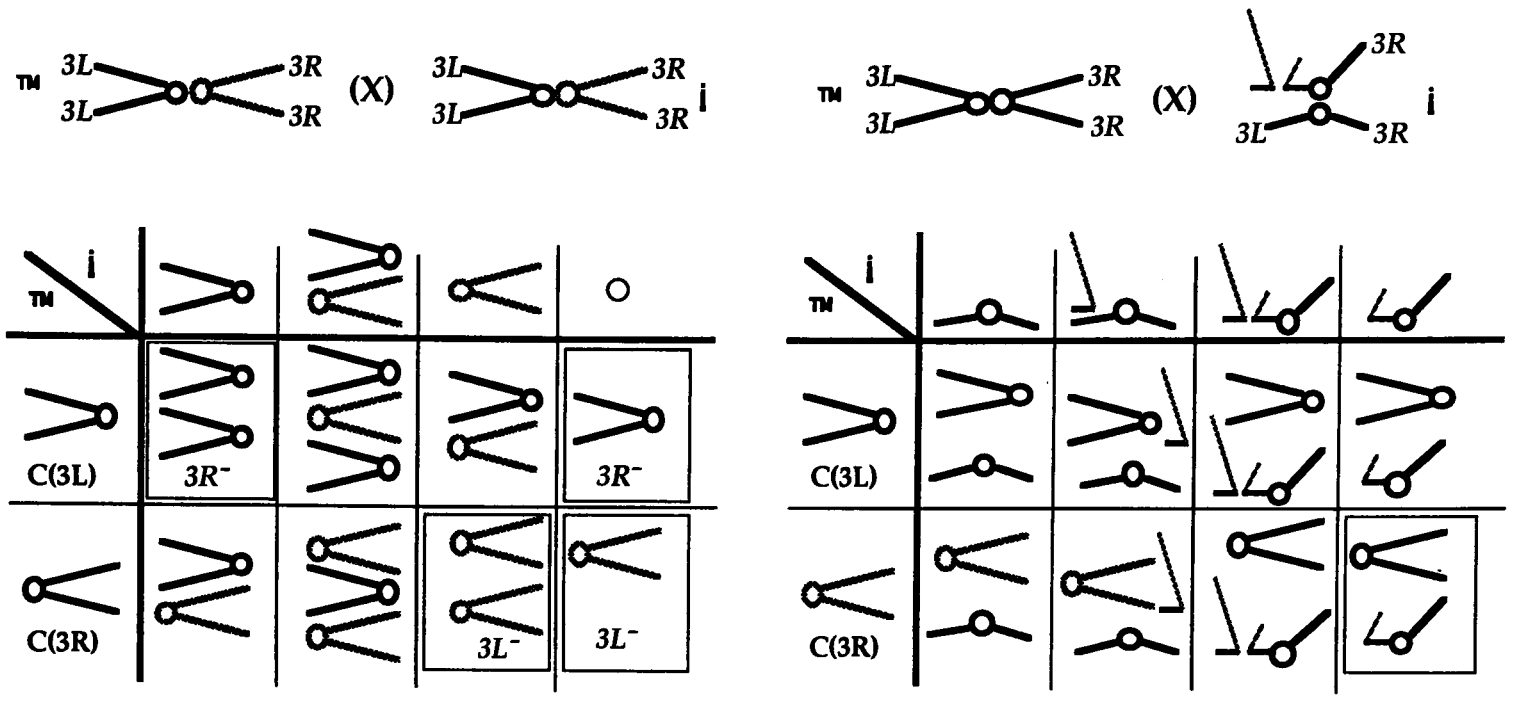

Figure 1.4 Generation of embryos deficient for large chromosomal regions

A. To generate embryos lacking entire chromsome arms, compound autosome stocks are used. Compound chromosomes have the same arms of the chromosome, eg. the left arms, attached to the same centrosome. The cross used to generate the embryos is shown at the top of the figure, and segregation of the gametes in the table below. 25% of the embryos lack the left arm, and 25% lack the right arm of the third chromosome. B. To generate smaller deletions, compound autosome females are crossed to males bearing Y-autosome translocations with breakpoints at various points along the chromosome. The Y chromosome is represented by the light gray lines originating from the break in the left arm of one of the male's third chromosomes in the cross at the top. Segregation of the gametes is shown below. As long as the required region is distal to the translocation breakpoint, one eigth of the embryos from the cross will lack the relevant region. (adapted from Merril et al., 1988).

Three of the zygotic genes required for cellularisation have been well characterised: *nullo*, *serendipity-α (sry-α)* and *bottleneck (bnk)*. Both *nullo* and *sry-α* display the same initial defect: the normally regular hexagonal actin array is highly variable, displaying unevenness in the thickness of the actin lines and occasional ruptures of the network. The result is formation of multinucleate cells with incompletely closed basal surfaces (Schweisguth et al., 1990; Rose and Wieschaus, 1992). In *bnk* mutants, there is premature and uneven closure of cells, and nuclei often get trapped between the fusing membrane furrows (Schejter and Wieschaus, 1993a). All three gene products immunolocalise to the leading edge of the advancing cellularisation front, consistent with roles in the structural regulation of the network during its formation and subsequent contraction. Localisation of the *sry-α* protein is dependent on *nullo*, and so *sry-α* appears to be functionally downstream of *nullo* (Postner and Wieschaus, in press). All three genes lack sequence homologies to known genes; *nullo* and *bnk* are notably basic.

While the events of morphogenesis unfold, other patterning events are occurring, in particular the establishment of the segmental organisation of the larval body. During the early mitotic cycles, maternal products required for segmentation are translated, and as the nuclei reach the cortex, the first transcription of zygotic segmentation genes is detectable. Ten minutes after cellularisation is complete, segmentation is also established.

1.7 Segmentation

The saturating genetic screens of Nüsslein-Volhard and colleagues identified a large number of genes required for the correct patterning of the embryonic cuticle (Nüsslein-Volhard and Wieschaus, 1980; Jürgens et al., 1984; Nüsslein-Volhard et al., 1984; Wieschaus et al., 1984). The larval cuticle is rich in anatomical landmarks allowing mutant phenotypes to be

Figure 1.5 Anatomical landmarks of the larval cuticle

This figure illustrates the anatomical landmarks of the cuticle of a wild type first instar larva. Anterior is to the left and the upper surface is dorsal. The most striking feature is the segmented pattern of the larva, as marked by the denticle (bristles) belts. The future abdomen is composed of eight segments, each marked by a ventral belt of denticles, denoted a1 to a8 corresponding to the abdominal segments they mark. The belts a2 to a7 cannot be distinguished unambiguously from each other; each is composed of six rows of denticles. Each row of denticles within the belt displays polarity as shown diagrammatically below a6, with rows 1 and 4 pointing anteriorly, and the remaining rows posteriorly. The denticle belt a1 is composed of four rows of denticles, and a8 has five rows. Each denticle belt has a characteristic trapezoidal shape in segments a2-a7, and rectangular in a8. On the dorsal surface, hairs point towards the posterior in the anterior half of each segment, and towards the anterior in the posterior half of each segment. The future thorax is composed of three segments, each marked by belt of fine denticles: t1, t2 and t3. The jaws are illustrated by a dotted line shape at the anterior end of the larva. At the posterior end, the filzkörper or posterior spiracles, part of the larval respiratory system are denoted sp; a crown of radiating bristles occurs at their exit point. Below the filzkörper, is the telson region (te) and the anal plate (ap). Also annotated are various sense organs, these were not examined during the screen (figure from Campos-Ortega and Hartenstein, 1985).

Figure 1.6 The segmentation gene hierarchy

The diagram illustrates the expression patterns of representative members of each class of genes operating in the segmentation hierarchy. A gradient of Bicoid protein diffusing from the anterior pole of the embryo represents the maternal co-ordinate class of genes. The embryonic axes are established by these genes; mutations in components of the systems lead to patterning defects affecting most of the embryo. The remaining classes of genes all act zygotically, although they may have maternal components, eg. the gap gene *hunchback*, or the segment polarity gene *shaggy/zeste-white 3*. Ilustrated is the gap gene *knirps (kni)*, which has two broad domains of expression. All the gap genes are expressed in one or two broad domains, and their name reflects their mutant phenotypes: a gap in the segmental patterning of the larval cuticle. The first sign of segmentation appears with the seven stripe expression of the pair-rule genes; mutations lead to the loss of every other segment. The action of the pair-rule genes defines fourteen parasegments, which are marked by the Engrailed protein which is present in a 1-2 cell wide stripe at the front of every parasegment. There is no stereotypic expression pattern for the segment polarity genes; the common theme is that they are responsible for patterning with the segment and maintaining segment boundaries. Parasegments acquire identities through expression of the homeotic or selector genes. Shown is expression of Ultra bithorax which defines the differentiation program for the sixth parasegment. The sixth parasegment constitutes the posterior half of the third thoracic and the anterior half of the first abdominal morphological segments (T3 and A1 in figure 1.5).

Maternal:*bcd*

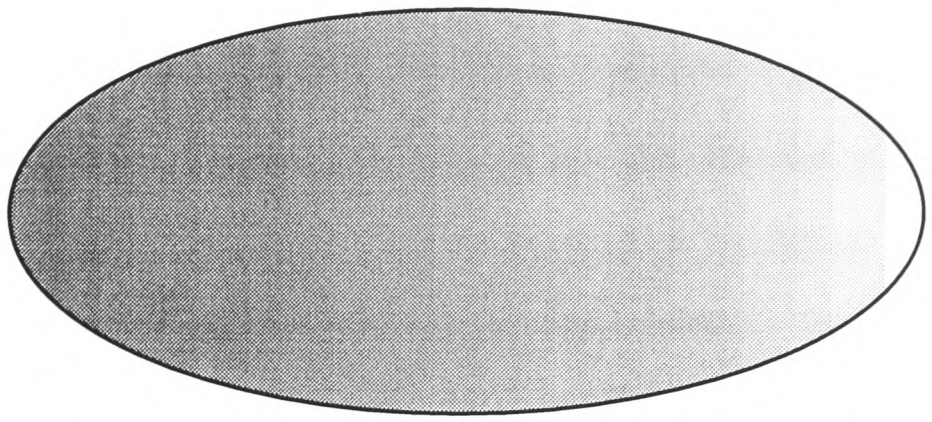

Gap:*knirps*

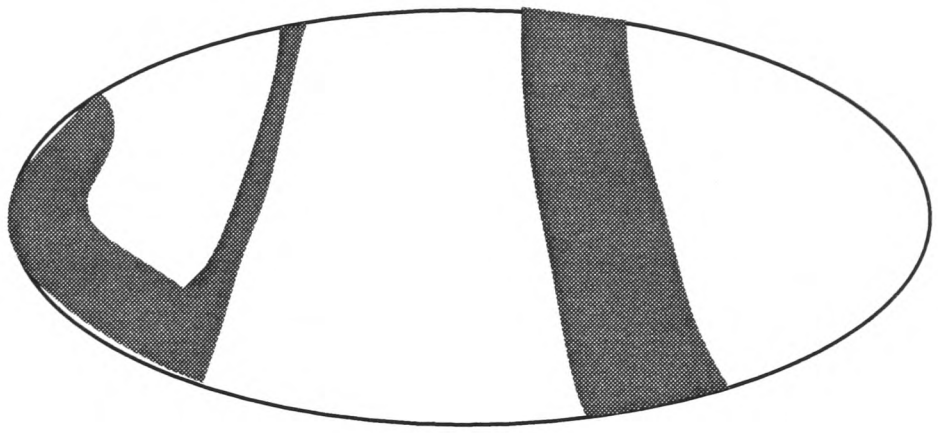

Pair rule:*hairy*

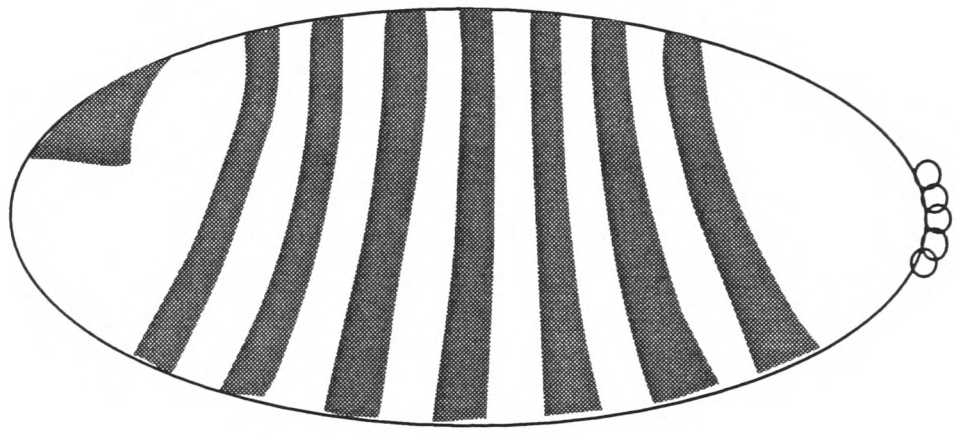

Segment polarity:*en*

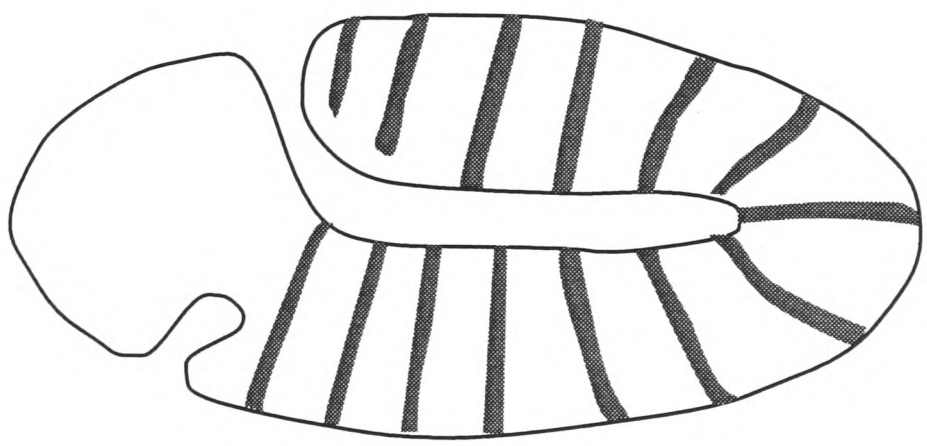

Selector:*Ubx*

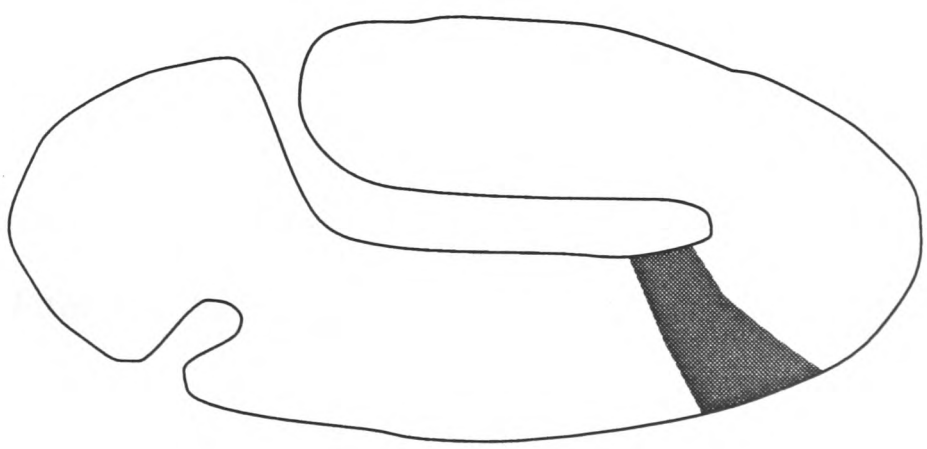

accurately classified according to their effects (figure 1.5). Three maternal systems are required for correct patterning along the anterio-posterior axis: the anterior, posterior and terminal systems (reviewed in (St. Johnston and Nüsslein-Volhard, 1992)). Positional information provided by these systems is interpreted by zygotic genes to subdivide the embryo into successively smaller domains (figure 1.6).

The segmentation genes subdivide the embryo into fourteen parasegments. Parasegments are defined in terms of gene expression (below) and are out of phase with the morphological segments visible in the late embryo and larva (Ingham et al., 1985; Martinez-Arías and Lawrence, 1985). The activities of the segmentation genes have been ordered into a hierarchy, proceeding from the gap genes, through the pair-rule genes, to the segment polarity genes. As specification of most of the thoracic and abdominal parasegments does not require positional information supplied by the terminal group genes, I will ignore the contribution of the terminal system to segmentation in this overview.

The segmentation genes act on positional information supplied by about fifteen known maternal effect genes. The anterior determinant is the *bicoid (bcd)* gene product. During oogenesis, *bcd* mRNA is transported to, and anchored at the anterior end of the embryo. Translation of the *bcd* mRNA, and diffusion of the Bcd protein after fertilisation leads to the formation of a morphogenetic gradient (Driever and Nüsslein-Volhard, 1988b; Driever and Nüsslein-Volhard, 1988a). The posterior determinant, *nanos (nos)* is localised to the posterior pole in the form of mRNA (Wang and Lehmann, 1991). Translation of *nos* mRNA also leads to a protein gradient (Gavis and Lehmann, 1994). The sole function of this gradient is to block translation of maternal mRNA from the *hunchback (hb)* gene in the posterior of the embryo. This has been proved by demonstrating the

viability and normal segmentation of embryos lacking in both maternal *hb* and *nos* (Hülskamp et al., 1989; Irish et al., 1989; Struhl, 1989).

It is therefore the Bcd gradient which initiates segmentation. Bcd acts as a concentration-dependent transcriptional activator of zygotic target genes (Tautz, 1988; Struhl et al., 1989; Finkelstein and Perrimon, 1990). Different genes respond to different areas of the gradient according to the number and affinity of Bcd binding sites within their promoters (Driever et al., 1989).

1.8 The gap genes and pair-rule genes

The gap and pair-rule genes all have been shown to be, or to have homology to transcription factors, and function as a transcriptional cascade within the syncytial blastoderm. The gap genes are so-called because their cuticular phenotype is a 'gap' in the segmental pattern. The phenotype is reflected in the expression patterns of the gap genes, either one or two broad bands of protein, corresponding to the area of cuticle they disrupt when mutated. Currently, there are nine gap genes: *hb*, *Krüppel (Kr)*, *knirps (kni)*, and *giant (gt)* which are discussed below; three which affect head development, and two which affect the terminal regions of the embryo.

The Bcd gradient both activates and regulates the expression domains of many of the gap genes (reviewed in (Driever, 1993)). The effects of Bcd are both direct and indirect; activation of the *hb* gene results in a morphogen gradient which is partly responsible for positioning the domains of *Kr*, *kni* and *gt* (Hülskamp et al., 1990; Struhl et al., 1992). Once expression of the gap genes is established, genes with adjacent domains of expression begin to cross-regulate each other. This cross-regulation refines the initial patterns of expressions by repositioning boundaries of expression and sharpening them (reviewed in (Pankratz and Jäckle, 1993)). The molecular

nature of the interactions is by no means understood; at least one of the gap genes appears capable of behaving as a transcriptional activator at low concentrations and as a repressor at high concentrations (Sauer and Jäckle, 1991). The role of the gap genes is to subdivide the embryo into broad domains, providing positional information for the correct spatial activation of the pair-rule genes.

The pair-rule genes have a characteristic mutant phenotype, the deletion of alternate larval segments. The phenotype is reflected in an expression pattern of seven stripes for all but one of the pair-rule genes (figure 1.6). Eight pair-rule genes are known, and all have homology to transcription factors. The pair-rule genes have been subdivided into the 'primary' and 'secondary' classes; the primary class consists of *hairy (h), even-skipped (eve)* and *runt (run)*. Mutations in the primary pair-rule genes affect the expression patterns of all the other pair-rule genes, but the converse is not true (Howard and Ingham, 1986; Ingham and Gergen, 1988). The role of the primary pair-rule genes is to integrate the positional information provided by the localised domains of expression of the gap genes. Consequently the promoters of *h, eve* and *run*, have been found to be large and complex, consisting of discrete elements responsible for generating individual stripes of expression (Goto et al., 1989; Harding et al., 1989; Howard and Struhl, 1990; Pankratz et al., 1990; Riddihough and Ish-Horowicz, 1991). For example, the element which generates the second *eve* stripe of expression has binding sites for Hb, Kr, Gt, and Bcd. Hb and Bcd are thought to activate expression of the stripe, whereas Gt and Kr are thought to establish the anterior and posterior borders respectively, by repression (Stanojevic et al., 1989; Small et al., 1991; Stanojevic et al., 1991).

The secondary pair-rule genes establish periodic patterns of expression based on the striping of the primary pair-rule genes. The necessary

promoter elements are simpler; in the case of the *fushi tarazu (ftz)* gene, a 600bp fragment (the 'zebra' element) is sufficient to confer a striped expression pattern, although a second element is necessary for high levels of expression (Hiromi et al., 1985; Hiromi and Gehring, 1987). Like the gap genes, the pair-rule genes undergo dynamic changes in expression patterns in response to each other, and also through autoregulation. In particular, the expression patterns of the Eve and Ftz proteins each change from seven stripes of uniform protein concentration, to seven stripes in which the highest concentration of protein is at the anterior end and diminishes towards the posterior end of the stripe (Lawrence et al., 1987; Frasch et al., 1988; Lawrence and Johnston, 1989).

The pattern of Ftz and Eve is thought to play a key role in activating the segment polarity genes *engrailed (en)* and *wingless (wg)* (reviewed in (Ingham and Martinez, 1992)). The function of the pair-rule genes is to establish fourteen stripes, 1-2 cells wide, of expression of the segment polarity *en* gene, and immediately adjacent, a 1-2 cell wide stripe of *wg* expression. The expression of *en* defines the anterior boundary of the parasegment, and the expression of *wg*, the posterior boundary. The boundaries are used by the homeotic genes to define their domains of expression when they establish the identities of the different parasegments. Further segment polarity genes pattern within each parasegment. As the embryo is by now no longer a syncytium, many of the segment polarity genes encode products required for intercellular communication.

1.9 The collection of zygotic segmentation genes is near saturation

The complexity of segmentation and the large number of known genes raises the question of whether there are further zygotic segmentation genes. The screens of Nüsslein-Volhard and colleagues recovered an average of five alleles at each locus, and statistics indicate that there is only

a slight chance that the screens were not saturating. Redundancy of function could have prevented detection of some genes. Several of the segmentation loci contain duplicated genes, for example the *sloppy-paired (slp)* and *gooseberry (gsb)* loci. In each case the duplicated genes appear to have different roles in development; both *slp* genes, *slp1* and *slp2*, contribute to segmentation, but a temporal difference in expression seems to reflect a functional difference (Grossniklaus et al., 1992). The *gsb* gene acts in segmentation, and the *gooseberry-neuro (gsbn)* gene in neural development; despite considerable sequence divergence, the genes are functionally interchangeable (Li and Noll, 1994). It is therefore possible to conceive of redundant loci generated by an event that duplicated and physically separated a segmentation locus. To see an effect on segmentation would require mutation of both loci simultaneously, an event highly unlikely in a conventional genetic screen. However, examination of duplicated genes shows that they rarely remain functionally equivalent (one exception is the *BarH1* and *BarH2* loci (Higashijima et al., 1992)).

To test if all zygotic genes contributing to segmentation have been discovered, Vavra and Carroll employed the same strategy as described for cellularisation, of generating embryos missing all or part of entire chromosome arms (see figure 1.4) (Vavra and Carroll, 1989). The aneuploid embryos were examined for altered expression patterns of *fushi tarazu (ftz)* and *even-skipped (eve)* not due to the effects of known segmentation genes. As *ftz* and *eve* are pair-rule genes, this screen could only detect novel gap or pair-rule loci. The authors identified only one potentially undiscovered zygotic gene acting in segmentation, a putative gap gene on chromosome 2L.

The final biological process I wish to give an overview of is the generation of the embryonic nervous system which occurs significantly later than the events so far described.

1.10 Neurogenesis

The *Drosophila* central nervous system (CNS) is derived from the ventro-lateral region of the embryo, the neuroectoderm (Hartenstein and Campos-Ortega, 1984). Within this region, groups of cells known as 'proneural clusters' acquire the competence to become neural. A significant proportion of proneural clusters are defined by expression of members of the *achaete-scute complex (AS-C)*. The *AS-C* is composed of four genes encoding proteins containing the basic-Helix-Loop-Helix (bHLH) DNA binding-oligomerisation motif. All the *AS-C* gene products can form heterodimers with the *daughterless (da)* gene product which are capable of transcriptional activation (Cabrera et al., 1987; Romani et al., 1987; Murre et al., 1989b; Cabrera and Alonso, 1991). Although all the cells of the proneural cluster initially express the *AS-C*, one cell is singled out to delaminate into the embryo and become a neuroblast. *AS-C* expression increases in this cell, and the remaining cells lose expression of the *AS-C* and are inhibited from assuming a neural fate by the neuroblast precursor. The precursor cell ultimately delaminates into the embryo, and the other cells of the proneural cluster remain epidermal unless they are singled out in a later phase of neuroblast formation. The peripheral nervous system (PNS) arises in a similar fashion to the CNS neuroblasts, except that the precursors are derived from the dorsal ectoderm, not the neuroectoderm.

The process of singling out a neuroblast precursor, and subsequently preventing the other cells in the proneural cluster from adopting the neural fate is known as lateral inhibition. A large number of genes are known to be involved in the cell-cell interactions required for lateral

inhibition, and are collectively known as the neurogenic genes. Mutations in the neurogenic genes result in all the cells in a proneural cluster delaminating and assuming a neural fate. The large decrease in the number of epidermal cells means very little larval cuticle is secreted, leading to a characteristic phenotype, allowing neurogenic mutants to be picked up in the screens of Nüsslein-Volhard and colleagues (Nüsslein-Volhard and Wieschaus, 1980; Jürgens et al., 1984; Nüsslein-Volhard et al., 1984; Wieschaus et al., 1984).

Two of the neurogenic mutants, the *Notch (N)* and *Delta (Dl)* loci, each code for transmembrane proteins with large extracellular domains (Wharton et al., 1985; Kidd et al., 1986; Vässin et al., 1987). Therefore, *N* and *Dl* are candidates for mediating the cell-cell interactions during lateral inhibition. In one analysis, N appears to act as a cell surface receptor, and *Dl* as a ligand during lateral inhibition (Heitzler and Simpson, 1991).

Four other zygotic loci produce neurogenic phenotypes: the *Enhancer of split complex (E(SPL)-C), mastermind (mam), big brain (bib)* and *neuralised (neu)*. All except *bib* show genetic interactions with *N*, and so are defined as the *N* group. *bib* has homology to membrane channel proteins, whereas *mam, neu* and *E(SPL)-C* are probably transcription factors, based either on sequence motifs or cellular localisation (Knust et al., 1987; Klämbt et al., 1989; Rao et al., 1990; Smoller et al., 1990; Greenspan, 1992). The *E(SPL)-C* consists of seven bHLH genes, all related to each other, probably redundant and with similarity to the *h* segmentation gene. Genetic epistasis experiments place them at the end of the lateral inhibition pathway, acting as transcriptional effectors of the epidermal cell fate (de la Concha et al., 1988). *mam, neu* and *bib* probably participate in the neural-epidermal decision, rather than reinforcing the outcome.

If *N* and *Dl* act in a signalling pathway, more components must be involved, for example in transduction of the signal from the cell surface to the nucleus. The neurogenic genes described above are the most well characterised of the neurogenic loci. Several other neurogenic loci are known, but have been less well characterised mainly due to the fact that they are maternal effect loci. Mutations in *almondex (amx), pecanex (pcx), l(1)EA24* and *l(1)3PP4* all produce a neurogenic phenotype when both their maternal and zygotic contributions are removed (Perrimon et al., 1989); *pcx* codes for a large transmembrane protein (LaBonne et al., 1989), while none of the others has been cloned. Two further loci, *l(1)1PP22* and *l(1)5PP1* lead to a neurogenic phenotype by removal of the maternal contribution alone.

All the maternal effect mutations just described, except *amx* and *pcx*, are also zygotic recessive lethals. It is genetically difficult to examine the maternal effects of zygotic recessive lethal mutations, and the reasons why are examined in the next section. Recent advances in the techniques required are also discussed. Following this, examples of why this class of genes is likely to be important for all the biological processes discussed in this introduction are presented.

1.11 Genetic techniques for examining maternal effect mutations

Maternal effect mutations lead to the failure to deposit a particular gene product in the oocyte. Such mutations are so called because they depend on the genotype of the mother, not that of the affected offspring. Therefore, to examine the effect of removing maternal gene products, it is necessary to generate females homozygous for a mutation in the gene of interest. Many genes are reused during development, and so are essential for viability, making it impossible to generate homozygous females. For example mitotic mutants cause cell cycle defects in the larval and pupal stages; as

these genes are essential for viability, when mutated they are generally recessive lethals.

To examine recessive lethal mutations for maternal effects requires the use of chimeric flies, heterozygous females whose germline is homozygous for the mutation of interest. Such females can be generated in two ways, (i) pole cell transplantation, or (ii) mitotic recombination (figures 1.7, 1.8). Pole cell transplantation relies on transplanting the pole cells of homozygous mutant embryos into a host embryo which lacks a functional germline. Alternatively, x-ray induced mitotic recombination can be used to produce females with homozygous germline clones. Pole cell transplantation is technically difficult, while x-ray induced mitotic recombination is labour intensive, due to the low frequencies of females with germline clones recovered.

The use of a dominant female sterile mutation (DFS) greatly simplifies the generation of germline clones by mitotic recombination (Perrimon and Gans, 1983; Perrimon et al., 1984). The DFS mutation is present in trans to the mutation of interest. If no mitotic recombination occurs, then the female cannot lay eggs because of the DFS mutation. Only females which have had a mitotic recombination event in their germline can lay eggs, as the daughter cell which has been homozygosed for the mutation of interest lacks the DFS mutation (figure 1.8). Analysis of zygotic lethals for maternal effects has focused on the X chromosome because the X-linked mutation, ovo^{D1}, is the most suitable DFS for generating germline mosaics. Oogenesis is blocked at an early stage, and wild type clones have a growth advantage allowing them to populate a full ovary. In addition, the viability of females heterozygous for the mutation is unaffected.

No DFS mutations with similar properties to ovo^{D1} have been recovered on the autosomes, making the generation of germline mosaics for

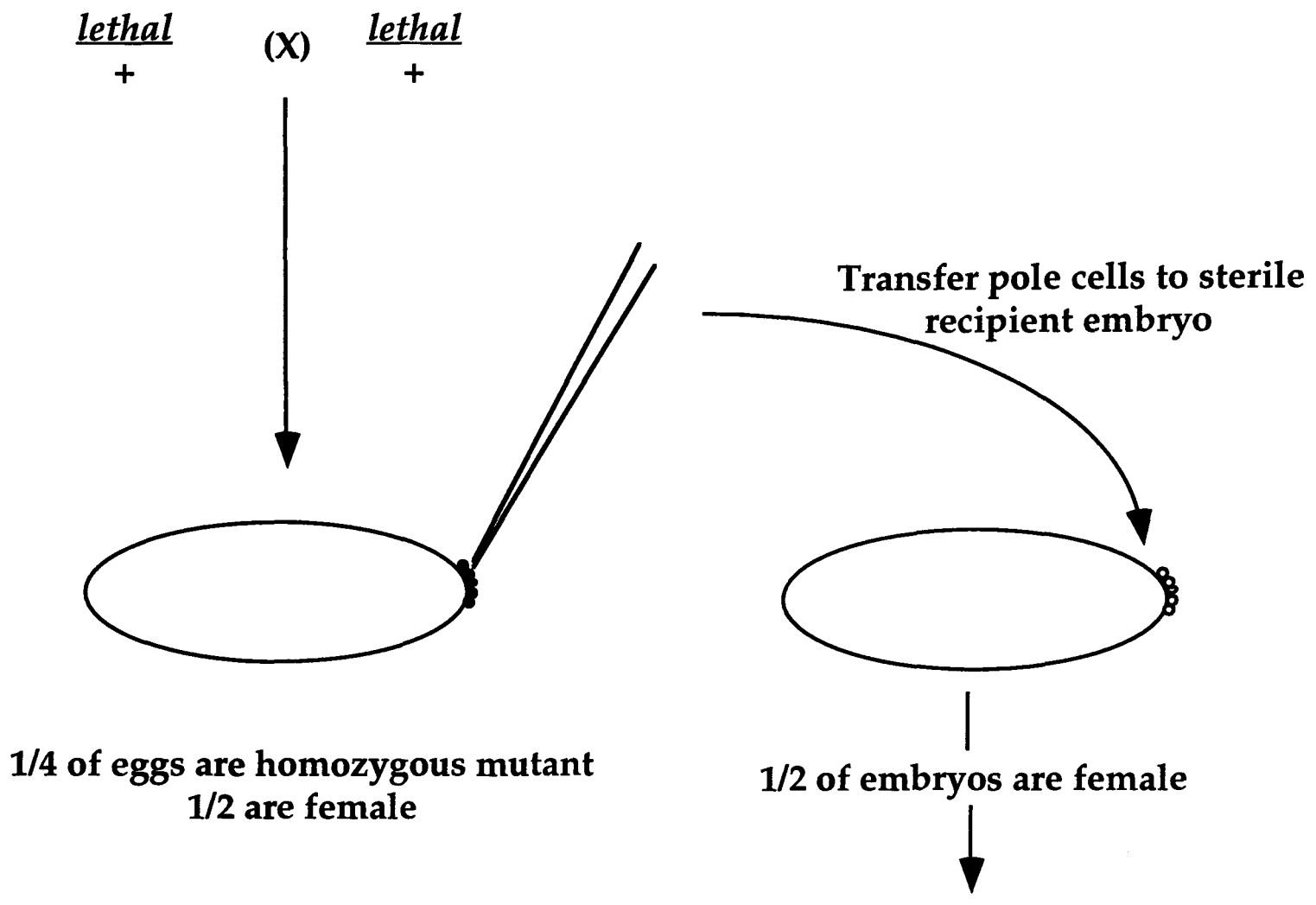

Figure 1.7 Generation of germline clones by pole cell transplantation

Use of pole cell transplantation to generate chimeric females whose germline is homozygous for a zygotic lethal mutation. The pole cells of donor embryos generating by crossing two heterozygotes are transplanted into recipient embryos with female sterility mutations. The recipient embryos are allowed to develop; only one in sixteen will be a female who received homozygous mutant germ cells from a female donor embryo.

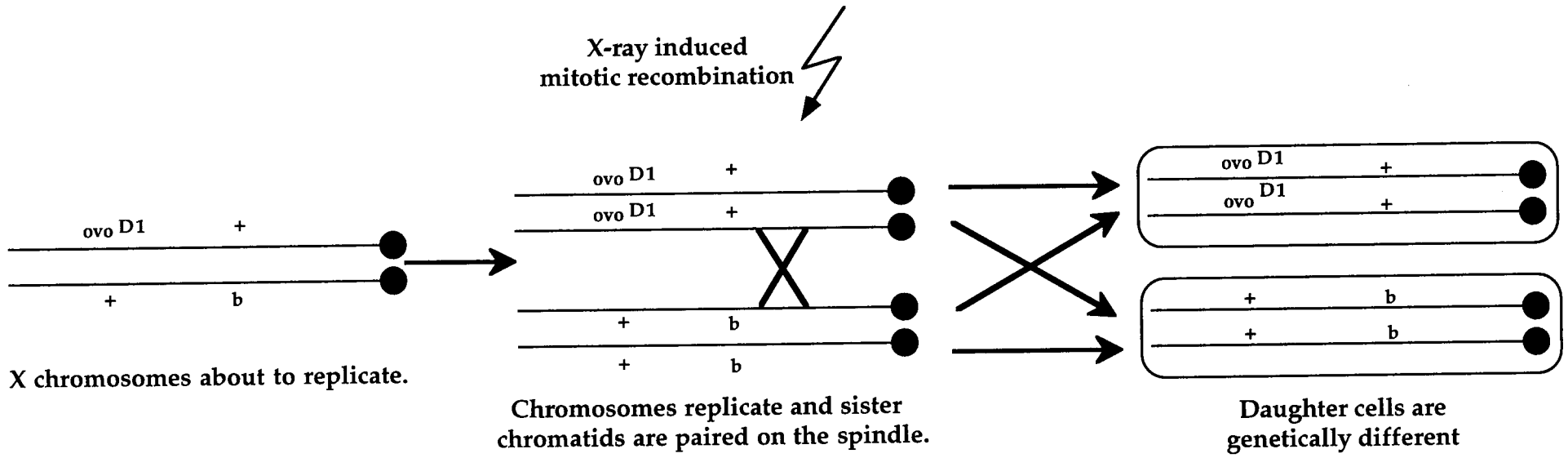

X chromosomes about to replicate.

Chromosomes replicate and sister chromatids are paired on the spindle.

Daughter cells are genetically different

Figure 1.8 Germline clones produced by mitotic recombination

Germline clones can be produced by the use of X-ray induced mitotic recombination. When sister chromatids are paired on the spindle, a mitotic exchange between non-sister chromatids leads to homozygosing of the region of the chromosome distal to the site of the exchange, as shown in the figure. The region proximal to the site is not homozygosed. Segregation leads to two non-identical daughter cells. In the case, illustrated, one of the daughter cells is homozygous for the 'b' locus. If the mitotic recombination event occurred in the germline, the effect of removing the maternal contribution of locus 'b' could be ascertained. However, the cell homozygous for 'b' may be at a growth disadvantage, and will be unable to populate the germline. The use of a dominant female sterile (DFS) mutation can prevent this from happening. The DFS, ovo^{D1}, is present in trans to the 'b' locus. If a mitotic crossover occurs proximal of both loci as illustrated, then the cell homozygous for 'b' is the only cell without a copy of ovo^{D1}, and is therefore able to populate the germline. X-ray induced mitotic recombination has two disadvantages, (i) germline mosaics are recovered at frequencies of about 5%, (ii) if the locus of interest is proximal to the DFS, then a crossover between them will lead to a female with a wild type germline. Both these disadvantages are overcome using the a yeast recombinase, FLP, to catalyse the exchange between non-sister chromatids. The FLP recombinase acts at target sites called FRTs, which can be integrated into the genome, so the mitotic recombination always occurs at the same location. Using a combination of a heat shock induced FLP recombinase, and a DFS, germline mosaic females can be recovered at frequencies of 90% or more.

autosomal mutations difficult. The construction of a P element carrying ovo^{D1} which was subsequently transposed to locations on the second and third chromosomes has overcome this problem (Chou et al., 1993). However, X-ray induced germline clones were recovered at frequencies of only 1-2%, even less frequent than the 1-5% rate reported for the X chromosome.

The importance of the maternal effects of essential genes for *Drosophila* embryogenesis was demonstrated by a genetic screen carried out by Perrimon et al. (Perrimon et al., 1989). They generated germline clones homozygous for over a thousand X-linked zygotic lethal mutations, and about 7% showed specific maternal effect phenotypes. They estimated that their screen had reached an 86% level of saturation, suggesting that there are at least four hundred genes with specific maternal effects in the *Drosophila* genome. Germline clone based screens cannot recover mutations which are lethal in the germline, so there are certainly more genes contributing to early embryogenesis.

The screen of Perrimon et al. relied on X-ray induced germline clones, with a frequency of females carrying germline clones between 1-5%. Recently a technique has been developed which allows the recovery of females carrying germline clones at frequencies of 90% or more (Chou and Perrimon, 1992). The technique relies on the discovery that a yeast recombinase, FLP, can catalyse recombination between sister chromatids at target sites (FRTs) integrated into the *Drosophila* genome (Golic and Lindquist, 1989; Golic, 1991). When combined with the use of a DFS mutation, the technique (FLP-DFS) makes the generation of germline clones for a given mutation straightforward. A genetic screen using this technique showed that 12% of X-linked zygotic lethal mutations tested had

a specific maternal effect, and a further 40% were germline lethal, in broad agreement with the screen of Perrimon et al.

Extension of the FLP-DFS technique by development of FRT sites on autosome arms (Xu and Rubin, 1993), which also carry the ovo^{D1} P element, should allow screening of autosomal zygotic mutations for maternal effects. The catalogue of genes with maternal effects in early embryogenesis should expand considerably. The potential for this class of genes to contribute to the areas of early embryogenesis discussed is presented next.

1.12 Maternal components for morphogenesis and cellularisation

Early morphogenesis relies entirely on maternal products, principally those required for mitosis, so many of these will be essential genes. However, if these genes are required for mitosis, mutations will be germline lethal, and will not be picked up in germline clone screens. There may be regulators for the early mitoses that are not ubiquitously required in all cell divisions; mutations leading to specific defects in the syncytial mitoses (when the nuclei have arrived at the cortex), have already been recovered. The maternal effect mutations *grapes (grp), scrambled (sced)* and *nuclear fallout (nuf)* all show defects during cycles 11-13 (Sullivan et al., 1993). Other gene products may interact with the known maternal effect mutations to control microfilament dynamics, both during axial expansion, and during the syncytial mitoses.

The small number of zygotic genes required for cellularisation suggested that they act on maternally supplied structures. No maternal effect genes specifically affecting cellularisation are known; cellularisation can be disrupted by mutations affecting earlier events, such as the syncytial mitoses: *grp, sced* and *nuf* all disrupt cellularisation (Sullivan et al., 1993). Earlier defects in mutant embryos could also mask later roles: the maternal

effect mutation *fs(1)1459* results in nuclei being displaced from the cortex, with the result that cellularisation does not occur (Zalokar et al., 1975).

One maternal effect mutation, *sponge (spg)*, is particularly interesting because it appears to link the microfilament and microtubule networks (Postner et al., 1992). In embryos derived from *spg* mutant mothers, actin does not concentrate in caps above nuclei during cycles 11-13. A hexagonal actin network is formed, but there are irregularities and multinucleate cells form. When an actin binding protein 13D2 was immunolocalised in embryos from *spg* mothers, it was found to be normally localised above the cortical nuclei, suggesting components of the caps were normally localised. The authors proposed that *spg* is required for localisation of actin to caps in response to centrosomal cues.

No maternal effect mutations have been shown to have a specific effect on cellularisation, possibly because the genes in question are all required in the preceding cell cycles and their actions are modified in some way by expression of the zygotic cellularisation genes. There is clearly potential to find more mutations, both in this category, and perhaps specific to cellularisation. Novel gene products have been isolated by biochemical means, when embryonic extracts were poured over columns of immobilised actin (Miller et al., 1985; Miller et al., 1989). A large number of embryonic actin binding proteins, including 13D2, were identified by this technique, and most await further characterisation, particularly at a genetic level.

1.13 Maternal components for segmentation

Molecular genetic analysis of the zygotic segmentation mutations has defined a transcriptional cascade which subdivides the embryos into parasegments. Transcription factors generally do not act alone, but often physically interact with partner proteins, cofactors for activation or

repression, and enzymes which modify their activity. Such activities are only now being defined for the segmentation genes.

The gene products of the segmentation genes are expressed in spatially localised patterns. Any factors which physically interact with the segmentation genes do not need to be spatially localised themselves, as activity will be dependent on interacting with the spatially localised partner. Such genes could therefore be maternally expressed and present ubiquitously throughout embryogenesis. The principle was illustrated by the cloning of the *odd-paired (opa)* pair-rule gene (Benedyk et al., 1994). Although mutation of *opa* leads to a pair-rule phenotype, the RNA and protein are not expressed in stripes, but throughout the embryo.

Embryonic lethal alleles of the *hairy (h)* gene display a pair-rule segmentation phenotype. The protein encoded by *h* contains the bHLH motif. Both the basic and the HLH domains are conserved in *D.virilis*, and mutations have been mapped to both regions suggesting they are required for *h* activity (Wainwright and Ish-Horowicz, 1992). It seems like that Hairy will homo- or hetero-dimerise. There are no published reports of Hairy protein binding to DNA, so Hairy may require a partner protein with which to bind DNA. Potentially, Hairy could bind DNA as a homodimer, but heterodimerisation is a theme that runs through all bHLH protein-protein interactions, probably because heterodimeric interactions greatly increase the control available for processes. Identification of a partner protein for Hairy was one of my original research aims when I began my thesis work. The absence of candidate zygotic mutations for a putative partner implied that it would be maternally expressed.

As expression of all the secondary pair-rule genes is not eliminated in any of the known mutants, there must be unidentified global activators. The pattern of Ftz evolves from a broad uniform expression to seven stripes,

suggesting that it is activated by factors present throughout the embryo, and subsequently refined by the actions of the primary pair-rule genes. Such factors are probably maternal supplied, and would be reused during development. A potential difficulty is that the phenotype of global activators when mutant might be too non specific to be recognised.

Evidence that more proteins than just transcription factors are required for segmentation comes from the screen of Perrimon et al. *hopscotch (hop)* is an X-linked larval/pupal lethal mutation (Perrimon and Mahowald, 1986). Embryos derived from mothers carrying germline clones homozygous for *hop* display segmentation defects. Cloning of *hop* revealed homology to the Janus (Jak) family of tyrosine kinases, and the authors suggest that *hop* phosphorylates factors that bind to specific regions of pair-rule gene promoters (Binari and Perrimon, 1994). By analogy with Jak, *hop* may be part of a signal transduction pathway, and so factors upstream and downstream, including transcription factors may also show specific maternal effects on segmentation as well.

The segment polarity genes operate within the cellularised embryo, so there is a requirement for cell-cell communication. It is known that many of the genes involved have maternal components: signal transducing machinery itself need not be localised, only the signal. An example is the *fused (fu)* gene which has both zygotic and maternal expression (Perrimon et al., 1989), and codes for a putative protein kinase (Preat et al., 1990).

1.14 Maternal components of neurogenesis

As neurogenesis occurs after cellularisation, the level of maternal components per cell is considerably titrated out, suggesting that maternal effect loci might not be as important as zygotic loci for neurogenesis. However, the six maternal effect neurogenic loci described above (section 1.10), are all on the X chromosome, suggesting there many be as many as

thirty maternal effect neurogenic loci in the total genome. Four of the loci are zygotic lethal mutations, as well as having maternal effects. The *groucho (gro)* locus is one of the few autosomal maternal effect genes with a zygotic lethal component which gives a neurogenic phenotype when mutated (Schrons et al., 1992), but more will almost certainly be discovered in FLP-DFS screens of autosomal lethal mutations.

This prediction is based on the finding that the neurogenic genes are active in many tissues in addition to the nervous system (Hartenstein et al., 1992). The neurogenic genes have been argued to constitute a "functional gene cassette", in each case acting to single out one cell from an equivalence group for a particular cell fate (reviewed in (Jan and Jan, 1993)). One example is choosing a muscle precursor cell (Corbin et al., 1991). Other maternal effect neurogenic genes will have zygotic effects, as many of the components required for generation of the CNS could be reused during processes requiring the neurogenic gene cassette.

The same argument can be presented in reverse. A large number of genes show genetic interactions with *N* in the generation and patterning of adult structures. Collectively these genes are called the *N* group, and many members will probably turn out to be maternal effect neurogenic loci when examined. A potential difficulty in removing the maternal expression of these genes is that *N*, and possibly the other neurogenic genes are required for oogenesis (Ruohola et al., 1991). If a *N* group member was also active during oogenesis, maternal effects on neurogenesis would be masked by female sterility. For example the *N* group member, *strawberry-notch (sno)* is needed for germline development (Coyle-Thompson and Banerjee, 1993).

The prediction of thirty maternal effect neurogenic genes may well be an underestimate. *N* and *Dl* are required not only for cell fate decisions

during oogenesis, but also for the microtubule based localisation of *bcd* RNA in the oocyte (Ruohola et al., 1991; Clark et al., 1994). This suggests that cytoskeletal genes may be present in the neurogenic group. This was confirmed by Poodry in experiments with the *shibire (shi)* locus, which codes for a homologue of dynamin, a microtubule organising protein (Chen et al., 1991; Vanderbliek and Meyerowitz, 1991). Embryos mutant for *shi* display defects very early in embryogenesis, but a heat pulse on a temperature sensitive mutant of *shi* at the correct time produces increased proliferation of neuroblasts (Poodry, 1990). In addition, embryos mutant for the *sno* locus display defects in the actin skeleton very early in development. If cytoskeletal functions are required for neurogenesis, they may be difficult to uncover, because neurogenic defects are masked by defects earlier in development, as is seen for *shi*.

The large number of genes able to produce a neurogenic phenotype has been described as "disturbing to some, since it suggests that a neurogenic phenotype can be produced rather non-specifically" (Greenspan, 1992). Perhaps it should be a surprise that so few genes are known to be required, especially if in addition to cell-cell signalling, cytoskeletal rearrangements are necessary during lateral inhibition.

1.15 Conclusion

This thesis has touched on all of the areas presented in this introduction. Screening of X-linked zygotic lethal mutations recovered mutations with maternal effects on segmentation, neurogenesis and cellularisation. I was most interested in mutations leading to pair-rule segmentation defects, and analysis of two such mutants is presented. In addition to the genetic screens, the protein-protein interactions of the Hairy protein, a member of the pair-rule class, were investigated.

Chapter 2. Protein-protein interactions of the Hairy protein *in vitro*

2.1 Introduction

During segmentation, the pair-rule gene *hairy (h)* acts as a transcriptional repressor of the pair-rule gene *fushi tarazu (ftz)*. In *h* mutant embryos, the seven stripes of *ftz* are broadened, expanding into the domains where *h* would usually be expressed (Carroll and Scott, 1986; Howard and Ingham, 1986). Conversely, when *h* is ectopically expressed under the control of a heat shock promoter, *ftz* stripes are repressed within thirty minutes of heat shock (Ish-Horowicz and Pinchin, 1987). Considering the short half life of *ftz* RNA and protein, this is consistent with Hairy acting as a direct transcriptional repressor (Edgar et al., 1986b).

The protein encoded by the *hairy (h)* segmentation gene contains the bHLH DNA binding-oligomerisation domain, implying that Hairy must function as a heterodimer or homodimer *in vivo* (Murre et al., 1989a; Rushlow et al., 1989). I examined whether Hairy can homodimerise or form heterodimers with known proteins *in vitro*. The results allow predictions about Hairy's mode of action as a transcriptional repressor to be made.

The pGEX expression system was employed to detect protein-protein interactions *in vitro* (figure 2.1) (Smith and Johnson, 1988; Kaelin et al., 1991; Bengal et al., 1992). Hairy and other bHLH proteins were fused to the glutathione-s-transferase (GST) enzyme in the pGEX vector, for expression and purification in bacteria. The fusion proteins were purified by affinity chromatography on glutathione-Sepharose beads, and their integrity confirmed by Coomassie staining or immunodetection on a Western blot (figure 2.2). ^{35}S-methionine labelled, *in vitro* translated proteins were incubated with beads carrying the immobilised fusion proteins, and

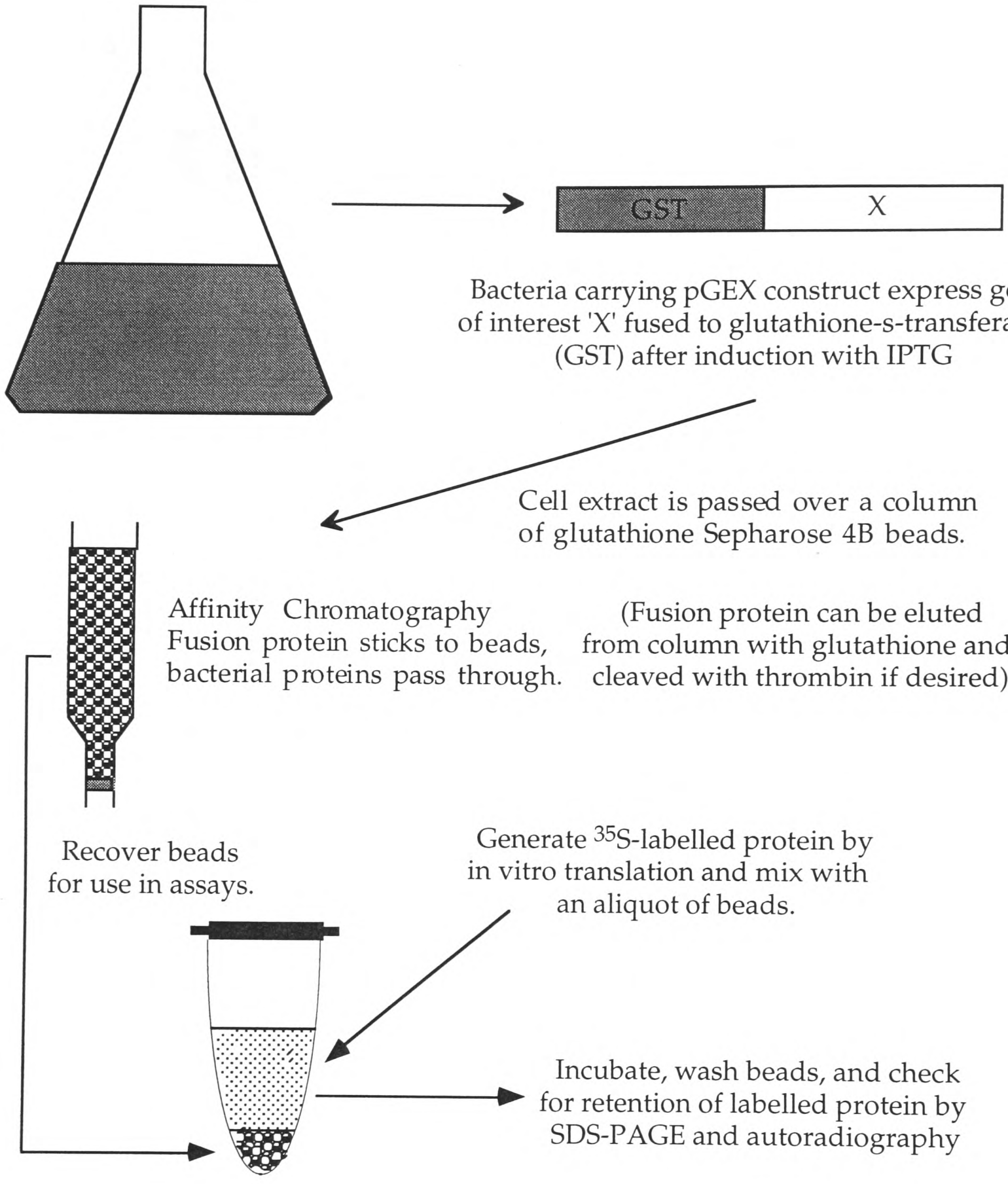

Figure 2.1 Principle of the pGEX expression system

The figure illustrates the purification of GTS fusion proteins by affinity chromatography and the subsequent use of beads with bound fusion protein for detecting protein-protein interactions.

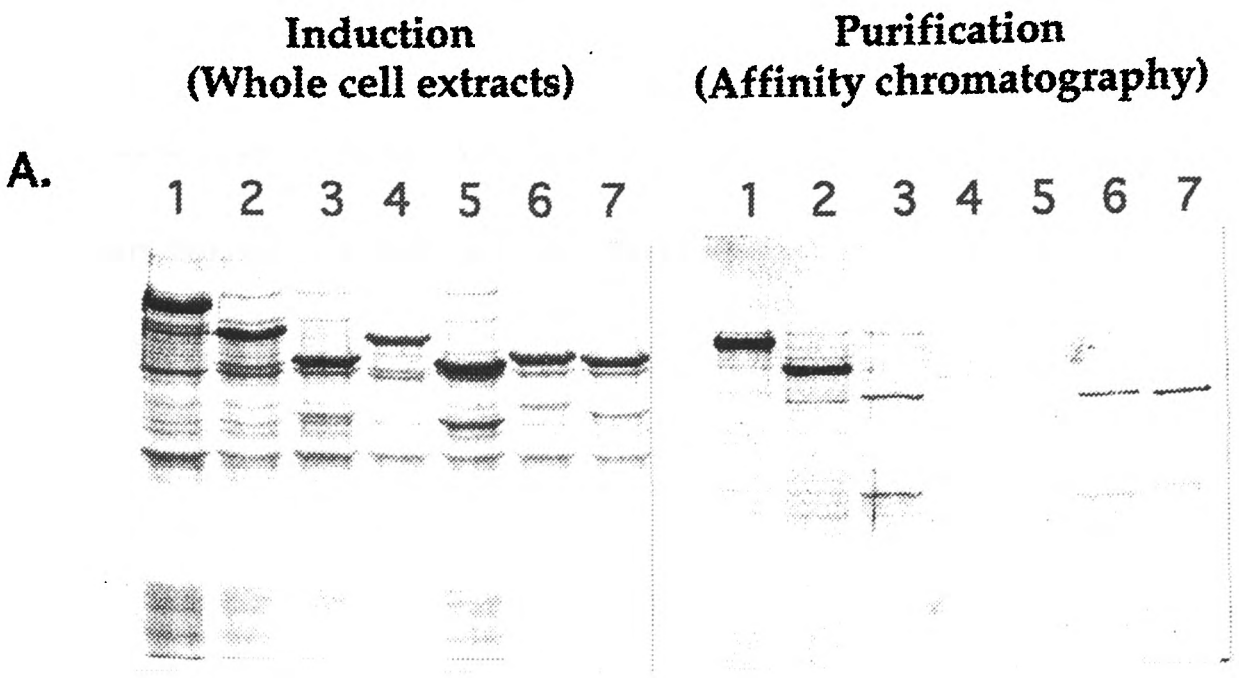

Figure 2.2 Expression of GST fusion proteins using the pGEX system

A. Coomassie stained SDS-PAGE gels showing induction and purification of GST fusion proteins from bacteria: Hairy (1), HairyΔNot (2), mC (3), m3 (4), m5 (5), m7 (6) and m8 (7). Although all the fusion proteins were induced, the levels of recovery varied greatly. The E(spl) proteins m3 and m5 are induced, but very little protein is recovered by affinity chromatography, presumably because they are insoluble and present in inclusion bodies within the bacteria. **B.** Confirmation of the integrity of three GST-HairyΔNot clones relative to a Hairy control and GST-Hairy by western blotting with a mix of anti-Hairy monoclonal antibodies. Some degradation of the control and fusion proteins is visible.

retention of the ^{35}S-labelled proteins examined by polyacrylamide SDS gel electrophoresis (SDS-PAGE) and autoradiography.

2.2 Hairy can form homodimers in vitro

HES1, a rat Hairy homologue and the Hairy related protein m8, a member of the *Enhancer of split complex (E(SPL)-C)* have been shown to bind DNA *in vitro* (Sasai et al., 1992; Tietze et al., 1992). The DNA binding experiments relied on purified proteins, suggesting they bind DNA as homodimers. As Hairy is highly related to these proteins, the ability of Hairy to homodimerise *in vitro* was tested.

Hairy was found to strongly homodimerise (figure 2.3). The HLH domain of Hairy is required for homodimerisation: a mutant Hairy protein, $Hairy_{mhx1}$, containing three missense mutations in helix 1, only interacted very weakly with wild type Hairy.

Hairy and the bHLH proteins of the *E(SPL)-C* all contain a conserved C-terminal tetrapeptide, WRPW (Knust et al., 1987). Two missense mutations in *h* have been mapped to this domain, showing that it is functional biologically (Wainwright and Ish-Horowicz, 1992). A derivative of GST-Hairy was constructed to test if the WRPW motif is required for homodimerisation. GST-HairyΔNot lacks the 84 carboxy terminal amino acids including the WRPW motif. Absence of the carboxy terminus and the WRPW motif did not affect homodimerisation (figure 2.3).

2.3 Assaying for protein-protein interactions between Hairy and the AS-C

Genetically, *h* acts as a repressor during adult bristle patterning (Botas et al., 1982). The phenotype of viable alleles of *h* is the appearance of extra microchaetae. Microchaetae are derived from proneural clusters defined by the expression of the Achaete-Scute Complex (AS-C). All four gene products of the AS-C *(T3, T4, T5, T8)* contain the bHLH motif, form

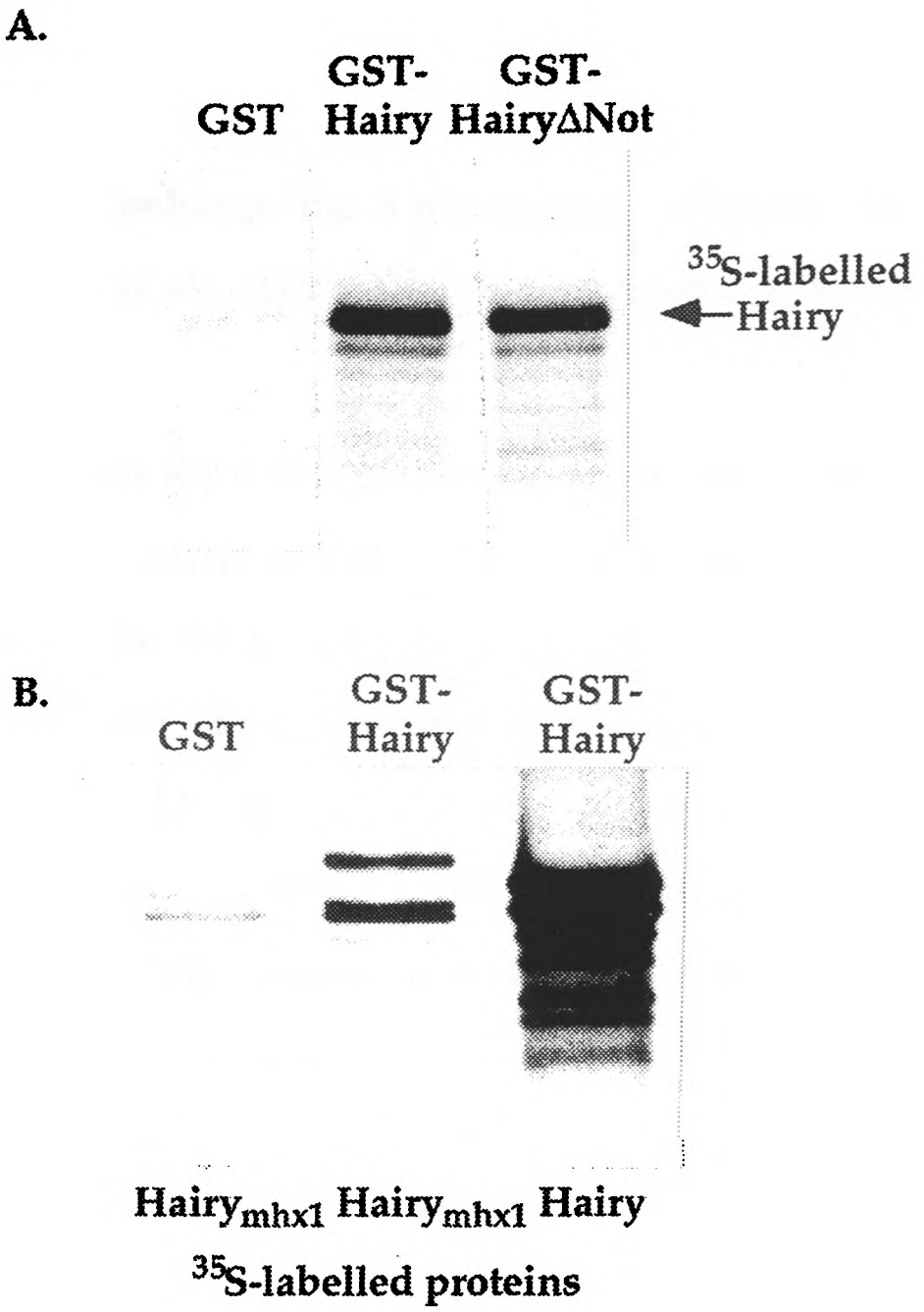

Figure 2.3 Homodimerisation of Hairy *in vitro*

A. Homodimerisation of Hairy. In vitro translated, ^{35}S-labelled Hairy is retained by beads carrying a Hairy or truncated Hairy fusion proteins, but not by beads carrying GST alone. **B. Homodimerisation requires an intact HLH domain.** A Hairy derivative, $Hairy_{mhx1}$, with three missense mutations in the first helix is only weakly retained by beads carrying a GST-Hairy fusion protein, when compared with unmutated Hairy. However, more $Hairy_{mhx1}$ is retained by GST-Hairy beads than Hairy alone, so the mutations in the first helix do not completely abolish homodimerisation. Note: $Hairy_{mhx1}$ preferentially forms a high and low molecular weight isoform, whereas unmutated Hairy usually forms low and intermediate isoforms. These isoforms are visible in the picture. The integrity of the $Hairy_{mhx1}$ construct has been confirmed by restriction digests.

heterodimers with the bHLH Daughterless (Da) protein and activate transcription (Cabrera et al., 1987; Romani et al., 1987; Murre et al., 1989b; Cabrera and Alonso, 1991). *h* acts as a repressor of the *achaete* (*ac;* T5) gene: extra doses of ac^+ enhance the *h* phenotype, whereas decreased doses suppress it (Botas et al., 1982). Therefore, *h* must act in the same genetic circuit as the AS-C.

Like *h*, mutations in the *Drosophila extramacrochaetae (emc)* gene lead to the appearance of extra bristles. *emc* also displays dosage sensitive interactions with the AS-C. Emc is a HLH protein, but lacks the DNA binding basic domain, and represses transcription by forming inactive heterodimers with T4 and/or Da, preventing formation of Da-AS-C heterodimers (Ellis et al., 1990; Garrell and Modolell, 1990; Van Doren et al., 1991). Hairy could repress transcription like Emc, by physically interacting with T5 and/or Da.

Ectopic Hairy expression early in embryogenesis interferes with sex determination and leads to female specific lethality (Parkhurst et al., 1990). Activation of the female specific gene *Sex lethal (Sxl)* depends in part on the activity of T4/Da heterodimers. The ectopic expression of Hairy could be antagonising heterodimer formation by sequestering T4 and/or Da. To test the prediction that Hairy functions as a repressor like Emc, the ability of Hairy to interact with Da and the AS-C bHLH proteins T4 and T5 was tested *in vitro*.

T5 and Da were found to only weakly interact with Hairy, whereas T4 interacted more strongly (figure 2.4). The result suggests that Hairy does not inactivate T5-Da complexes. The AS-C bHLH protein T4 is known to form heterodimers with Da (Cabrera and Alonso, 1991; Van Doren et al., 1991). As figure 2.4 shows, T4 forms heterodimers with Da, and also

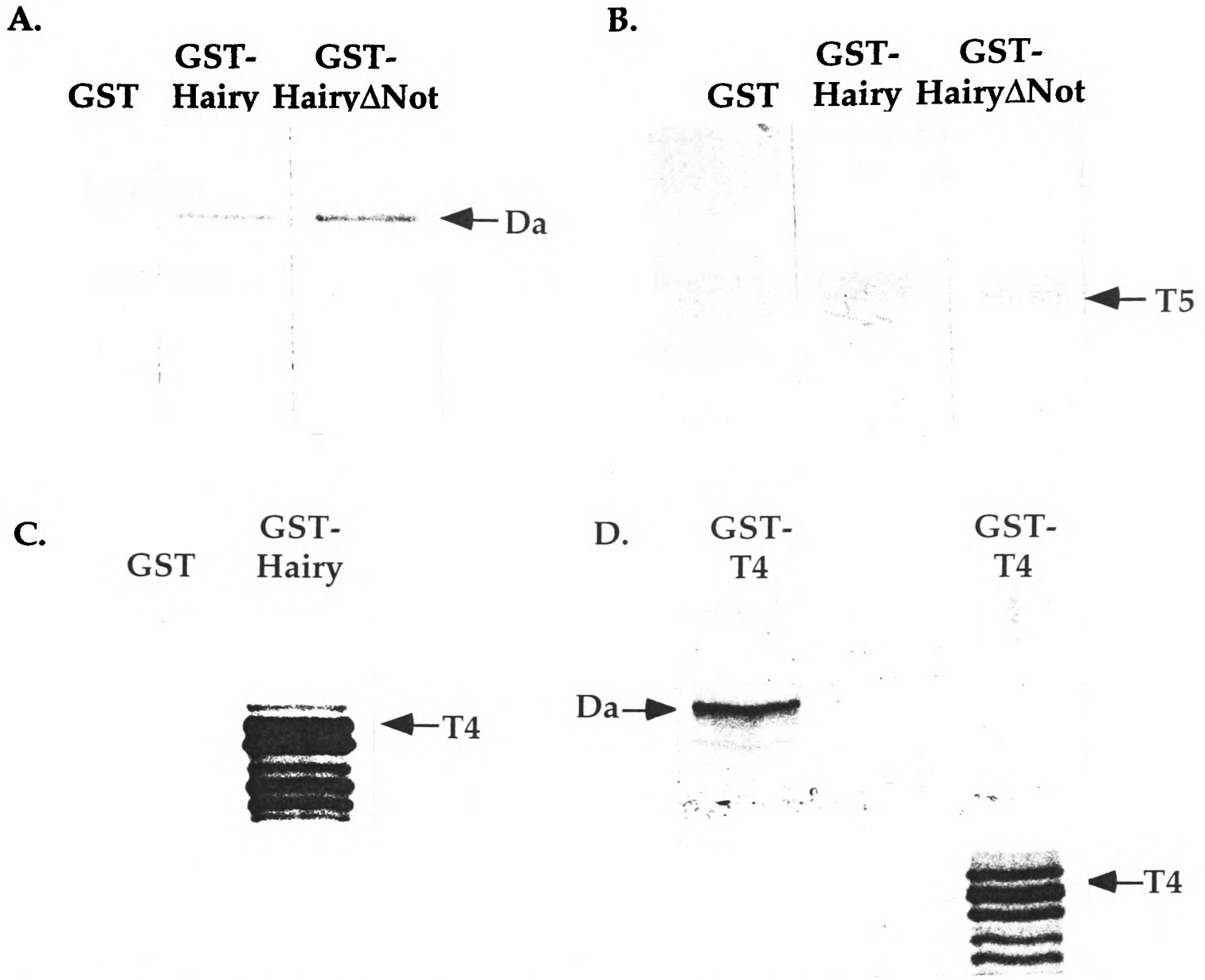

Figure 2.4 Interactions between Hairy and the AS-C

A. ^{35}S-labelled Da protein is not retained by the GST-Hairy, or GST-HairyΔNot fusion proteins. **B.** T5 is not retained by GST-Hairy or GST-HairyΔNot. **C.** T4 is retained by the GST-Hairy fusion protein. **D.** Positive controls. ^{35}S-labelled Da and T4 are retained by a GST-T4 fusion protein.

homodimerises. Interestingly, although T5 does not interact with Hairy, T4 does.

2.4 Groucho

The yeast two hybrid system has been utilised in our laboratory to select for proteins that interact with Hairy (Fields and Song, 1989; Gyuris et al., 1993). One of the partner proteins identified is the product of the neurogenic locus, *groucho (gro)*. Gro does not contain a bHLH motif, and there is no previous evidence that *gro* participates in segmentation (Hartley et al., 1988; Schrons et al., 1992). *gro* shows genetic interactions with the *E(SPL)-C*. The E(spl) proteins are structurally very similar to Hairy, and experiments in yeast show that Gro can interact with members of the E(spl) bHLH proteins (Z. Paroush).

To test whether this interaction is unique to the yeast system, I tested the ability of Groucho to interact with Hairy and the E(spl) proteins mC, m7 and m8 *in vitro*. When Hairy, E(spl) mC, m7 and m8 were expressed as GST fusion proteins in bacteria, and adsorbed to glutathione-Sepharose beads, *in vitro* translated ^{35}S labelled Gro protein was retained by the beads (figure 2.5). These results independently confirm those obtained in the yeast two hybrid system.

Further experiments in yeast revealed that physical interactions with Gro depend on the WRPW motif, not the HLH domains of Hairy or m7. To verify that the observed *in vitro* interactions also rely on the WRPW motif, a derivative of m7 was expressed in bacteria and adsorbed to glutathione-Sepharose beads. GST-m7ΔWRPW lacks the WRPW motif. GST-HairyΔNot was also used as it lacks the 84 carboxy-terminal amino acids. Gro was incubated with beads carrying these proteins. In both cases, removal of the WRPW motif abolished binding of Groucho to the bHLH

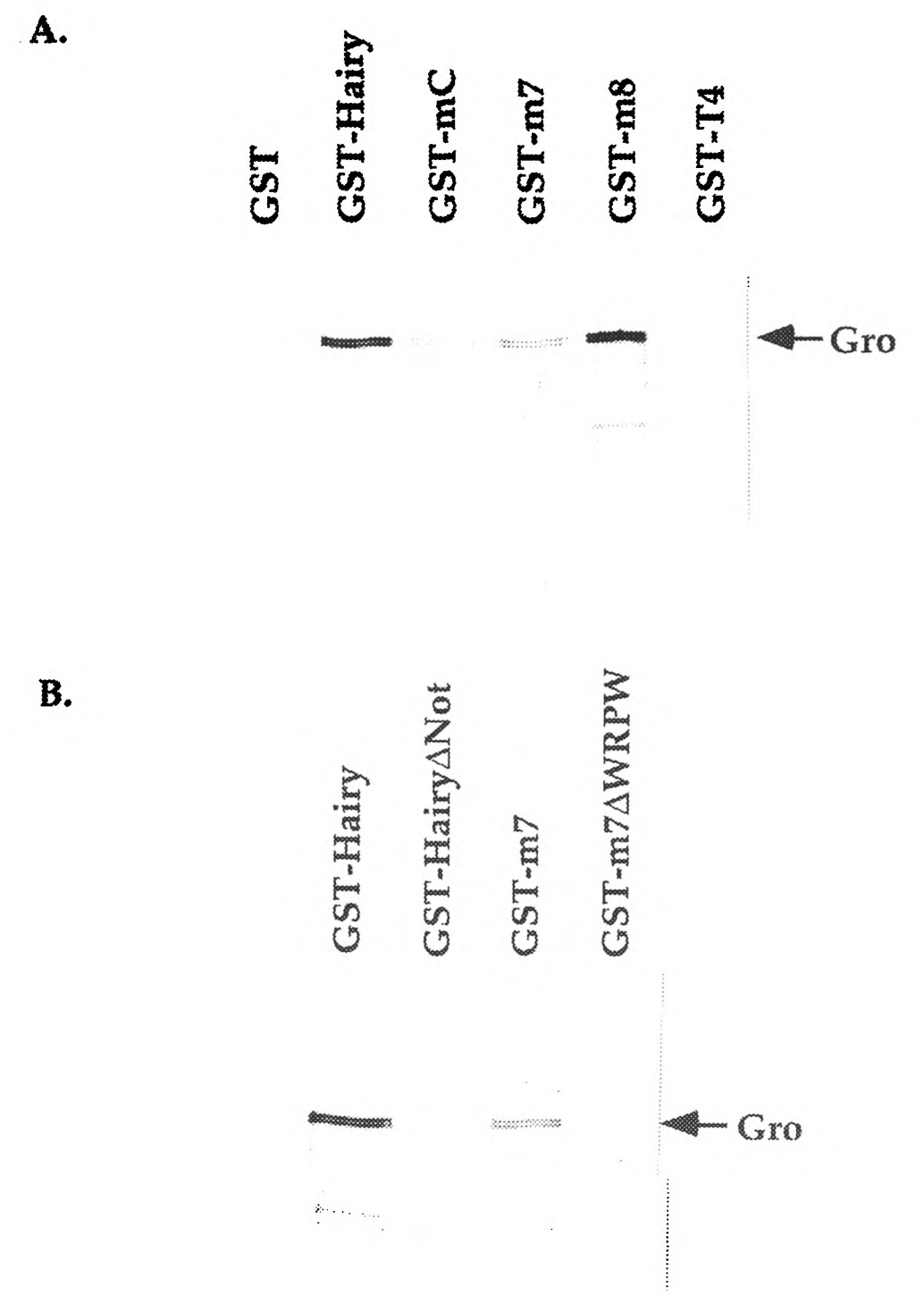

Figure 2.5 Interactions between Groucho, Hairy and E(SPL)-C proteins

A. Retention of in vitro translated ^{35}S-labelled Groucho protein by Hairy, and E(SPL)-C proteins mC, m7 and 8. Gro is not retained by GST, or GST-T4. **B.** Interaction of Groucho is dependent on the carboxy-terminal WRPW motif of Hairy and m7. Gro interacts with GST-Hairy and GST-m7, but not Hairy lacking its carboxy terminus, GST-HairyΔNot, including the WRPW motif, or m7 lacking the WRPW motif, GST-m7ΔWRPW.

proteins (figure 2.5). The WRPW motif is therefore required for interaction with Groucho *in vitro*.

2.5 Discussion

Heterodimerisation is a theme that appears to run through bHLH protein-protein interactions. For example, the c-Myc protein is not seen to form homodimers *in vivo* (Amati et al., 1992), and c-Myc homodimers have been shown to be biologically inactive (Amati et al., 1993). Therefore, the ability of Hairy to homodimerise *in vitro* may not reflect an interaction *in vivo*. Hairy might have a partner protein *in vivo* with a HLH domain very similar to that of Hairy, so that the stability of the heterodimer is greater than that of the homodimer. However, as HES1 and E(spl) m8 bind DNA on their own, I favour a model in which Hairy is able to bind DNA as a homodimer.

Hairy physically interacts only weakly with T5 or Da. These results are in agreement with *in vitro* experiments of Van Doren et al., which showed that Hairy is unable to antagonise the binding of Da/T5 and Da/Da dimers to sites in the *ac* promoter (Van Doren et al., 1991). However, Van Doren et al. did not test the ability of Hairy to interfere with T4/Da heterodimers. The interaction observed between Hairy and T4 implies that Hairy could sequester T4, to repress transcription in the same manner as Emc. This mechanism was proposed to explain how ectopic Hairy expression can interfere with sex determination (Parkhurst et al., 1990). The rat Hairy homologue HES1, has been reported to effect transcriptional repression by sequestering the E47 bHLH protein in cultured cells (Sasai et al., 1992). At the moment it is not possible to say whether the Hairy-T4 interactions are biologically significant.

Although Gro is a not a bHLH protein, Hairy physically interacts with Gro in yeast and *in vitro*. There is evidence that non-bHLH proteins interact

with bHLH proteins. MyoD and the leucine zipper protein jun interact, but the interactions depend on MyoD's bHLH domain (Bengal et al., 1992). The Gro interaction is reliant on the carboxy-terminus WRPW motif, but not an intact HLH domain. Recent experiments suggest that Gro-Hairy interactions are biologically significant and that Gro is required for transcriptional repression *in vivo* (Paroush et al., submitted).

2.6 Conclusion

The results I have obtained and other experiments favour a model in which Hairy homodimerises and binds DNA. Hairy can also interact with the AS-C T4 protein, and may sequester it in inactive heterodimers. Hairy does not interact with T5 or Da, suggesting that Hairy does not antagonise the formation of T5-Da heterodimers, and must repress transcription in another way. It could do this by binding to the T5 promoter and directly repressing transcription. PCR based *in vitro* selections can be used to define Hairy DNA binding sites, and the promoters of target genes examined for the occurrence of such sites. Mutating candidate sites *in vivo* using transgenes and checking for phenotypic effects would show that Hairy acts through the putative sites. Finally, Hairy is capable of interacting with non-bHLH proteins; these proteins may be required for Hairy to effect repression of transcription (Paroush et al., submitted).

Chapter 3. Genetic screens for zygotic lethal loci with maternal effects

3.1 Introduction

The original aim of my thesis research was to identify novel genes required during segmentation, particularly genes required for pair-rule gene function. Such genes are likely to be maternally expressed and reused several times during development, and so will be zygotic recessive lethal mutations (chapter 1). The development of the DFS-FLP system has greatly facilitated the generation of germline clones, making screening of zygotic recessive lethal mutations for maternal effects more straightforward than before.

During the period of my DPhil research, X chromosome stocks for using DFS-FLP to generate germline mosaics became available (Chou and Perrimon, 1992), whereas stocks for generating autosomal germline clones are not yet available. Although the X chromosome had been previously screened for zygotic lethals with maternal effects (Perrimon et al., 1989), I decided to generate X-linked lethal mutations and screen them for maternal effects using the FLP-DFS system. Although the previous screen had an estimated level of 86% saturation, it was quite possible that further loci were missed in addition to the estimated 14% unscreened loci,.

A screen carried out by Tricoire had indicated that a maternal effect locus in 10E1-10F3 showed genetic interactions with *h* (Tricoire, 1988), suggesting that there would be at least one locus which might display a *h* like segmentation phenotype, as well as others with gap gene phenotypes. Like *gro*, such loci could have multiple roles in development, or even be housekeeping genes. An example is two mutations mapping to RNA polymerase which are known to show dominant maternal interactions with segmentation genes (Parkhurst and Ish-Horowicz, 1991; Mortin et al., 1992). Although I wanted to avoid mutations with global rather than

specific effects on patterning, it was not feasible to introduce a genetic bias into the screen favouring recovery of mutations involved in segmentation.

3.2 Generation of zygotic recessive lethal mutations

The genetic screen carried out was divided into two parts (figure 3.1). The first was generation of X-linked recessive zygotic lethals. The second part was to screen the recessive lethal mutations for maternal effects using the DFS-FLP system, whilst maintaining stocks to recover mutations of interest.

Two different mutagens were utilised, ethyl methanesulfonate (EMS) and diepoxy butane (DEB). EMS preferentially induces point mutations, whereas DEB causes a significant number of chromosomal aberrations and small deletions (Ashburner, 1989). In this respect, DEB is similar to X-rays which preferentially generate deletions and chromosomal abnormalities, making subsequent cloning of genes simpler.

Males carrying a marked X chromosome with a target site for the FLP recombinase inserted at 14A-B (FRT^{101}) were mutagenised and mated to *runt*/FM3 females. Neither the *runt* nor the FM3 balancer chromosome are hemizygous viable, so no F1 males are recovered. FRT^{101}/FM3 females were selected and mated individually to FM7 males. In the F2, the absence of males in a tube indicated that a zygotic lethal mutation had been induced on the mutagenised FRT^{101} X chromosome (designated in bold script: $\mathbf{FRT^{101}}$). These stocks were analysed further (section 3.3).

A trial screen in which male flies were fed 0.025M EMS yielded X-linked zygotic lethals at a rate of 46%, higher than the standard 30% rate for this dosage (table 3.1). 380 lethals were recovered making it unnecessary to perform a large scale EMS screen. A trial screen for DEB yielded a 10.5% rate of X-linked zygotic lethals at 5mM DEB. Although using higher

concentrations of mutagen increased the proportion of zygotic lethal mutations recovered, the number of sterile tubes increased too. For example, at a concentration of 25mM DEB, a third of the tubes with F1 progeny had induced lethals, but the number of tubes not showing F1 progeny was 88% (table 3.1).

For a large scale screen, male flies were fed DEB at concentrations of 2.5mM, 5mM and 10mM, compromising between a significant mutation rate and an acceptable level of sterile tubes. X-linked zygotic recessive lethal mutations were induced at rates of 6.5%, 7.8% and 13% respectively (table 3.1), in agreement with the results of the trial DEB screen. A total of 3859 individual matings were established and screened.

A total of 696 lines carrying X-linked zygotic lethals were recovered from all the screens, of which 380 were induced by EMS, and 316 were produced by DEB mutagenesis. Stocks were established by mating the **FRT^{101}**/FM7 virgin females to FM7 balancer males. I screened 193 of the EMS induced, and 165 of the DEB induced X-linked lethal lines for maternal effects on patterning. The remaining stocks were screened by S. Pinchin.

3.3 Generation of germline mosaics

To generate germline mosaics, **FRT^{101}**/FM7 females were mated to *ovo^{D1}* FRT^{101}/Y; F38/F38 males. The males carry the dominant female sterile mutation (DFS), *ovo^{D1}*, on an X chromosome with an integrated FRT^{101} site; the second chromosome is homozygous for a heat shock inducible FLP recombinase. The female F1 progeny can only lay eggs if a mitotic recombination event occurs in their germline (chapter 1).

The parents were allowed to lay eggs for 48h, and after a further 48h of ageing, the expression of the FLP recombinase was induced in the F1 larvae by heat shocking for 4h at 37°C. F1 adult **FRT^{101}**/*ovo^{D1}* FRT^{101}; F38/+ females were mated to males in blocks of test tubes on apple juice agar

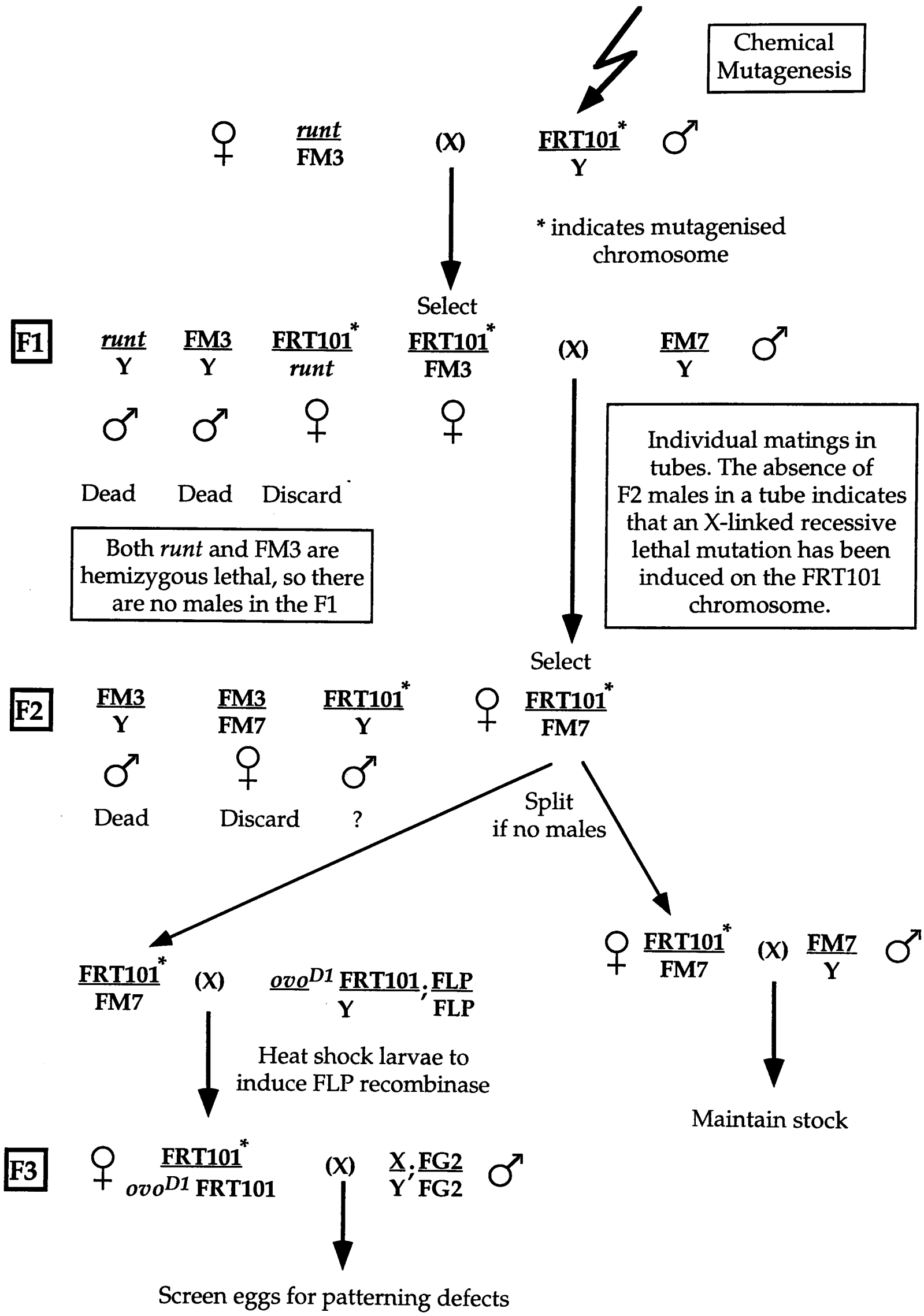

FIGURE 3.1 FLP recombinase based germline clone screen

A. Trial EMS screen

[EMS]	Lethal	Viable	Sterile	Frequency
0.025mM	380	446	nr.	46%

B. Trial DEB screen: 411 individual matings

[DEB]	Lethal	Viable	Sterile	Frequency
25mM	4	8	88	33%
5mM	16	135	3	10.5%
2.5mM	11	129	17	8%

C. Large scale DEB screen: 3859 individual matings

[DEB]	Lethal	Viable	Sterile	Frequency
10mM	113	758	139	13%
5mM	88	1040	136	7.8%
2.5mM	84	1350	151	6.5%

Table 3.1: Frequencies of sex linked recessive lethal mutations induced

The tables illustrate the frequencies at which X-linked zygotic recessive lethal mutations were induced by different concentrations of the chemical mutagens EMS (A.) and DEB (B., C.). The numbers represent the number of individual matings scored; absence of male F1 progeny indicated that a zygotic lethal had been induced (figure 4.1). Sterile tubes, in which no F1 progeny emerged, are not included in the frequencies of lethal mutations. The proportion of sterile tubes generally increased with increasing concentration of mutagen, eg. 25mM DEB. nr., not recorded.

plates. The apple juice plates were changed every 24 hours. Five egg lays (plates) per line were scored in total. After 24h ageing, the plates were examined for the presence of eggs. If eggs were present, the number that hatched, or failed to do so was noted. Unhatched eggs were further scored for fertilisation. Embryos which develop but fail to hatch turn a brown colour due to phenol oxidase enzymes in the gut being released. Abnormal egg morphology was also noted.

The lethal lines were classified according to the frequency of unhatched fertilised eggs (table 3.2). If a lethal mutation had a maternal effect, then no embryos hatched (or <10%) and the eggs went brown except for unfertilised eggs. The presence of a wild type copy of the recessive lethal mutation on the father's X chromosome could also be sufficient to rescue the maternal effect, and in this case, 50% of the fertilised eggs would hatch (figure 3.2A). However, this class was indistinguishable from lethal mutations with no maternal effect, so a further cross was necessary (figure 3.2B). Failure to lay any eggs indicated that the gene's function was required in the female germline. Some females laid eggs that were visibly abnormal, indicating a requirement for the gene product during oogenesis. The proportions of each of the classes are shown in table 3.2.

Unhatched, brown eggs were prepared for cuticle examination under dark field microscopy. The morphological landmarks used to classify cuticular phenotypes are shown in figure 1.5. Any disruption to segmentation leads to a disruption in the pattern of the denticle (bristle) belts secreted by the larval epidermis. In cases where there was a large reduction in the amount of cuticle secreted or gross alterations to the cuticle, segmentation defects could be masked. The males used as the fathers in the cross, FG2 males, contain a lacZ enhancer trap inserted at the *fushi tarazu (ftz)* pair-rule gene, so that lacZ is expressed in 7 stripes. This allows examination of the

A.

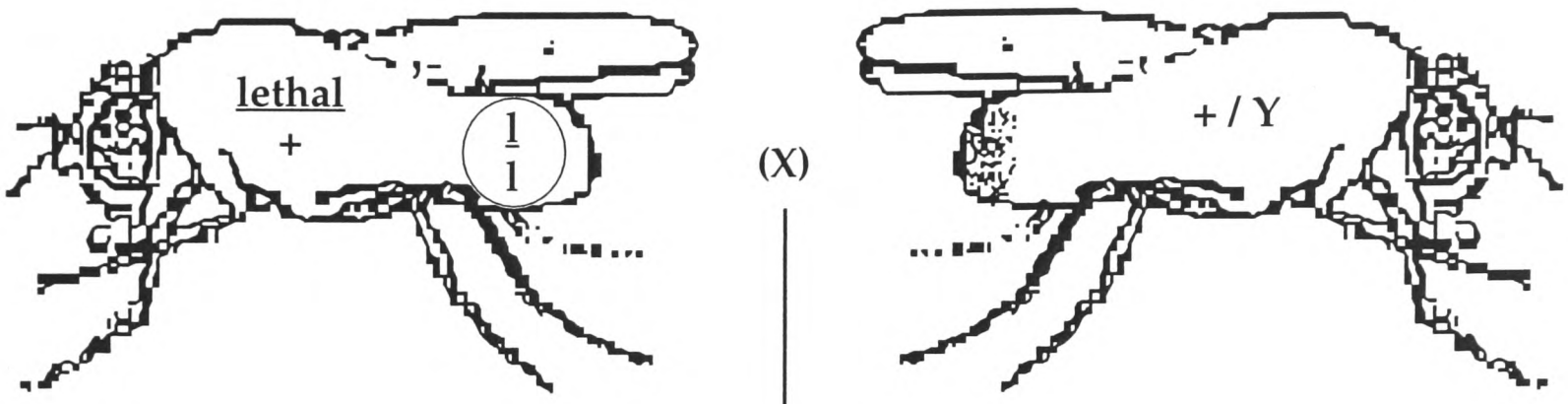

Female heterozygous for a recessive lethal mutation, with a germline clone homozygous for the lethal mutation

Wild Type Male

F1 ♀ $\frac{\text{lethal}}{+}$ $\frac{\text{lethal}}{\text{Y}}$ ♂

B.

$\frac{\text{lethal}}{+}$ (X) $\frac{\pm}{\text{Y}}$

$\frac{\text{lethal}}{+}$	$\frac{\pm}{+}$	$\frac{\pm}{\text{Y}}$	$\frac{\text{lethal}}{\text{Y}}$

Figure 3.2 The genetics of maternal effect and zygotic mutations

A. The genotypes of the progeny of a female with germline clones homozygous for a zygotic lethal mutation are shown. If the lethal mutation has a strict maternal effect, neither male nor female progeny are viable. If transcription of the wild type copy of the lethal mutation on the paternally derived X chromosome can rescue the maternal effect, female progeny are viable. Distinguishing between a zygotic lethal with no maternal effect and a rescuable maternal effect is not possible with this cross shown, and requires a second cross: **B.** As the female is heterozygous for the lethal, there is no maternal effect, so hemizygous males display only the zygotic phenotype of the lethal. There is a maternal effect if this phenotype is different from that seen in the male progeny of cross A.

Phenotypes	EMS	DEB
Total number of lines	193	165
Germline lethal	45.5%	33%
Abnormal oogenesis	6%	8%
Maternal effect	13%	21%
Maternal effect rescuable	16%	24%
No maternal effect	19.5%	13%

Table 3.2 Phenotypes of germline clones of X-linked lethals

The germline clone phenotypes of the lethal lines generated by the EMS (193 lines) and DEB (165 lines) screens are expressed as percentages of the total number of lines examined. The phenotypic classifications were defined as follows:

Germline lethal: females failed to lay any eggs.

Abnormal oogenesis: eggs with abnormal morphology; this class also includes flies which laid a large number of eggs, none of which went brown. Either they were unfertilised or they failed to develop normally either due to abnormal oogenesis or halted development prior to gut formation (the gut produces phenol oxidases which turn unhatched developed embryos brown).

Maternal effect: <10% of fertilised eggs hatched.

Maternal effect rescuable: approximately 50% of fertilised eggs hatched, the maternal effect being rescued by a paternally supplied wild type copy of the lethal. This class needs further testing to distinguish true maternal effects from zygotic lethals (see figure 3.2).

No maternal effect: >80% of the eggs hatched.

ftz expression pattern for by X-gal staining, to reveal segmentation defects. None of the embryos examined by X-gal staining revealed *ftz* expression abnormalities. Lines with no cuticular defects or a high degree of phenotypic variability were discarded.

In addition, a collection of 35 X-linked lethals showing cuticular phenotypes was sent from the Perrimon laboratory, which was conducting a similar screen of the X chromosome at the same time. Females carrying germline clones of these mutations were generated and their progeny screened for segmentation defects. The phenotypes of all the mutations which underwent further analysis are described in the next section.

3.4 Phenotypes of mutations with maternal effects

Stocks which had not been discarded in the first round of screening were analysed further in two ways: (i) the zygotic component of the lethality was examined and compared to the maternal effect to establish that the observed maternal effect was an independent phenotype (figure 3.2b), and (ii) the maternal effect phenotypes were re-examined. Twelve X-linked lethal bearing stocks were kept for further analysis (phenotypes summarised in table 3.4). All other lines were discarded. The positions of these twelve lethal mutations on the X chromosome were investigated using a collection of chromosomal duplications (figure 3.3 and table 3.3). Seven mutations were successfully mapped using the duplications and the positions are given below and in table 3.4. The other mutations were either not covered by the duplications or had more than one lethal mutation and so could not be rescued by a single duplication.

The maternal effect phenotypes of each line are described below, using the cuticular anatomical landmarks shown in figure 1.5. The following is a rough guide to how the maternal effect mutations are classified. There are four maternal co-ordinate systems (as described in Chapter 1), mutations in

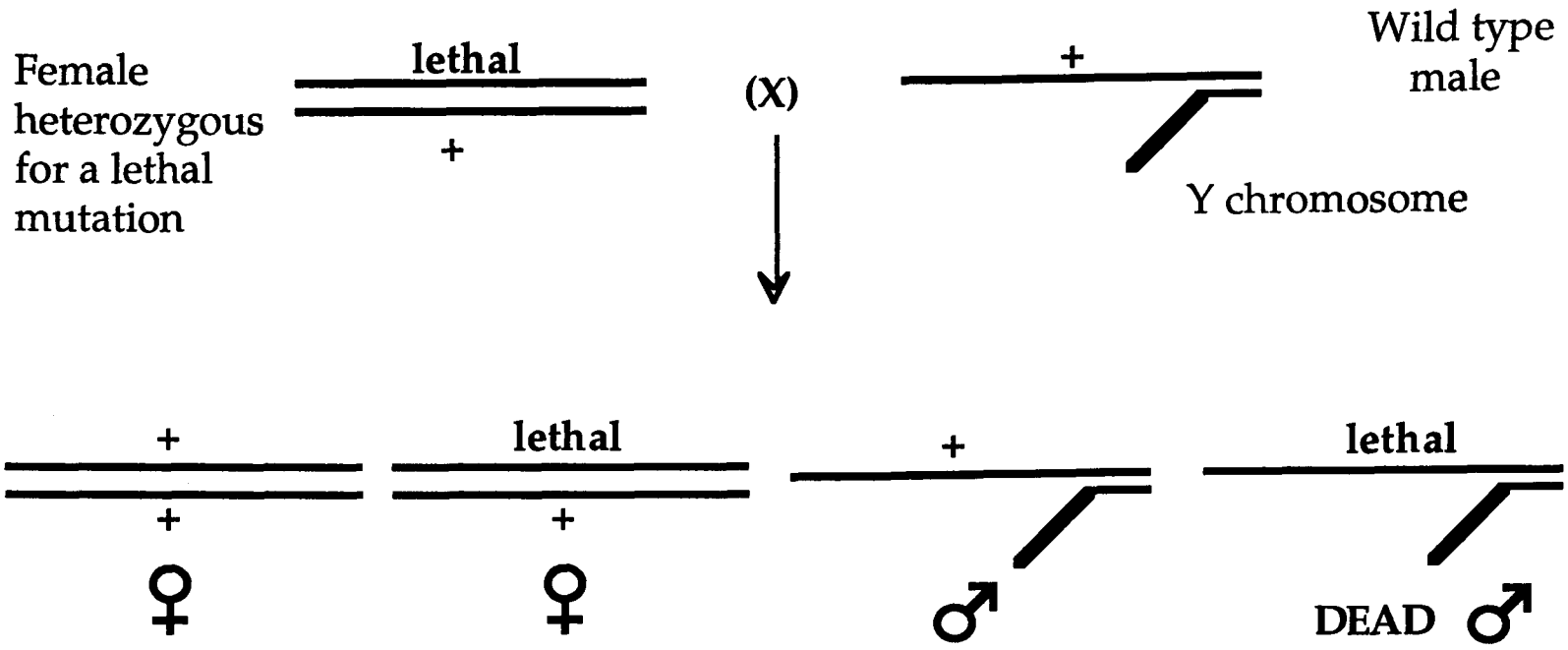

Inheritance of X and Y chromosomes in a mating between a wild type male and a female heterozygous for an X-linked recessive lethal mutation. Only one class of male is seen because half the male progeny inherit the lethal mutation and die.

If the male's Y chromosome (or autosome) carries a small portion of the X chromosome, (a duplication) including a wild type copy of the lethal mutations, then that class of male will now be found in the progeny.

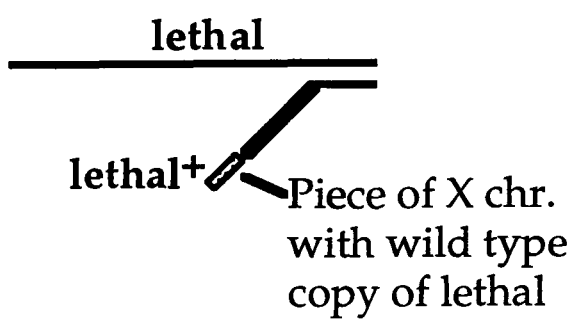

Figure 3.3 Principle of mapping with duplications

The figure illustrates how a male carrying a recessive lethal mutation can survive because of a small duplication of the X chromosome on the Y chromosome (or one of the autosomes). Mutations can be mapped by mating heterozygous females to a collection of known duplications to see which duplications allow males to survive. Table 4.4 lists the duplications used to map lethal mutations obtained in the FLP screen.

Genotype of duplication stock	Extent	Origin
Df(1)svr, spl ras^{2} fw/Dp(1;Y) y^{2}Y67g/C(1)DX, y f	1A-2B	#901
Df(1)w258-45, y/Y; Dp(1;3)w^{vco}	2B-3C	#1527
Df(1)A113/C(1)DX, y w f; Dp(1;2)w^{+64b}/+	3C-5A	#940
Df(1)ct4B1, oc ptg; Dp(1;3)ct^{J8}/Ubx; C(1)DX y w f	4D-7B	#3209
Df(1)ct-J4, In(1)dl-49, f/C(1)DX, y w f; Dp(1;3)sn^{65b}/Ki	6C-7C	#948
Df(1)C128/C(1)DX, y f; Dp(1;2)sn^{+72d}/bw^{D}	7A-8A	#2984
y lz$^{89d18-15}$ f/Dp(1;Y)lz	8D-9A	#3610
Df(1)v-L15, y/C(1)DX, y w f; Dp(1;2)v^{+}75d/+	9A-10C	#929
Df(1)GA112/Dp(1;Y)B^{s}v^{+}y^{+}Y/FM7	9F-10E	#3559
Df(1)v-L3/C(1)DX, y w f; Dp(1;2)v^{+}63i/+	9E-10A	#903
Df(1)KA7/C(1)DX, y w f; Dp(1;2)v^{65b}/+	10A-11A	#957
Df(1)D15, v f/C(1)DX, y f; Dp(1;4)r^{+}/+	13F-16A	#906
In(1)dl-49, y^{2} sc we^{1}/Dp(1;Y)B^{s}Y	16A-20F	#2495

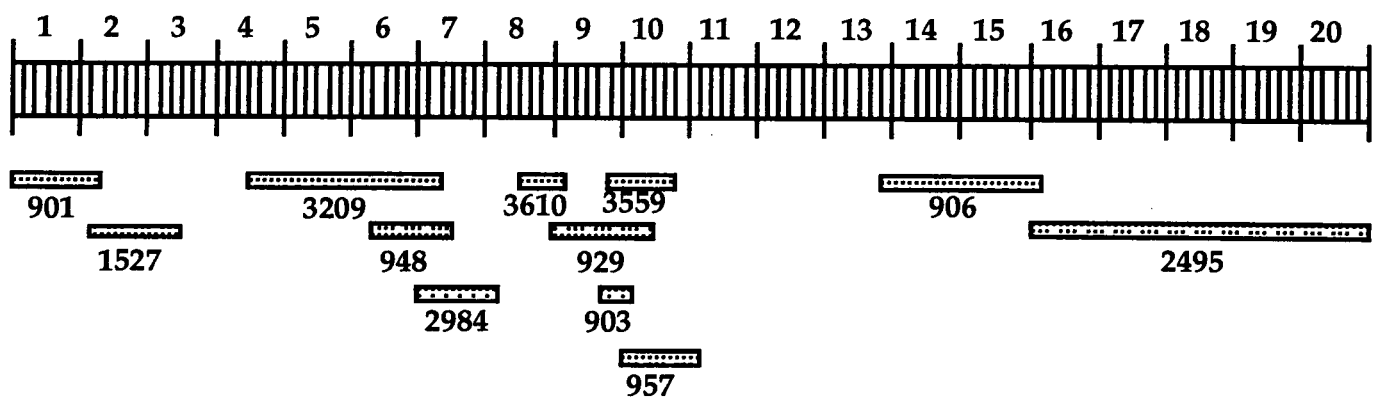

Table 3.3 Duplications used for mapping the lethal mutations

The genotype of each of the duplications used to localise the lethal mutations is shown in the left hand column; the cytologically defined extent of each duplication is shown in the middle column; all duplications were obtained from the Bloomington stock centre and the stock numbers are listed in the right hand column. The regions of the X chromosome covered by the duplications are illustrated diagrammatically below the table.

which lead to defects in the regions of the embryo patterned by the system. If the anterior system is affected, the normal structure of the head is disrupted, including the jaws, the thoracic denticle belts and some of the abdominal denticle belts. Mutations in the posterior system lead to disruptions of the posterior structures such as the abdominal denticle belts, and the filzkörper, anal plate and telson. Alterations to the terminal system disrupt the head structure, and the filzkörper, telson, anal plate and abdominal denticle belts A7/A8. Mutations in the dorsoventral system to increased width of the ventral denticle belts (ventralised) or the belts of dorsal hairs (dorsalised). If the activities of the gap and pair-rule genes are changed, then the pattern of the thoracic and abdominal denticle belts can be altered, as well as the head structure (there are at least three head segments, but they are involuted and not visible in cuticle preparations or figure 1.5). Pictures of the mutant cuticles which accompany the descriptions are shown in figure 3.4.

3.5 Strict maternal effect lethal mutations

T60

The maternal effect phenotype of T60 was deletion of the odd numbered abdominal denticle belts (odd-skipped) in a 'classical' pair-rule phenotype (deletion of every other denticle belt). Examination of the zygotic component revealed a phenotype identical to the X-linked pair-rule gene *runt (run)* (see chapter 5). Weak hypomorphic alleles of *run* lead to an odd-skipped pair-rule phenotype, while stronger alleles give rise to an odd-skipped phenotype with pattern duplications within the abdominal denticle belts, altering their shape from trapezoidal and asymmetric to rectangular and symmetrical. The zygotic phenotype displayed such pattern duplications, whereas the maternal effect did not. The difference

was sufficient to justify further analysis which is described in the following chapters.

T188

T188 has a variable but distinctive phenotype of a large ventral hole situated towards the posterior of the larva with necrosis around the edges of the hole. Embryos which lacked the hole show variable segmentation defects. The filzkörper were missing in many cases whereas the jaws were present even in severely affected embryos. The mutation may be in one of the posterior group genes, but it is unusual in consistently giving a ventral hole phenotype, which is not seen in other posterior group mutants. No zygotic embryonic cuticle phenotype is seen. The lethal mutation maps to the region 9E-10A.

P435

P435 displays a fairly consistent cuticle phenotype ranging from fusion of abdominal denticle belts 3 to 7, to complete fusion of all the abdominal denticle belts. These segmentation defects are often accompanied by ventral holes, particularly near the posterior of the embryo. The phenotype suggests that this may be a posterior group mutant. No zygotic segmentation phenotype was seen. The lethal mutation maps to 1A-2B.

P748

The maternal effect phenotype of P748 is variable; most noticeable are segmentation defects leading to pair-rule type phenotypes, both 'classical' and more severe. The manner in which the abdominal denticle belts fuse is reminiscent of weak alleles of the segment polarity gene *engrailed (en)*, which was originally characterised as a pair-rule gene. In addition, there are occasional ventral holes, the jaws are often messed up or missing, and filzkörper are usually present. The zygotic phenotype leads to cuticles with

non-specific defects but wild type with respect to segmentation. The lethal mutation maps to the region 9F-10A.

D140

D140 has a maternal effect leading to ventral holes of various sizes, often edged by necrotic material. It is possibly a posterior group mutation. The lethal mutation maps to the region 9E-9F.

D149

The cuticle of progeny derived from D149 germline clones have a dorsal hole, with necrosis around the edge. The ventral denticle belts are unaffected as are the filzkörper. Although the head is severely affected, jaws are present. It seems likely that this mutation affects the process of dorsal closure, an event which occurs 11-13 hours after egg laying, and involves the migration of epidermal cells dorsally and the seaming of the dorsal midline. Embryos lacking the zygotic component of D149 do not show any cuticular defects. The lethal mutation maps to the region 6C-7A.

3.6 Maternal effect mutations susceptible to paternal rescue

T44

The most consistent phenotype is fusion of all eight abdominal denticle belts to form one large denticle belt. The thoracic denticle belts and terminal structures are unaffected. The phenotype is reminiscent of the gap gene *knirps*, but also resembles a weak posterior group gene. The phenotype is variable: there are often signs of necrosis amongst the ventral denticle belts, and some cuticles have holes without segmentation being affected. The zygotic phenotype of the lethal did not affect segmentation; occasional embryos displayed non-specific cuticle defects.

T62

Mutant embryos display fusions of abdominal denticle belts, with most embryos showing only one or two fusions. Occasionally more severely affected embryos show pair-rule or segment polarity phenotypes. The mutation was tested for allelism with the X chromosome segment polarity mutants *armadillo, dishevelled* and *porcupine,* and all three mutations complement T62. The zygotic phenotype of the lethal is occasional malformation of the jaws, but the number and morphology of the abdominal denticle belts appear to be wild type. The lethal mutation maps to the region 13F-16A.

T69

T69 displays a highly variable phenotype in which denticle belts fuse. Re-examination of the cuticle phenotype suggests that the epidermal cells might be dying because they have exhausted a vital component, rather than there being a patterning defect. The lethal mutation maps to the region 6C-7A.

T160

T160 displays segmentation defects in which the abdominal denticle belts are decreased in number, and the remaining belts increase in size. In addition the anterior of the larva is severely disrupted, the jaws always being absent or deformed. Occasionally, thoracic denticle belts 2 and 3 can be seen. Filzkörper are absent from the posterior in the more severely affected cuticles. It is difficult to classify this phenotype. The T160 lethal mutation was lost from the balanced stock.

D60

One chimeric female laid fourteen eggs of which four failed to hatch and displayed deletion of the even-numbered abdominal denticle belts. Two

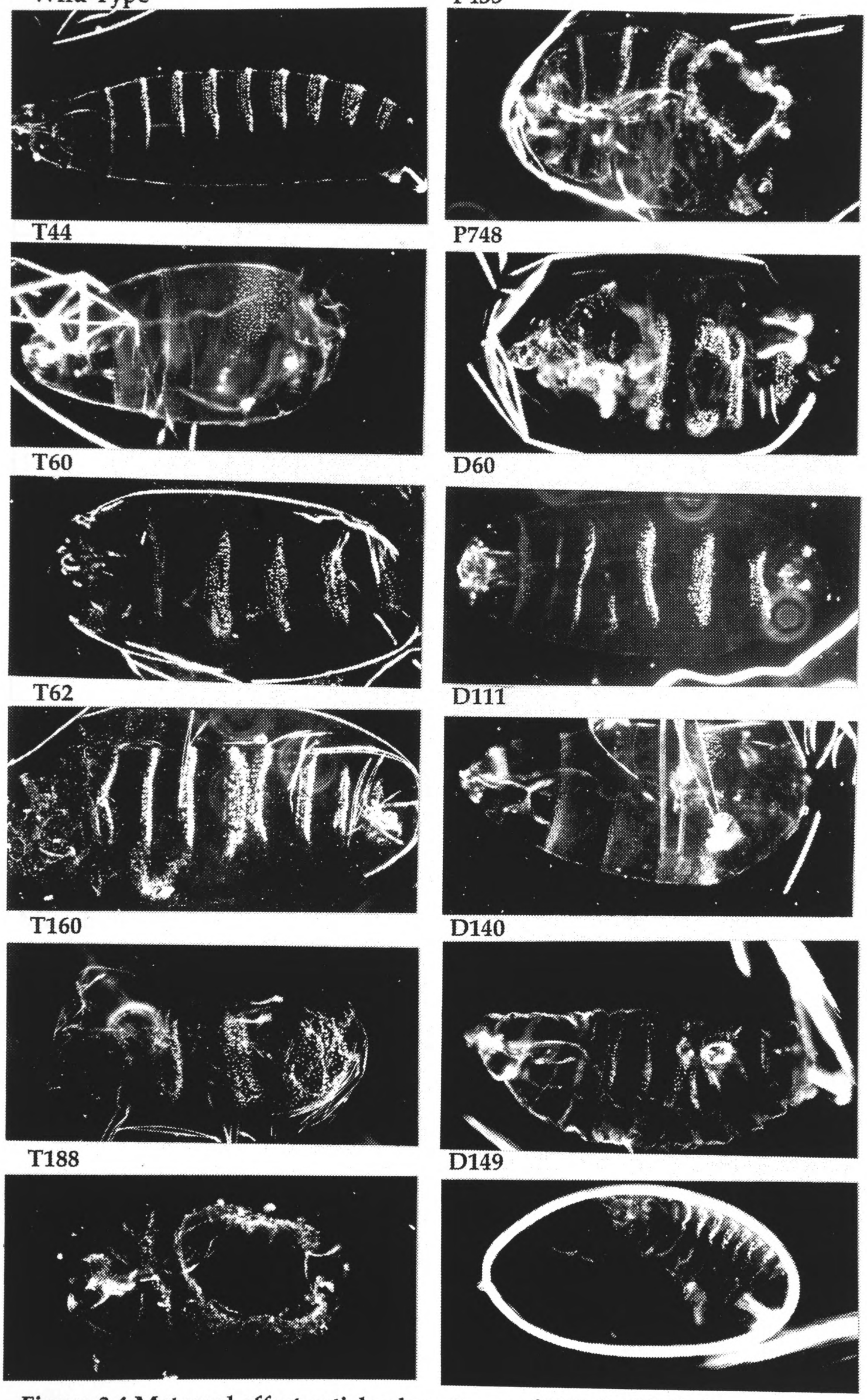

Figure 3.4 Maternal effect cuticle phenotypes of X-linked lethals

LINE	MUT	MAP	ME	CUTICLE PHENOTYPE
T44	EMS	-	P	Posterior group or gap gene phenotype
T60	EMS	13F	M	Odd-skipped pair rule phenotype
T62	EMS	13F-6A	P	Segmentation defects
T69	EMS	6C-7A	P	Segmentation defects
T160	EMS	-	P	Segmentation and terminal defects
T188	EMS	9E-10A	M	Ventral hole
P435	EMS?	1A-2B	M	Segmentation defects
P748	EMS?	9F-10A	M	Segmentation defects
D60	DEB	-	P	Even-skipped pair rule phenotype
D111	DEB	-	P	Segmentation defects: posterior group
D140	DEB	9E-9F	M	Ventral hole
D149	DEB	6C-7A	M	Dorsal open

Table 3.4: Summary of maternal effect phenotypes

Line: the number of the lethal line producing the phenotype; the prefix indicates the origin of the stock: T,D=my screens; P=isolated by T.-B. Chou.

Mut: indicates whether the mutation was induced by EMS or DEB.

Map: position on X chromosome if known.

ME: strict maternal effect (M) or maternal effect rescuable (P)

Cuticle phenotype: summary of cuticular phenotype.

showed a 'classical' pair-rule phenotype, and the other two showed weaker 'even-skipped' phenotypes. Only one other mutant female has laid eggs despite multiple attempts, revealing a requirement for the function of the lethal mutation in the germline. Perrimon et al. showed that *l(1)1P2* has a maternal effect leading to deletion of the even-numbered abdominal segments, and also thoracic segment 3 (T3), but not thoracic segment 1 (T1) (Perrimon et al., 1989). However, T1 is deleted in stronger D60 phenotypes, and D60 appears to map more proximal than *l(1)1P2*. The phenotype of the maternal effect prompted further work, (described in the next chapter) and the mutation was renamed *leprechaun (lep)*. The zygotic phenotype is a strict embryonic lethal and unhatched embryos display wild type segmentation.

D111

The maternal effect phenotype of D111 is segmentation defects in the abdomen, in a manner reminiscent of T44, although probably less severe. D111 could either be a member of the posterior group genes or the gap genes.

3.7 Summary of germline clone screen

EMS and DEB mutagenesis generated 358 X-linked recessive zygotic lethal mutations which were examined for maternal effects on the larval cuticle. Twelve were retained for further study. Two lines, T60 and D60 (*leprechaun*), had maternal effects leading to pair-rule mutant phenotypes, the class in which I was most interested. I decided to concentrate my subsequent research on investigating these two mutations.

Three other lines, P748, T69 and T62, have maternal effects on segmentation. P748 has a fairly consistent phenotype which resembles that of a pair-rule mutation. In contrast, T62 and T69 lead to segmentation defects which are probably non-specific: neither mutation seemed to give

rise to a consistent phenotype. Five mutations had maternal effects which can be loosely classified as falling into the posterior group of mutations. T188, P435 and D140 all give rise to holes in the ventral cuticle; T188 and P435 often showed abdominal segmentation defects, especially in embryos lacking the ventral holes. T44 and D111 give rise to abdominal segmentation defects similar to the gap gene knirps. One mutation, D149 has a very consistent phenotype of a large hole on the dorsal surface of the cuticle, and is probably defective in dorsal closure. Finally, the maternal effect of T160 could not be classified in any of the conventional groupings by its cuticular phenotype.

The principle reason for undertaking the screen was to recover mutations of the pair-rule class. Two, possibly three, X-linked lethal mutations gave rise to pair-rule phenotypes, despite it being a relatively small scale screen (393 lethals screened for maternal effects). These mutations were not picked up in the larger scale screens of Perrimon et al, and Chou and Perrimon (Perrimon et al., 1989; Chou and Perrimon, 1992). This could be due to the fact that more time was spent scrutinising the phenotypes. The phenotype of P748 is highly variable, so it would probably be discarded in a large scale screen. Further studies of T60 revealed that it probably does not have a segmentation phenotype (Chapter 6). *lep* exemplifies a class of genes that are not easily recovered, those that are required for germline development as well as early embryogenesis. In my screen one female was fertile, and laid only a small number of eggs. Many similar mutations could have been missed in the larger screens. It is not possible to say how many more genes affecting segmentation lie on the X chromosome. As the X chromosome only constitutes about 20% of the genome, the autosomes provide scope for identification of maternal effect mutations with pair-rule phenotypes. As the gap and pair-rule genes are all transcription factors, the molecular identity of novel autosomal maternal effect genes can be

guessed. However, the discovery that the segmentation gene *l(1)hopscotch* encodes a tyrosine kinase, indicates that there could be many surprises.

Chapter 4. The genetics of the *leprechaun* mutation

4.1 Introduction

Two zygotic lethal mutations with maternal effects leading to pair rule phenotypes were recovered from the germline clone screen. This chapter examines the genetics of the zygotic lethal D60, which was renamed *leprechaun (lep)*. The maternal effect phenotype of *lep* is the deletion of even-numbered abdominal denticle belts in a 'classical' pair rule phenotype (figure 4.1). The first and third thoracic denticle belts are also missing in more severely affected cuticles. As I was particularly interested in maternal pair rule genes, I examined *lep* more closely.

lep appears to affect germline development in addition to segmentation, making the recovery of chimeric females with germline clones which are able to lay eggs very difficult. This prevented further analysis of the segmentation phenotype. The *lep* mutation was induced by DEB, a mutagen which preferentially induces small deletions. Therefore, the *lep* mutation could be a null allele, or cover more than one locus. Hypomorphic alleles might permit germline development and allow analysis of the segmentation phenotype. To generate further alleles of *lep* requires a duplication which rescues the *lep* lethality in males, otherwise genetic crosses and analysis are not possible. To identify a rescuing duplication, I mapped *lep* by meiotic recombination.

4.2 Mapping the *leprechaun* mutation

The FRT element used in the screen was inserted at 14A-B. Therefore, any zygotic lethal mutations with maternal effects must therefore lie distal to 14A-B, as only the part of the chromosome distal to the FRT is homozygosed during mitotic recombination (see chapter 1.11). The zygotic lethal component of *lep* was not rescued by any of the duplications used to map the location of lethals isolated in the screen (see table 3.3). Therefore,

Wild type

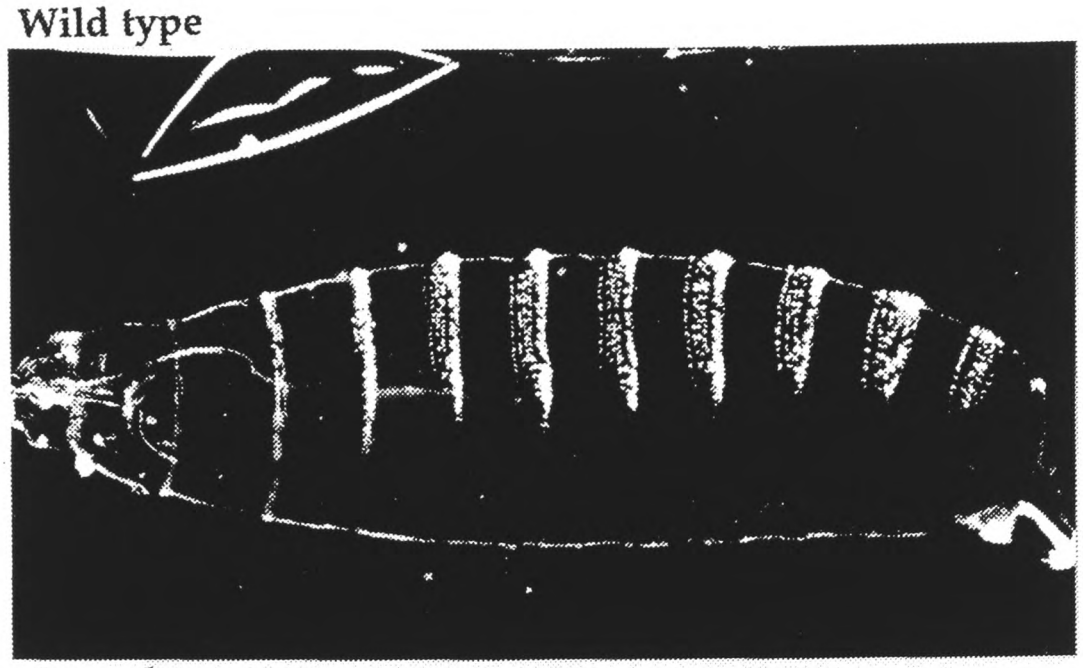

leprechaun

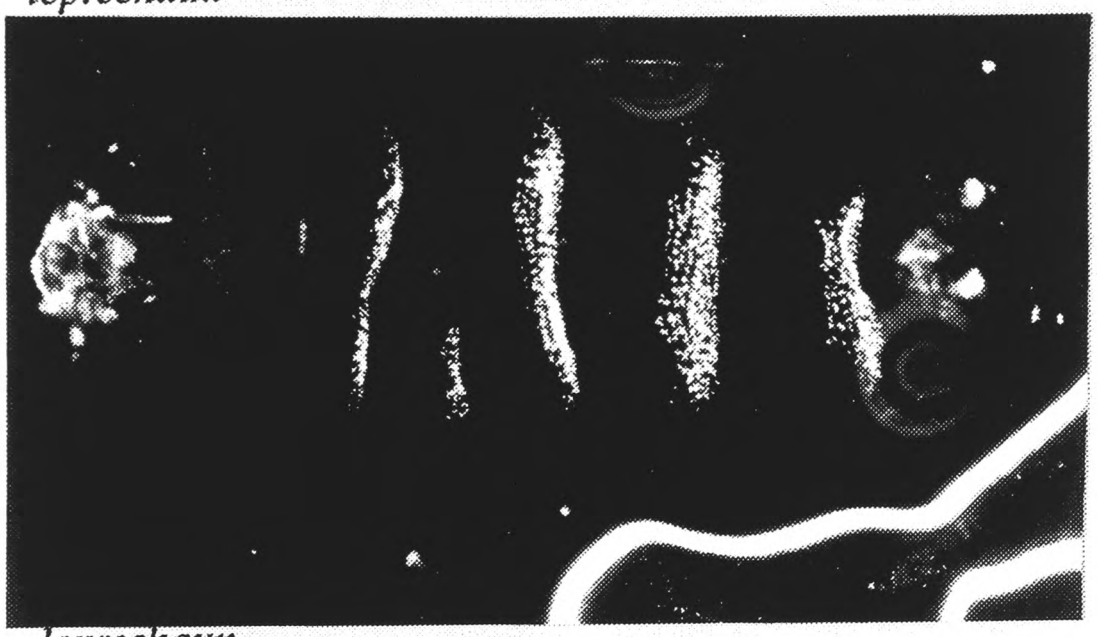

leprechaun

Figure 4.1 The *leprechaun* maternal effect cuticle phenotype
A wild type cuticle is shown at the top; below are two examples of the *leprechaun* maternal effect phenotype. In each case the even numbered abdominal denticle belts are missing.

lep is either located in a region not covered by the duplications used, or it is a double mutant, not rescuable by a single duplication. An alternative mapping procedure had to be employed to map the location of *lep*.

The multiply marked chromosome *sc cv ct v g f* was used to map the *lep* zygotic lethal mutation by meiotic recombination. Male progeny from *lep/sc cv ct v g f* mothers were scored for the presence of phenotypic markers. The results are shown in table 4.1 and indicate that *lep* lies between the markers *ct* (7B) and *f* (15F). The lep bearing chromosome is mutant for *white (w)*, a gene responsible for pigment distribution in the eye, so the eye colour markers *v* and *g* cannot be scored in all progeny. However, some males had acquired the w^+ gene by recombination and examination showed they were all *g*. This suggested that *lep* must be close to *g* (12B), in the cytological region 11A-14B. Of this region only 13F-14B was covered by the duplications used.

Another multiply marked chromosome *m wy sd* os^s was also used for mapping *lep* as the markers *m*, *wy* and *sd* all lie close to the predicted location of *lep* in 12B-13F. The results obtained with the *m wy sd* os^s chromosome confirmed the predicted location of *lep*, and suggested that *lep* is closer to *wy* at 11E than to *sd* at 13F as both of the recombinants between *wy* and *sd* were *wy* sd^+ (table 4.2).

The genetic position of a locus describes its position on the chromosome in units of percent recombination between the locus and other loci. The genetic distances between the markers used for the mapping crosses were calculated, based on the frequencies of observed recombination between each pair of markers. The recombination frequencies obtained were compared to the expected frequencies. The values for *sc-cv* and *cv-ct* correlated well with what was expected, but there was a decrease in recombination between *ct-f*. For the *m wy sd* os^s chromosome, there was a

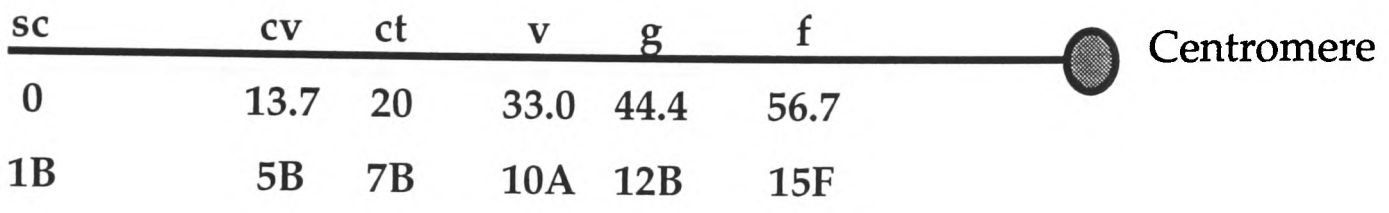

Multiply marked chromosome

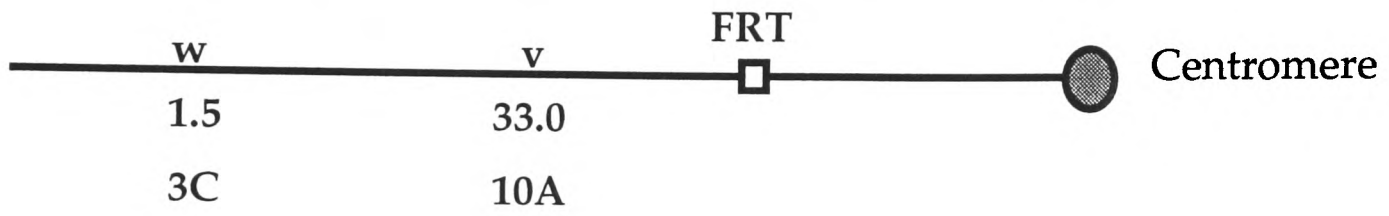

leprechaun chromosome

Genotypes				# Males
sc	+	+	+	0
sc	cv	+	+	0
sc	cv	ct	+	16
sc	cv	ct	f	228
+	cv	ct	f	43
+	+	ct	f	23
+	+	+	f	23
+	+	+	+	18

Table 4.1 Results of mapping *lep* with the *sc cv ct f* chromosome

The markers on the chromsomes used are shown at the top with the map and cytological positions of the markers. The table lists the number of male progeny of each genotypes scored from *lep/sc cv ct v g f* mothers. The *v* and *g* eye colour markers were not scored as the lep FRT chromosome has the *white (w)* mutation which prevents their accurate scoring. However, *sc* is linked to *w*, so all *sc* flies could be scored and found to show the *g* phenotype. The data indicates that *lep* lies between *ct* and *f*, closely linked to *g*.

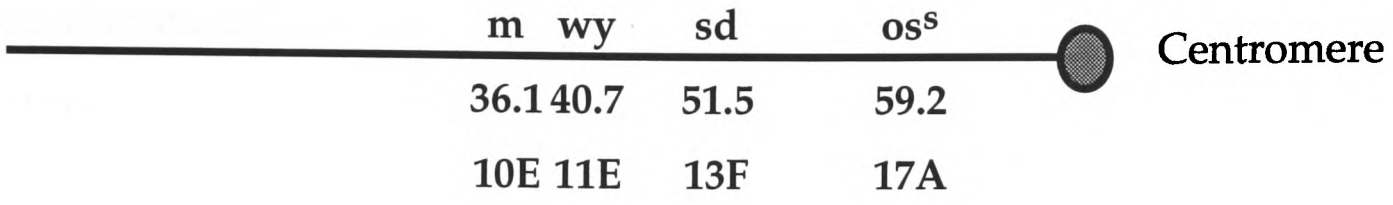

Genotypes				# Males
m	+	+	+	0
m	wy	+	+	2
m	wy	sd	+	11
m	wy	sd	os^s	801
+	wy	sd	os^s	0
+	+	sd	os^s	0
+	+	+	os^s	0
m	wy	sd	os^s	106 white

Table 4.2 Results of mapping *lep* with the *m wy sd* os^s chromosome

The multiply marked chromosome used is shown at the top with the map and cytological positions of the markers. The table lists the number of male progeny of each genotype scored from *lep/m wy sd* os^s mothers. The marker os^s was difficult to score, and so there may some inaccuracy based on this in the scoring. The bottom row of the table are flies that showed all the markers, but also had white eyes, implying that there had been a recombination event with the *lep* chromosome distal to the *m* marker. The results confirm the previous mapping of *lep* to the cytological region 12-13. In addition, the two recombination events (*m wy*) suggest that *lep* is closer to *wy* than it is to the *sd* marker.

decrease in recombination between all the markers. The decrease in recombination in the region 10E-17A could be due to experimental error through infamiliarity with the markers, or insufficient progeny examined to yield a better correlation. It is also possible that an inversion or a similar event occurred on the *lep* chromosome causing the depression in recombination. The *lep* chromosome has not been examined cytologically.

Database searches for duplications covering regions of the X chromosome uncovered two related duplications: *Dp(1;f)LJ8* and *Dp(1;f)LJ9* (both covering approximately 12A10-13A2) (Hardy et al., 1984). Neither rescued the *lep* zygotic lethality, implying that if *lep* is proximal of *g* at 12B, *lep* must lie in the region 13A-13F. If *lep* is distal of *g*, it must lie in the region 11A-12A.

4.3 A genetic screen for *leprechaun* duplications

As no *lep*$^+$ duplication had been found, I attempted to generate duplications *de novo*. The approach chosen was to attempt to produce a 'free' duplication by irradiating an X-Y translocation (Brosseau et al., 1961).

X-Y translocations were chosen as the starting material for a genetic screen for *lep* duplications as this allows one end of the desired duplication to be defined. I chose translocations with breakpoints in the cytological regions 12F, 13B and 13C-D as this is where *lep* appeared to map. The structures of the translocations are shown in figure 4.2.

Individual translocation arms are lethal due to gross aneuploidy, and males hyperploid for part of the X chromosome only occur at low frequencies. However, a large interstitial deletion in one half of an X-Y translocation would generate a free duplication that is viable in males carrying an intact X chromosome (figure 4.3). Such a free duplication would carry a wild type copy of *lep*, and so allow *lep* males to survive. A

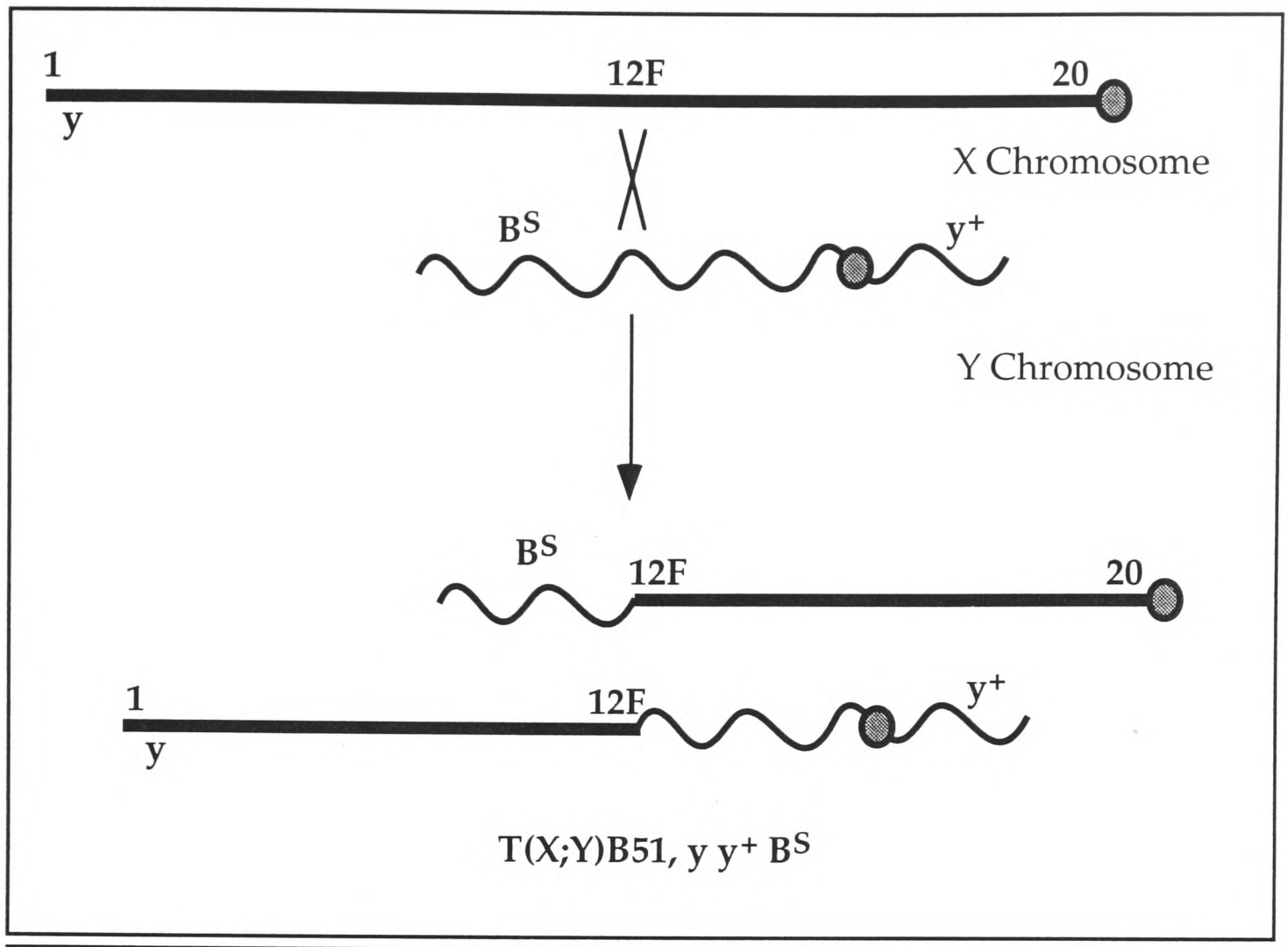

Figure 4.2 Structures of translocations used to generate duplications

The top panel illustrates an illegitimate recombination event between an X and Y chromosome which produces the two halves of an X-Y translocation. Each half is identified by dominant markers, y^+ or B^S. The bottom panels show the two other translocations used in a screen for duplications to rescue *lep*.

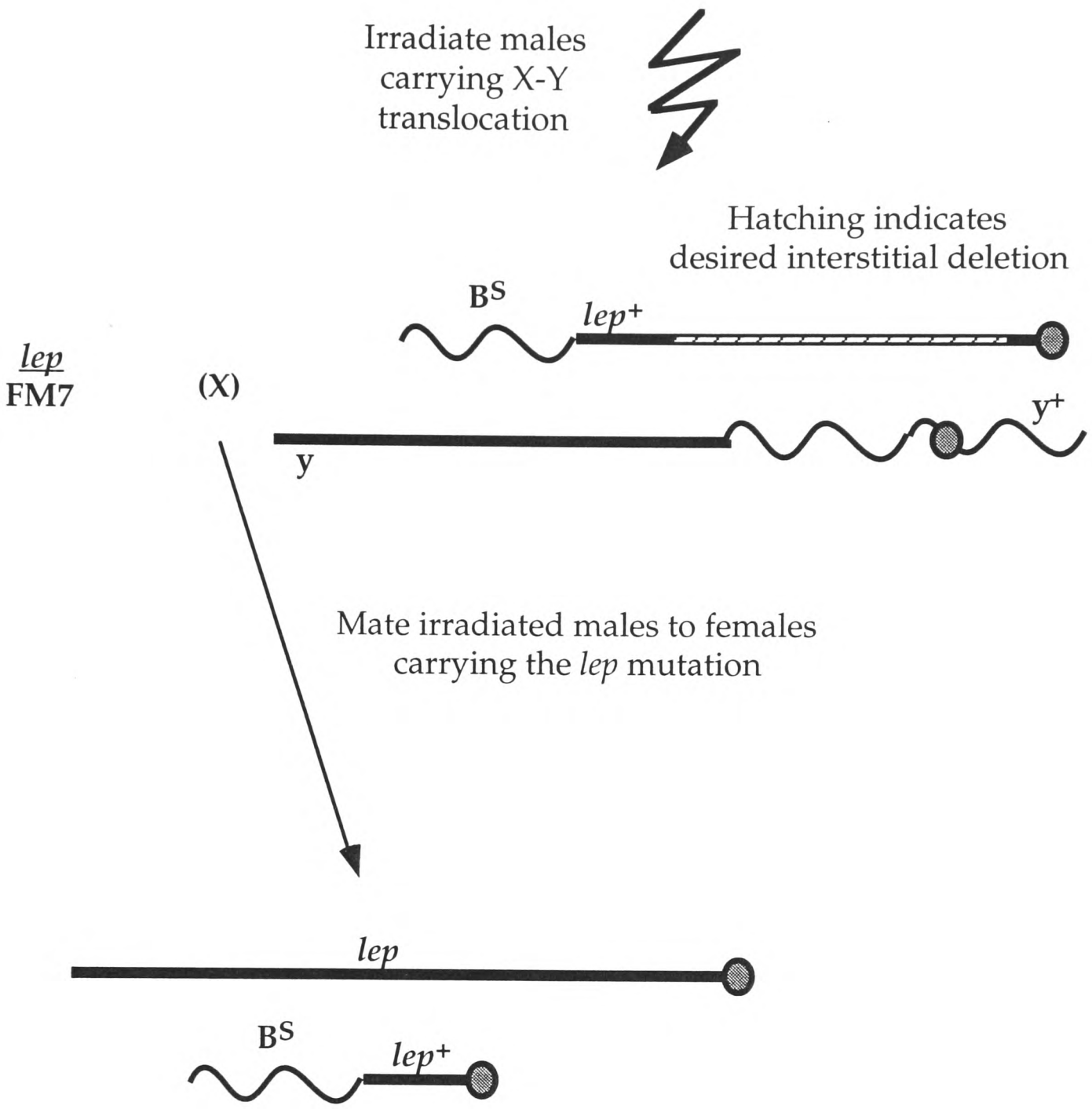

If there is an X-ray induced large interstitial deletion of X chromosome material, then males carrying the *lep* mutation and the free duplication can survive. In the example shown, the proximal half of the T(X;Y) has lost most of the X chromosomal material, leaving behind a small region carrying a wild type copy of *lep*. Markers can be used to identify the origin of the duplication, eg. B^S.

Figure 4.3 Experimental design for first duplication screen

The diagram illustrates how irradiation of T(X;Y) males should produce a large interstitial deletion (hatched pattern); the resulting free duplication rescues *lep*.

breeding scheme was designed in which surviving *lep* males are rapidly identified amongst the other progeny (figure 4.4).

The *Drosophila* Y chromosome carries six fertility groups essential for male fertility, which are usually carried on both halves of X-Y translocations. As a result, male progeny inheriting a free duplication derived from a T(X;Y) half will not have all the fertility loci, and will be sterile. To overcome this, I introduced a second Y chromosome into the T(X;Y) males. Provided the Y chromosome segregates into the male progeny to-gether with any free duplications, the male progeny will be fertile. The males carrying the T(X;Y) and Y chromosome were exposed to a dose of 4000 rads of gamma rays, which is sufficient to induce a high frequency of chromosomal aberrations and rearrangements with minimum sterility (Grigliatti, 1986). A total of 450 irradiated males were mated at a ratio of 1:2 to either *lep/FM7* (640) or *stunted (sun)/FM7* (260) females. (*sun* is a zygotic lethal mutation mapping to the same region of the X chromosome and is discussed in the next chapter). Unirradiated males were mated in parallel as a control.

The progeny were examined for males with a bright orange eye colour (due to the presence of a mini-w^+ gene next to the FRT element) as these are *lep* males, presumably rescued by a free duplication. The other class of males, carrying the FM7 balancer chromosome, had white eyes. To assess the frequency at which candidate males occurred amongst the progeny, the number of females emerging was recorded, as FM7 males have a slightly decreased viability compared to wild type. The number of candidate males was 25, and the number of female progeny was 11,710. Only one of the candidate males showed the expected markers; the other males were either FM7 males carrying the distal half of the T(X;Y) which carries w^+, rescuing the w mutation on the FM7 chromosome, or the products of non-

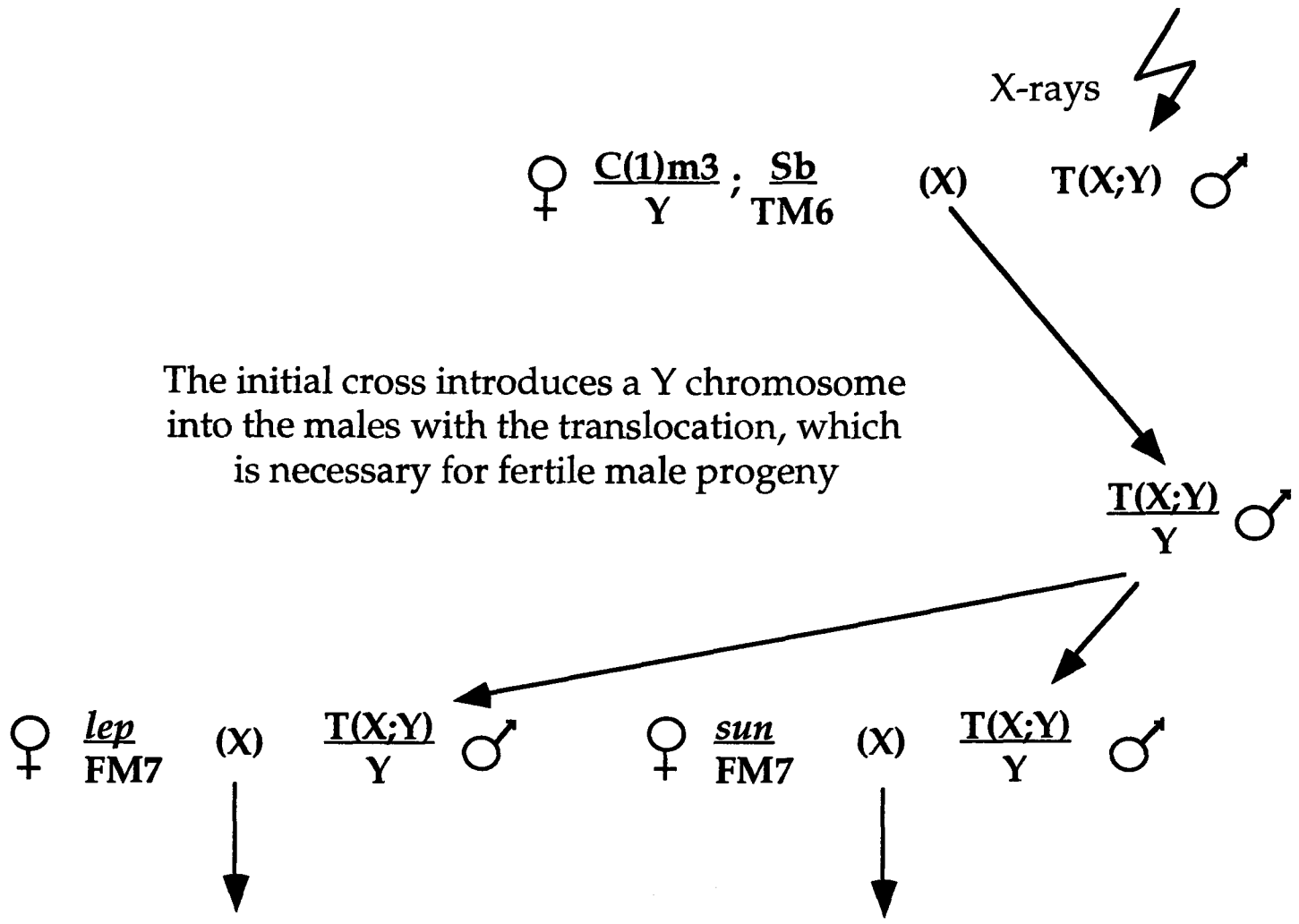

Number of female offspring:	11,710
Number of candidate males:	25

Figure 4.4 First genetic screen for *lep* duplications

Breeding scheme to screen for duplications of the *lep* locus. The screen was also used to screen for duplications of the *stunted (sun)* locus which maps to the same approximate region of the X chromosome (see next chapter). Of the 25 candidate males, 24 did not show the correct markers. The remaining candidate male of the 25 showed the expected phenotypic markers, was derived from T(X;Y)B117 (13C-D), and rescued the *sun* mutation, placing *sun* proximal of 13C-D. Unfortunately the male was sterile, either because it was hyperploid, or had failed to inherit a Y chromosome.

disjunction of the T(X;Y) males. The candidate male was derived from T(X;Y) B117 which has a breakpoint at 13C-D. It rescued the *sun* mutation. The male was *y* B^S indicating that it had inherited the proximal portion of the T(X;Y), and so the *sun* mutation must be proximal to 13C-D (see figure 4.2). Unfortunately the candidate male was sterile, and no duplication was recovered.

The sterility of the candidate male could have been due to two reasons. If the proximal portion of T(X;Y) had not lost any X chromosomal material, then the male would have been hyperploid for almost half the X chromosome. Such males survive, but are sterile (Stewart and Merriam, 1973). The second reason is that the Y chromosome did not segregate with the free duplication into the *lep* male. To solve the former problem requires screening increased numbers of progeny, but it was possible to overcome the latter problem by altering the screen.

4.4 A second genetic screen for *lep*$^+$ duplications

A variation of the first duplication screen was designed to negate the previous requirement for co-segregation of the free duplication and a Y chromosome. The key alteration was construction of an attached X-Y chromosome bearing the *lep* mutation, so that all *lep* males would carry all the Y chromosomal male fertility loci.

The breeding scheme for construction of the C(X;Y) *lep* chromosome is shown in figure 4.5. The C(X;Y) *lep* stocks recovered could not be tested for the presence of the Y chromosome fertility loci as *lep* is lethal in males. Despite it being unlikely that recombination could have removed any of the fertility loci, all of the C(X;Y) *lep* stocks were used in the revised duplication screen to avoid relying on one stock (figure 4.6). 1100 males were irradiated with 4000 rads of gamma rays and mated to over 2,200 C(X;Y) *lep/FM7* virgin females at a ratio of 2 females per male, and 25

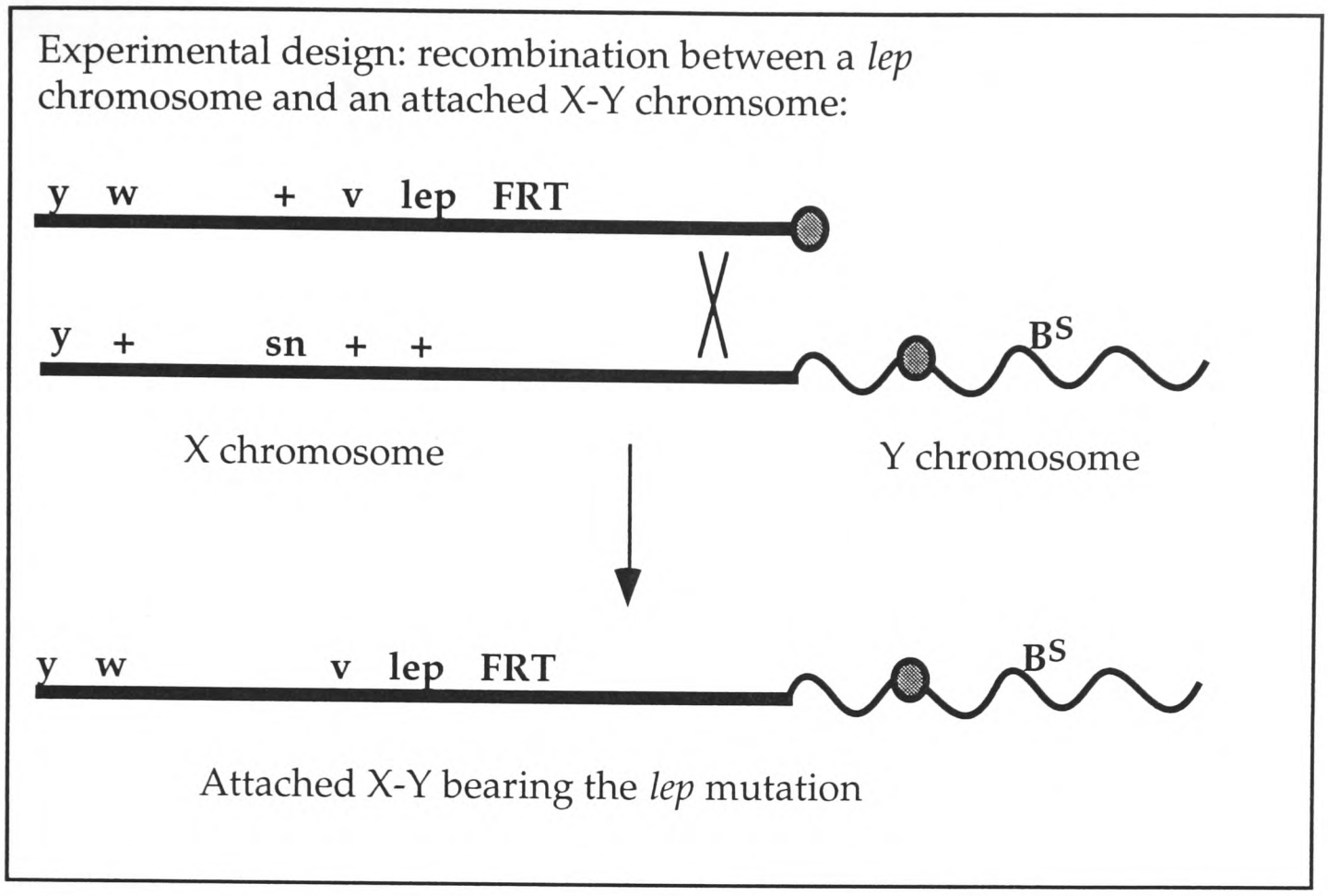

y w lep **FRT^{101}** **(X)** ***y sn*** B^S

FM7

Males are either C(X;Y)P2 or C(X;Y)P3. Both conform to the diagram above.

y w lep **FRT^{101}** **(X)** **FM7**

y sn B^S

Select *sn*$^+$ B^S females. **(X)** **FM7**

(FM7 carries *sn* and *B*; B^S/B can be distinguished from *B*/+)

Establish stocks from single females

Check that *sn*$^+$ B^S chromosome carries *lep*.
(Absence of *sn*$^+$ B^S males in stock)

Figure 4.5 Generation of a C(X;Y) *lep* chromosome

The top panel diagrams the experimental design for the recovery of a C(X;Y) chromosome; the genetic crosses are shown underneath.

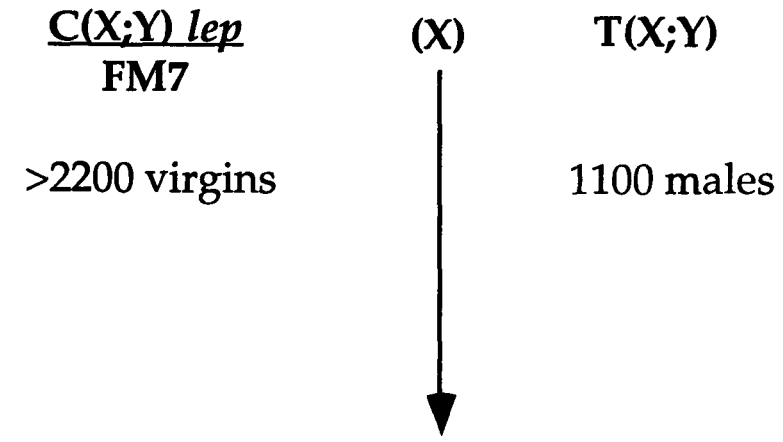

Number of female progeny:	2887
Average per bottle:	34
Average per control bottle:	73
Number of candidate males:	39

Origin of candidate males:

	Irradiated	Control
T(X;Y)S29	1	-
T(X;Y)B51	8	6
T(X;Y)B117	19	5

Figure 4.6 Second screen for duplications for *lep*

The genetic cross for the second screen for duplications to rescue the *lep* mutation is shown at the top. The results of the screen are shown in the box immediately below. Of the 39 candidate males, only 1 showed the correct phenotypic markers for a *lep* male. It was derived from T(X;Y)S29 which has a breakpoint in 13B4-6. The presence of the marker B^S indicated that the *lep* male had inherited the distal half of the T(X;Y), implying that the location of *lep* is in 1A-13B4-6. The male was sterile, probably due to hyperploidy. The box at the bottom indicates the origin of the candidate males. As all the males derived from T(X;Y)B51 and T(X;Y)B117 didn't show all the correct phenotypic markers, they have a high background rate (FM7 males carrying the distal half of the T(X;Y)). This background appears absent in T(X;Y)S29, as the one candidate male was a genuine *lep* male.

males per bottle; the flies were transferred to a second bottle after 3 days laying, for a further 3 day lay before being discarded. Only 2887 females emerged in the F1 progeny, an average of 34 per bottle. In the first duplication screen, an average of 130 females per bottle emerged. Examination of the unirradiated control bottles showed an average of 73 females per bottle, suggesting that the X-ray dosage had been too high, inducing a high level of male sterility.

Only one of the candidate males displayed all the phenotypic markers of a *lep* male. The fly was derived from T(X;Y)S29 which has a breakpoint in 13B4-6. The male also showed the B^S marker, indicating that it had inherited the distal half of the T(X;Y), implying that *lep* lies somewhere between 1A and 13B4-6. As *lep* was not rescued by *Dp(1;f)LJ9* which covers 12A10-13A2, this suggests that *lep* lies in 13A2-13B4-6, or distal to *g*. The male proved to be sterile, suggesting that it was hyperploid and that the T(X;Y) had not undergone any interstitial deletion.

4.5 Conclusion

The recovery of a candidate, albeit sterile, *lep* male in the second duplication screen suggests that the experimental approach should work. The search for a lep^+ duplication has been taken over by M. Seki, who has recovered nineteen lep^+ males in screens following the same protocol. One lep^+ male proved to be fertile, but the stocks established were sickly, and died after two generations.

A more recent search for suitable duplications revealed that a chromosomal transposition, Tp(1;2)eag^{X6}, covers 13A1-13E8. This was shown not to rescue *lep* by M. Seki. Tp(1;2)eag^{X6} and Dp(1;f)LJ9 have breakpoints 22kb from each other (Drysdale et al., 1991). This leads to three possibilities: either that *lep* is a double mutant or a deletion that cannot be rescued by either duplication alone, or that it maps somewhere else.

As *lep* was induced in the DEB screen, which had a low frequency of X-linked lethals, the probability of *lep* being a double mutant occurring is low. In addition the meiotic mapping data is consistent, implying that both mutations of a double mutant would have to be close to-gether. If they had been further apart, the recombination data would have been more complicated. It appears most likely that lep maps distal to *g* (12B). Testing with available duplications leaves 11A-12B as a possible region. In any case, more promising results were first obtained in studying T60, so I concentrated attention on analysing this chromosome.

Chapter 5. The genetics of the *stunted* mutation

5.1 Introduction

This chapter examines the genetics of the zygotic lethal T60, whose maternal effect is the deletion of the odd-numbered abdominal denticle belt, (like *odd-skipped*). The zygotic phenotype of the T60 mutagenised chromosome was pair-rule, suggesting the presence of a mutation in the *runt (run)* pair rule gene, as *run* is the only X-linked pair rule gene (figure 5.1).

Closer examination of the maternal and zygotic effects of the T60 chromosome revealed subtle differences between the two phenotypes. The normal shape of the abdominal denticle belts is roughly trapezoidal and this is seen in the T60 maternal effect phenotype. In the T60 zygotic phenotype, the denticle belts are rectangular in shape with partial mirror image symmetry (figure 5.1). The cuticle phenotypes suggested that there might be a maternal effect mutation on the T60 chromosome which modifies *run* activity. To test this hypothesis, it was necessary to check if there was a *run* mutation present and to remove it to allow examination of the maternal effect phenotype.

5.2 The *stunted* maternal effect segmentation phenotype

To determine if a *run* mutation was present, I employed two strategies: (i) a complementation test with a *run* mutation, which indicated a *run* mutation on the chromosome as *run*/T60 females were not viable, and (ii) testing for rescue with a chromosomal duplication carrying a wild type copy of the *run* gene. T60 males with run^+ on a duplication did not survive (figure 5.2). These results imply either that (i) the T60 chromosome carried two zygotic lethal mutations, *run*, and another which falls outside the run^+ duplication preventing rescue of T60 males, or (ii)

Wild type

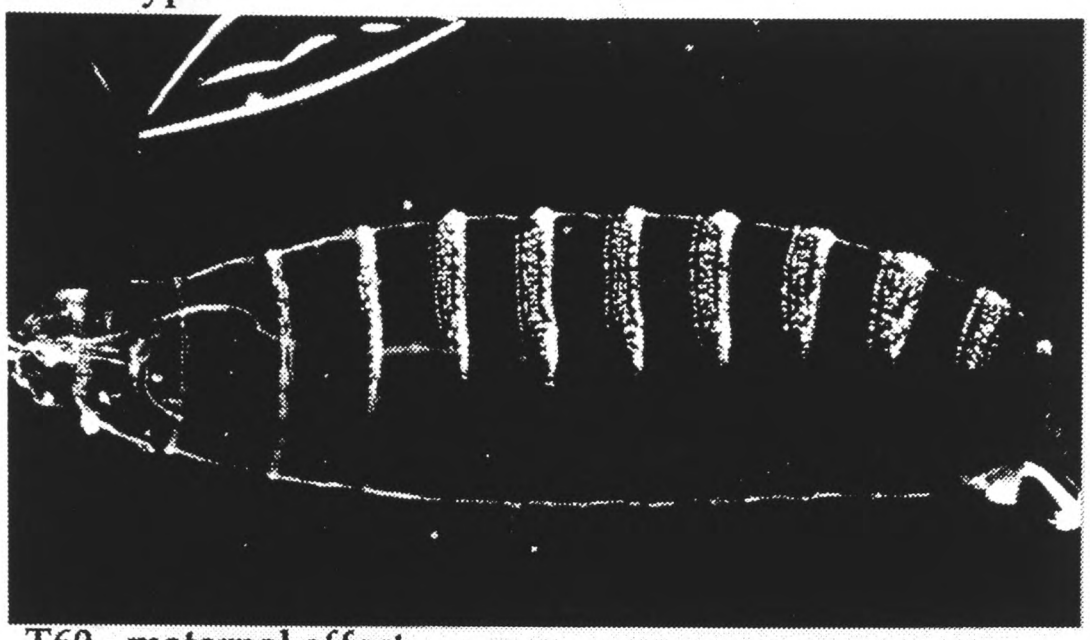

T60 - maternal effect

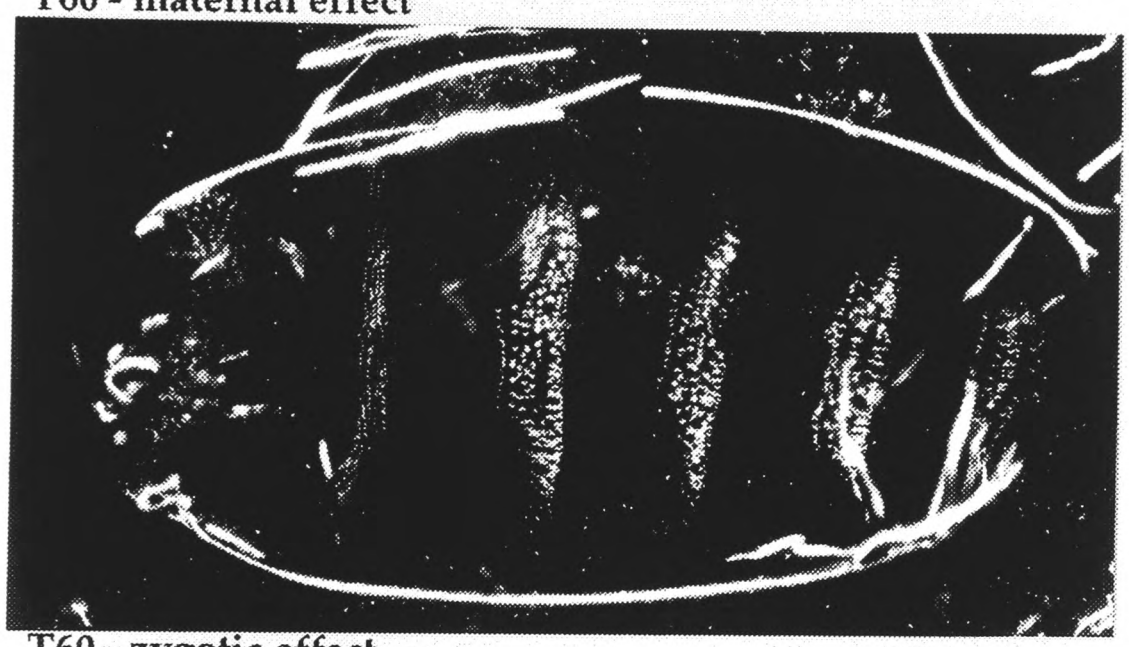

T60 - zygotic effect

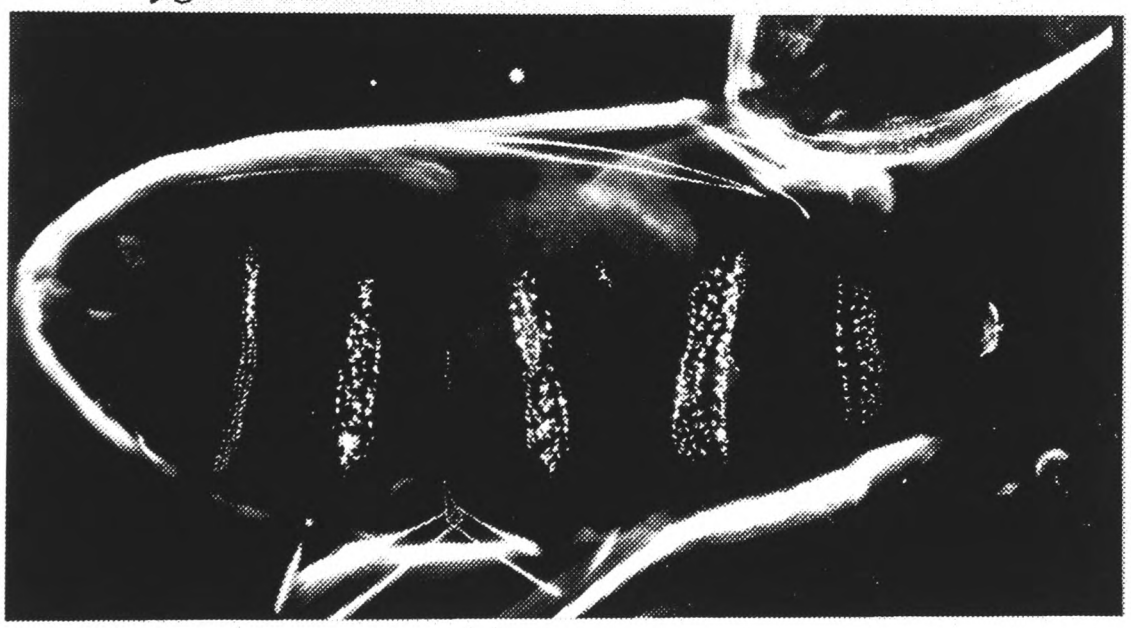

Figure 5.1 The T60 maternal effect cuticle phenotype
A wild type cuticle is shown at the top; in the middle is the T60 maternal effect phenotype; at the bottom is the T60 zygotic phenotype, note the differences in the shape of the denticle belts between the maternal and zygotic effects.

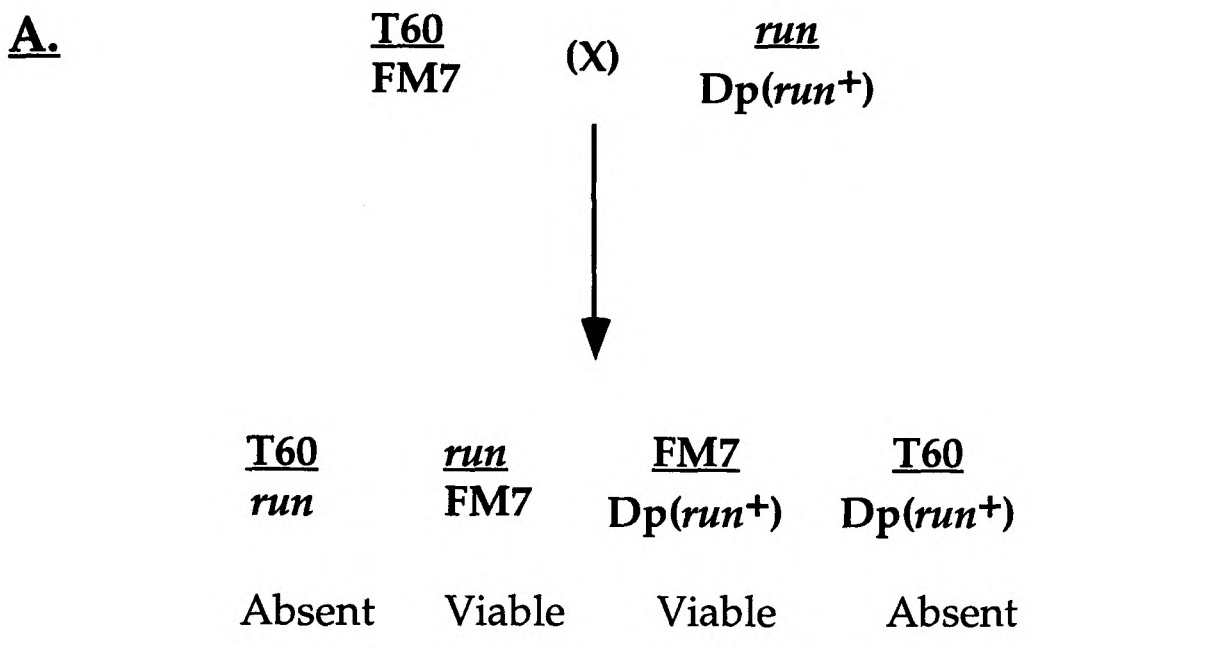

Figure 5.2 Genetics of the T60 chromosome

To test for the presence of a *run* mutation on the T60 chromosome, the genetic cross shown in A was carried out. The female carries the T60 chromosome balanced over FM7, and was mated to a male mutant for *run* (*Df(1)B102*), and carrying a duplication with a wild type copy of *run* (y^+ *Y mal*$^+$). F1 females carrying the T60 chromosome and the *run* mutation were not viable, but neither were males carrying the T60 chromosome and the *run*$^+$ duplication. Two explanations for this result are shown in B. The actual explanation was that T60 carries both a *run* mutation and another lethal which lies outside the duplication. An alternative was that the T60 chromosome contained a lethal locus which when trans-heterozygous to *run*, displays a lethal interaction.

the T60 chromosome carried a locus which displays a lethal trans-heterozygotic interaction with *run* (figure 5.2).

It was possible to distinguish between these two possibilities by separating the proximal and distal regions of the T60 chromosome (figure 5.3). Any maternal effect mutation must lie between 1A and 14A-B: as the FRT element is inserted at 14A-B, only the region of X chromosome distal to the FRT is homozygosed after a mitotic recombination event; *run* is proximally located on the X chromosome, at 19E1-3.

Recombinant lines with either the proximal or distal end of the T60 chromosome were recovered which carried zygotic lethals. Cuticle preparations of egg lays from the recombinant lines were examined for patterning defects (figure 5.4). This established that the proximal part of the T60 chromosome did indeed carry a *run* mutation.

Eighteen recombinant lines carrying the distal part of the T60 chromosome did not show any zygotic patterning defects in egg lays. The majority of the eggs from these lines hatched, establishing the lethal phase of the recessive mutation as during the larval or pupal stages. The eighteen lines were checked for maternal effects by making germline clones. Hatched larvae and brown unhatched eggs were observed. Cuticle preps of the brown eggs revealed an unusual phenotype (figure 5.4), highly similar to that of a null mutation of the *run* locus. The similarity of the maternal effect mutation to *run* prompted the naming of the maternal effect as *stunted (sun).* sun^{mat-} will be used to describe embryos lacking maternal sun activity.

All the germline mosaic females were pooled to conduct preliminary antibody staining. The segmentation genes *ftz* and *engrailed (en)* are both downstream of *run.* Examination of their expression patterns in the *sun* maternal effect embryos showed alterations highly similar to patterns seen when staining embryos completely lacking *run* activity. Mutations with

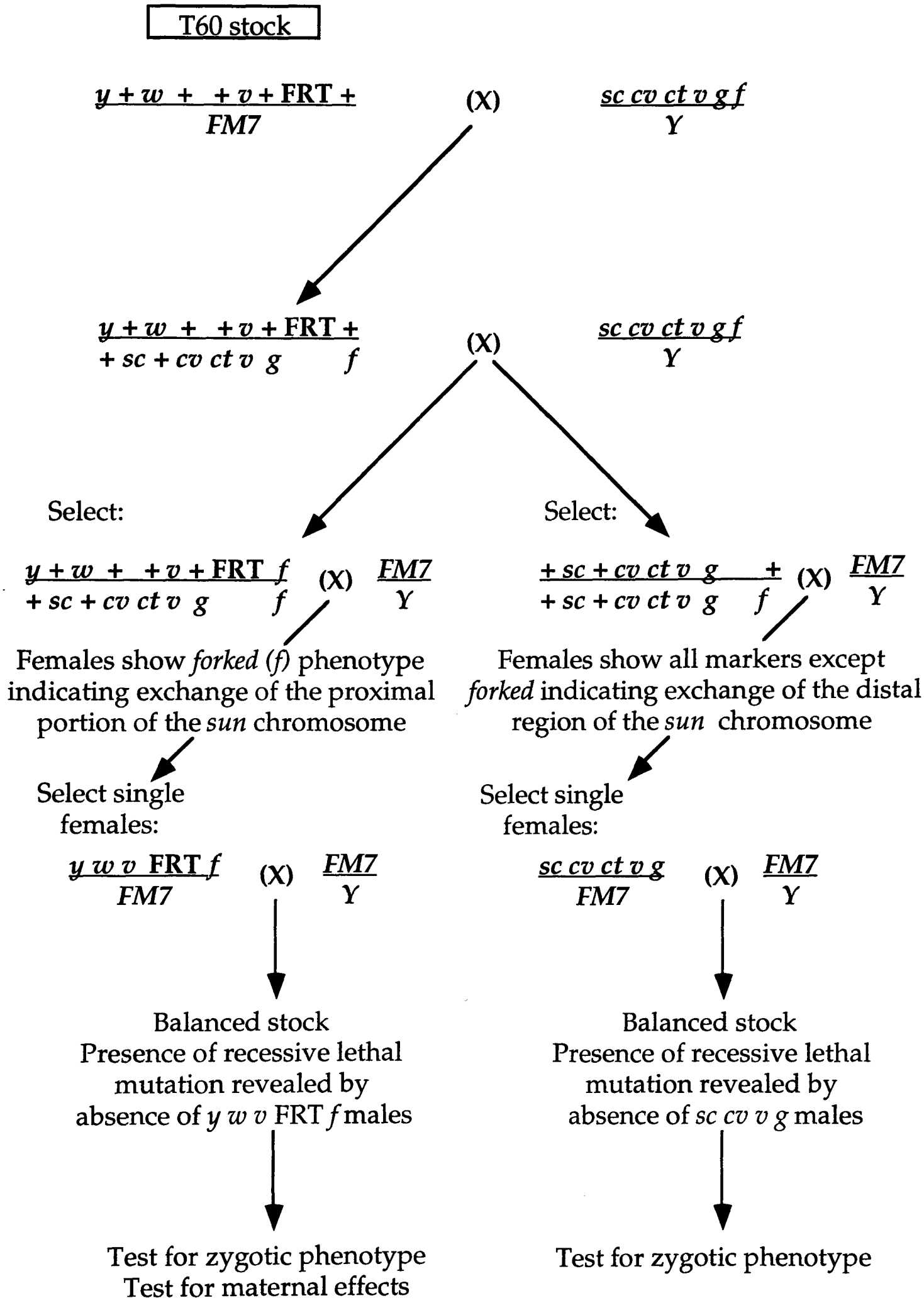

Figure 5.3 Breeding scheme to analyse the T60 chromosome

The scheme illustrates genetic crosses between the T60 chromosome and a multiply marked chromosome to recover the proximal and distal (1A-14B) regions of the T60 chromsome as independent stocks, in order to separate the putative maternal effect and *run* mutations.

Figure 5.4 Cuticle phenotypes of the T60 recombinant lines

A. Maternal effect cuticle phenotype of a recombinant line carrying the distal part of the T60 chromosome. The phenotype is highly similar to a strong hypomorphic allele of the *run* pair-rule locus. Only four abdominal denticle belts are visible and they display mirror image symmetry. The similarity of the phenotype to that of a *run* allele led to the maternal effect mutation being named *stunted (sun).*

B. Cuticle of a null allele of the *run* pair-rule locus. The phenotype is more severe that of A. The two posterior abdominal denticle belts have almost fused, and the next denticle belt has almost disappeared.

C. Cuticle phenotype seen in subsequent attempts to reproduce the *sun* maternal effect phenotype. There is a severe reduction in the amount of cuticle present. The phenotype is similar to that of the neurogenic mutants.

D. Neurogenic cuticle phenotype: larger numbers of cells adopt a neural fate, so there are less epidermal cells and consequently less cuticle is secreted.

A.

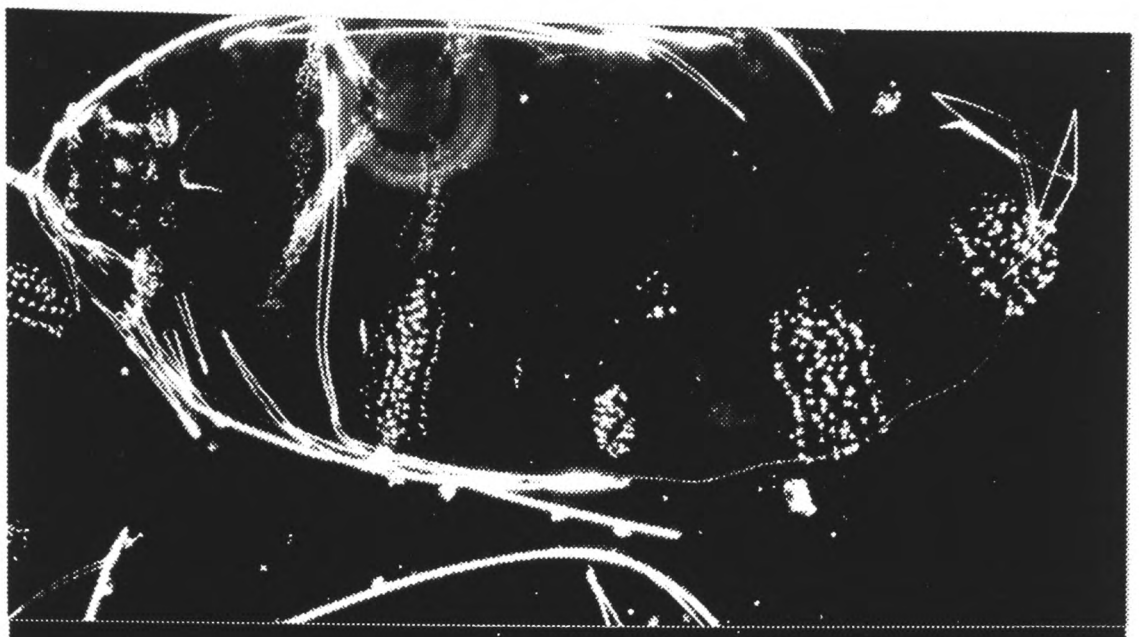

B.

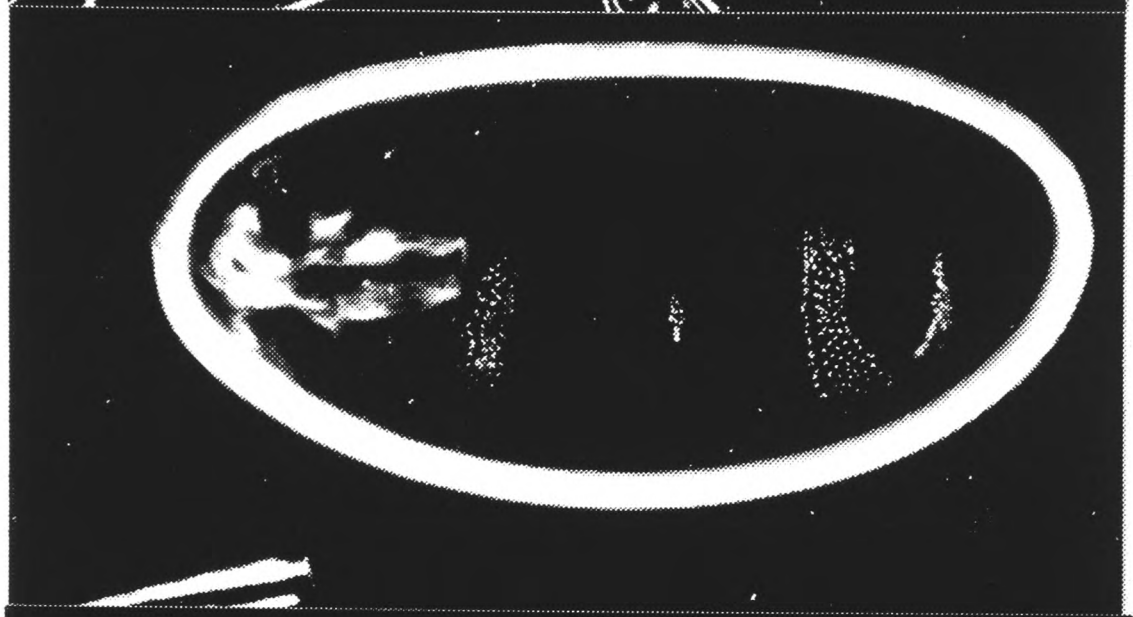

C.

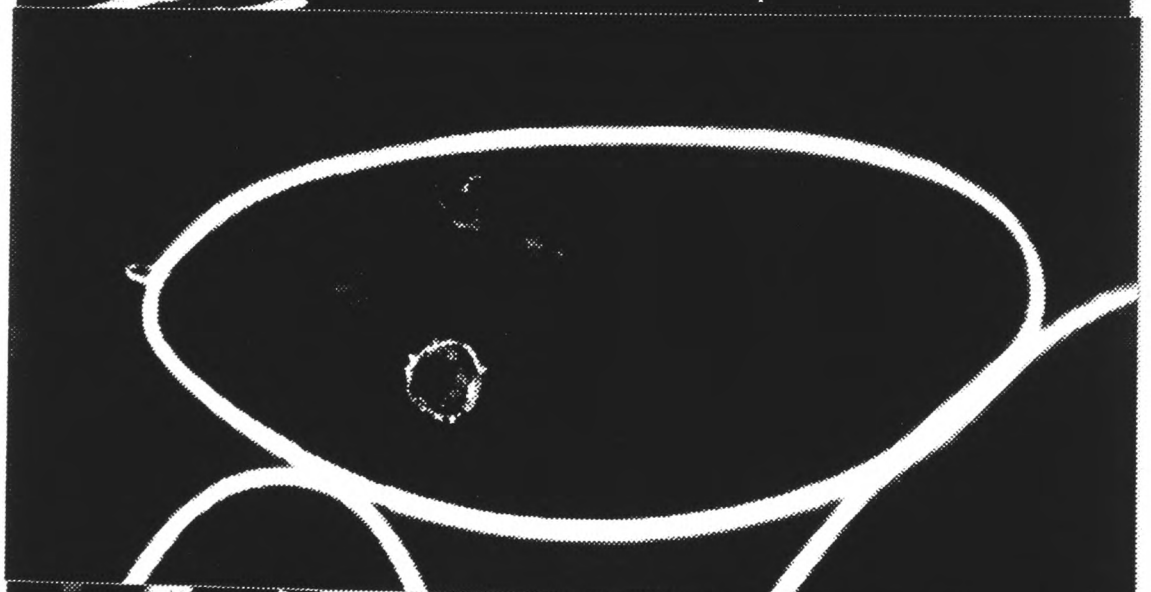

D.

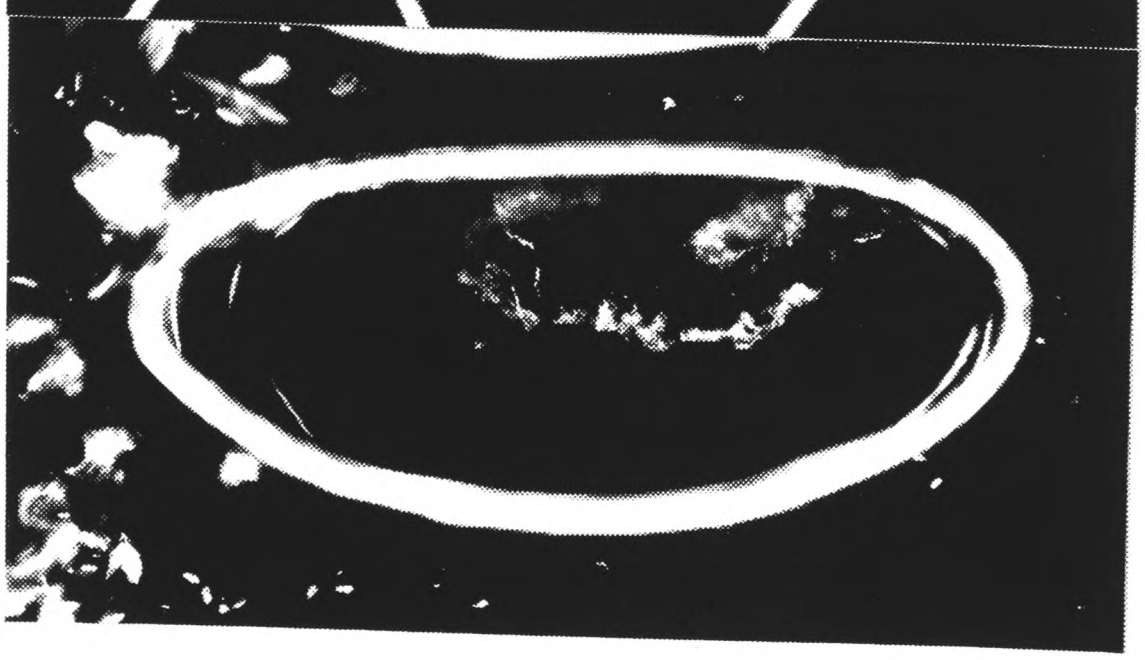

the same phenotype are usually operating within the same genetic pathway, suggesting that the *sun* gene product is required for normal *run* activity.

The *sun* maternal effect phenotype raised questions about the molecular identity of the *sun* gene product. The nuclear location of Run protein, and its position in the transcriptional cascade within the segmentation gene hierarchy suggested that it is also a transcription factor (Kania et al., 1990). The mouse polyoma enhancer binding protein 2α (PEBP2α) was found to be a vertebrate homologue of *run* (Ogawa et al., 1993b), and requires a second protein to bind the polyoma virus enhancer, PEBP2β (Ogawa et al., 1993a). *Drosophila* Run also binds the polyoma enhancer in the presence of mouse PEBP2β (Kagoshima et al., 1993). No PEBP2β homologue had been identified in flies, and so *sun* was a candidate gene to encode such a homologue which is why I concentrated my efforts on characterising the *sun* maternal effect.

All subsequent attempts to reproduce the maternal effect segmentation phenotype of *sun* failed. I am unable to explain why this was so. Although contamination of the egg lay chambers by *run* flies seems a possibility, it is unlikely as all lines were tested independently for maternal effects, and several of them displayed the severe segmentation phenotype. In subsequent experiments, eggs laid by females with *sun* germline clones failed to exhibit any hatched larvae, and the eggs developed a very light brown colour only after 2-3 days of incubation at 25°C. The initial testing had produced hatching larvae, indicating probable paternal rescue, as well as unhatched eggs with intact cuticles (although showing segmentation defects). Examination of the unhatched eggs in cuticle preparations revealed a very small amount of cuticle, or no cuticle at all (figure 5.4). Despite this change of phenotype, the initial segmentation phenotype

Genotypes				# Males
sc	+	+	+	-
sc	cv	+	+	1
sc	cv	ct	+	2
sc	cv	ct	f	109
+	cv	ct	f	30
+	+	ct	f	16
+	+	+	f	82
sc	cv	+	f	5
+	cv	ct	+	1
sc	+	+	f	12

Table 5.1 Mapping of T60 with the *sc cv ct v g f* chromosome

The table lists the frequencies of occurrence of different male progeny from T60/*sc cv ct v g f* females. Males carrying w^+ were further scored for the *v* and *g* eye colours: *sc cv f* - 4 showed *v*, and 1 showed *v* and *g*; *sc f* - 1 showed *v* and *g*. T60 carries *run*, in addition to the *sun* mutation. The cytological positions of *run* and *f* are 15F and 19B respectively, so there is expected to be linkage between *run* and *f*, although they are separated by a recombination distance of 10%. Examination of the figures above shows *f* is present in 97% of the recombinant progeny. This suggests that the *sun* maternal effect is closely linked to *f*. The w^+ flies indicate that *sun* lies proximal of *g* also.

Genotypes				# Males
m	+	+	+	-
m	wy	+	+	-
m	wy	sd	+	-
m	wy	sd	os^s	495
+	wy	sd	os^s	1
+	+	sd	os^s	29
+	+	+	os^s	-
+	+	+	+	19

Table 5.2 Mapping of *sun* with the *m wy sd* os^s chromosome

The table lists the frequencies of occurrence of different male progeny from *sun/m wy sd* os^s females. Tight linkage of *sun* to the *sd* (13F) marker is seen. I had difficulty in scoring os^s, so figures for this marker may be not be reliable, but as it is located at 17A it was not really required for mapping.

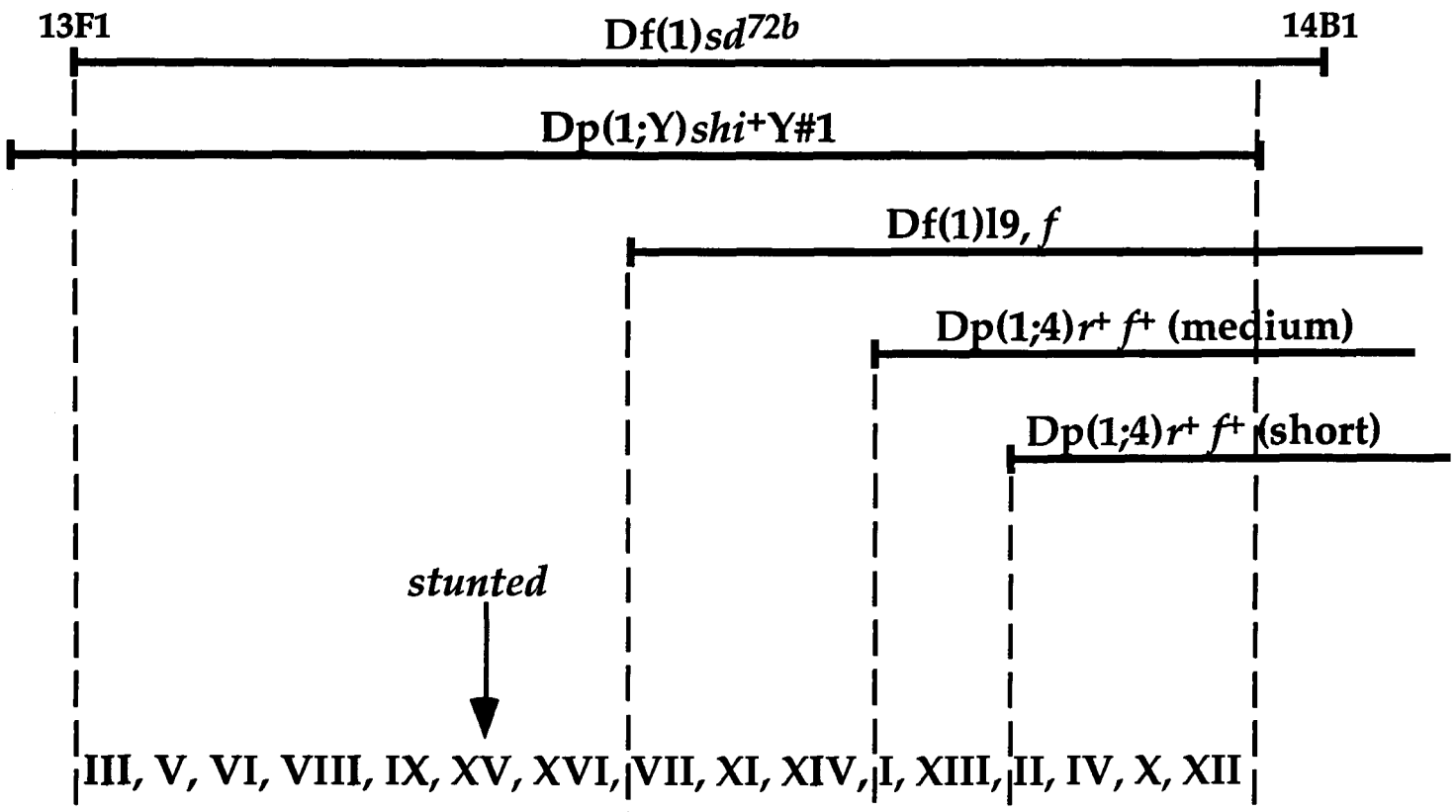

Figure 5.5 Position of *sun* within the region 13F

The *sun* mutation was positioned within Df(1)sd^{72b} by complementation and rescue crosses with the deficiencies and duplications shown. The Roman numerals represent a collection of complementation groups within *Df(1)*sd^{72b}. Group XV, represented by one allele, *l(1)EM67*, failed to complement *sun*. The complementation groups were isolated in a saturation mutagenesis of *Df(1)*sd^{72b} by A. Katzen, and some correspond to known genes: III, lethal alleles of *sd*; VI, clathrin heavy chain; XVI, D-Myb; VII, *shibire*; IV, *extra denticle*. (Diagram based on the data of A. Katzen).

prompted me into trying to show that there was an underlying segmentation defect as well as a reduction in cuticle secretion (sections 5.6 and 5.7). The next sections describe the mapping of the *sun* mutation and isolation of further alleles.

5.3 Mapping of the *stunted* mutation

Prior to separation of *sun* and *run* I attempted to map the locations of recessive lethals on the T60 chromosome by recombination with a multiply marked chromosome. As the existence of a maternal effect mutation on T60 was uncertain, the mapping experiment could provide early conformation of a lethal mutation in the distal part of the T60 chromosome, and yield its approximate location.

Male progeny from T60/*sc cv ct v g f* females were scored for the presence of phenotypic markers (table 5.1). The mapping results suggested the presence of *run*, and another lethal mutation linked to *f* and located in the region between *ct* and *f* (7B-15F). The marker *f* appeared in 97% of the male progeny. As *f* is located at 15F and *run* at 19B, a *run* mutation should show linkage to the *f*. However, *f* and *run* are separated by a genetic distance of 10% expected recombination between them, so the prevalence of *f* amongst the progeny cannot be explained by the presence of a *run* mutation alone, suggesting a second lethal was linked to *f*.

After the separation of *sun* and *run*, the location of *sun* was mapped by recombination with the *m wy sd* os^s chromosome. Male progeny from *sun/m wy sd* os^s females were scored for phenotypic markers (table 5.2). Tight linkage of *sun* to the *sd* (13F) marker was seen. The duplication screen described in chapter 5 placed *sun* proximal to 13C-D, implying that *sun* is in the region 13C-14B, as maternal effect mutations must be distal to 14A-B, the position of the FRT element.

sun is not rescued by $Dp(1;4)r^+$ which covers the region 13F-16A. *Dp(1)sdY#3m* which extends more distally into 13F was found to rescue the *sun* recombinant lines, placing *sun* in the distal end of 13F. Further duplications and deficiencies for the region refined the location of *sun* (figure 5.5). The mutation *l(1)EM67* is located in 13F (A. Katzen, unpublished results) and failed to complement *sun*. *l(1)EM67* is immediately distal of the *Drosophila* homologue of the Myb proto-oncogene. A P element construct containing 11.6kb of DNA from the Myb region rescues *l(1)EM67* (A. Katzen, unpublished results) and was also found to rescue *sun*, strengthening the argument that *sun* and *l(1)EM67* are allelic.

A second mutation located in 13F, *42-3.0B*, also appears to be a *sun* allele. *42-3.0B* is lethal over a deficiency for 13F, $Df(1)sd^{72b}$ (13F-14B), but otherwise viable. The lethality of $42\text{-}3.0B/Df(1)sd^{72b}$ females is rescued by the P element construct which rescues *sun* and *l(1)EM67*. Complementation tests between *sun* and *42-3.0B* showed that *sun/42-3.0B* females emerge late and are all sterile (59 females tested). *l(1)EM67/42-3.0B* females also emerge late and only 10% of females are fertile (53 females tested). The female sterile phenotype and the P element rescue argue that *42-3.0B* is another *sun* allele. As *sun/42-3.0B* females are viable, and $Df(1)sd^{72b}/42\text{-}3.0B$ females are not, *sun* resembles a hypomorphic allele rather than a null mutation. By the same criteria, *l(1)EM67* is a weaker hypomorph than *sun*.

The zygotic lethality of *sun* was investigated by mating *sun/FM7* females to $Df(1)sd^{72b}/Dp(1)sdY\#3m$ and doing egg lays. $sun/Df(1)sd^{72b}$ females should have less *sun* activity than *sun* hemizygotes. 94% (498/527) of the eggs hatched, and all but three of the unhatched eggs showed wild type segmentation. The remaining three had very subtle segmentation defects.

Therefore the zygotic component of *sun* has a larval-pupal lethal phase, with the maternal component rescuing any embryonic requirements.

5.4 Screening for further alleles of *stunted*

An important consideration in genetics is the nature of mutant alleles, usually assessed by comparison to other alleles. The *sun* allele *42-3.0B* did not display a maternal effect on cuticle development. *l(1)EM67* was recombined onto a chromosome carrying FRT^{9-2}, but chimeric females with germline clones did not lay any eggs. This is surprising as *l(1)EM67* appears to be a weaker hypomorph than *sun* (above). *l(1)EM67* may be a double mutant in which a second mutation affects germline development.

A screen was designed to recover further mutations in the *sun* locus on an FRT bearing chromosome (figure 5.6). Putative *sun* mutations are recovered in males carrying a *Dp(1)sdY#3m;* one disadvantage to the screen is that it cannot recover doubly mutant chromosomes if the other mutation lies outside *Dp(1)sdY#3m.*

Chromosomes mutagenised with EMS were examined for failure to complement *sun;* 4636 mutagenised chromosomes were screened (figure 5.6). None showed lethality when combined with the *sun* mutation. However, one of the mutant lines displayed a wing phenotype in trans to *sun*. These females were recovered and used to establish stocks, and the mutation named *shrinkled (shk). shk* is a homozygous and hemizygous viable mutation. The stocks all displayed the wing phenotype in about 10% of males and 30% of females (figure 5.7). The penetrance of the *shk* phenotype increased to 60% when the *shk* chromosome was in trans to the *sun* mutation. The phenotype was also visible over *l(1)EM67* and $Df(1)sd^{72b}$, at approximately the same degree of penetrance as for *shk/shk* females.

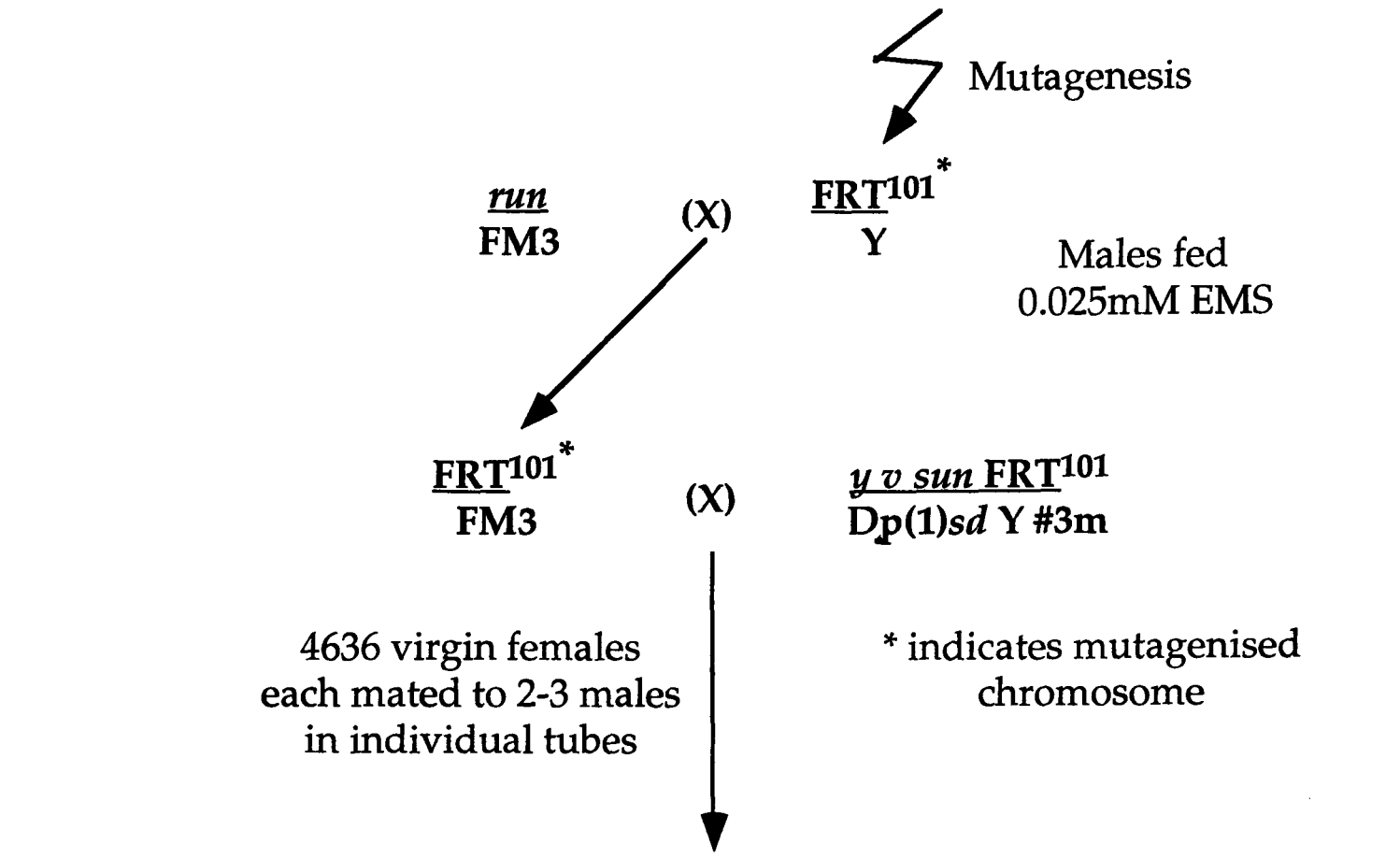

RESULTS	
Total:	4636
Lethals:	2606
Non-lethals:	1138
Sterile:	892
Lethal frequency:	0.56
Candidates:	1

Figure 5.6 F2 screen for *sun* alleles

Breeding scheme to isolate alleles of the *sun* mutation. Screening is in the F2 for the absence of females carrying the mutagenised chromosome and the *sun* mutation. Candidate mutations are recovered as males with Dp(1)*sd*Y#3m. The frequency of lethals induced was based on mutagenised chromosomes not rescued by Dp(1)*sd*Y#3m. No lethal alleles of *sun* were recovered, but a chromosome which showed a wing phenotype when trans to *sun* was observed and retained.

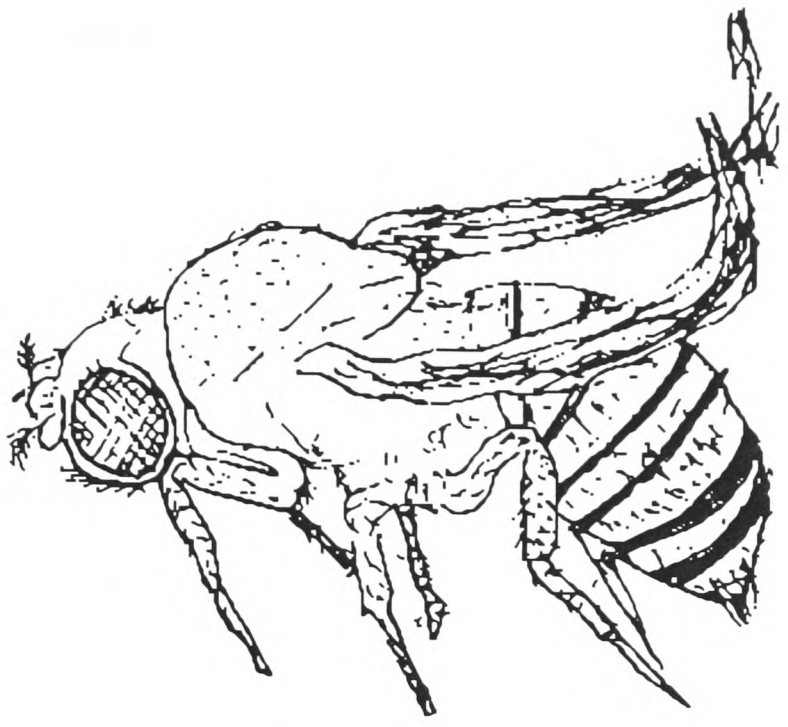

Genotype	N	Wing Phenotype
shk/Y	92	10%
shk/shk	320	29%
shk/sun	131	60%
shk/EM67	181	20%
shk/Df(1)sd^{72b}	177	36%

Figure 5.7 The *shrinkled* wing phenotype

The drawing shows a *shk/sun* fly displaying the *shk* wing phenotype. The table indicates the penetrance of the wing phenotype in various genotypes: N = number of flies examined, wing phenotype = percentage of flies showing an obvious wing phenotype (more subtle phenotypes could be detected on closer examination).

It is not possible to definitively say whether *shk* is an allele of *sun*. The low penetrance of the wing phenotype in males makes it difficult to score for rescue by *Dp(1)sdY#3m*. As the duplication is carried on the Y chromosome it cannot be tested for rescue in females. *shk* males seem to show partial sterility that is rescued by *Dp(1)sdY#3m*, and by the P element which rescues *sun*. Although these results are based on small scale experiments, they suggest that *shk* is an allele of *sun*.

5.5 Screening for further alleles of *stunted* with the *shrinkled* mutation

Although it was not clear if *shk* is a *sun* allele, its strong interaction with *sun* alleles presented a way of doing rapid genetic screens for novel alleles by looking for female which show wing phenotypes when heterozygous for a mutagenised chromosome and *shk* (figure 5.8). Not all *sun* mutations would be detected by this method as the *sun/shk* interaction is not fully penetrant, but this is compensated for by the ease of screening.

The *y w v* FRT^{101} chromosome to be mutagenised had the *f* marker placed on it by recombination: *y w v* FRT^{101} *f* males were selected from the progeny of *sc cv ct v g f/ y w v* FRT^{101} females and used to establish stocks. The presence of *f* differentiates between the original *shk* chromosome and any novel mutations, as well as simplifying subsequent testing of candidate mutations for allelism with *sun*. The *y w v* FRT^{101} *f* males were mutagenised with EMS and mated with *shk/shk* females. 4035 F1 females were screened for a wing phenotype, and 118 flies showing disrupted wings were tested for allelism with *sun*. Three failed to complement *sun* and two of the mutagenised chromosomes were recovered in males carrying *Dp(1)sdY#3m*.

Stocks were established and the two mutations, sun^{Y6} and sun^{Y52}, were tested for maternal effects. Both exhibited the same severe reduction in cuticle secretion at 25°C as is seen in the original *sun* allele (sun^{1}). This

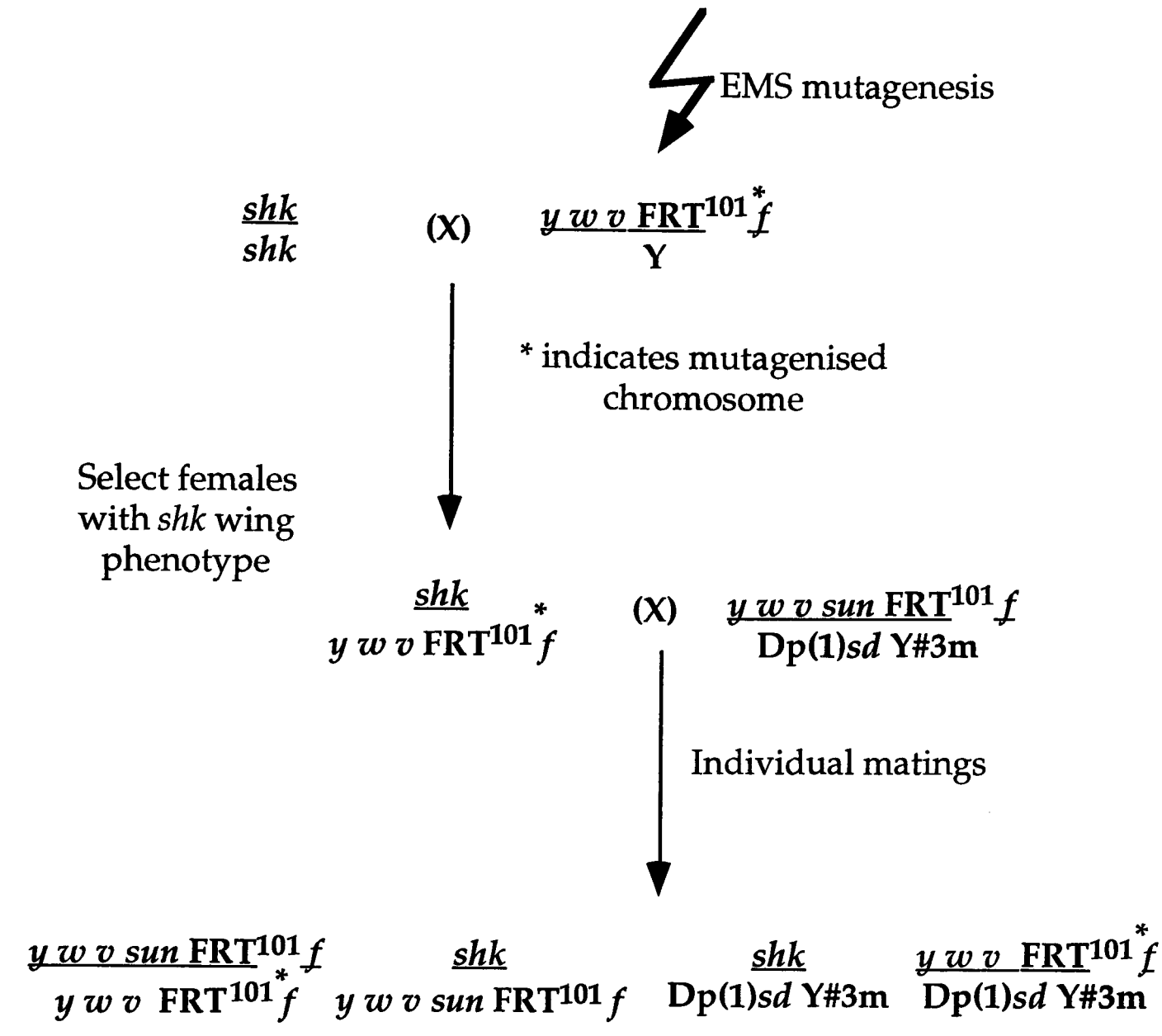

Number of females examined:	4035
Number with wing phenotypes:	118
Number which didn't complement sun:	3
Number of alleles recovered:	2

Figure 5.8 F1 screen for *sun* alleles

The diagram illustrates the breeding scheme for an F1 screen for novel *sun* alleles. The screen relies on the wing phenotype shown when *sun* is trans to the *shk* mutation. Two *sun* alleles were recovered by the screen.

Allele	Zygotic effect	Maternal effect
sun^{1}	Lethal	Severe reduction in cuticle at 25°C; temperature sensitive
sun^{EM67}	Lethal	Females do not lay eggs
sun^{Y6}	Lethal	Severe reduction in cuticle at 25°C; temperature sensitive
sun^{Y52}	Lethal	Severe reduction in cuticle at 25°C; temperature sensitive
shk	Viable; wing defect	Shows weak cuticle disruptions in trans to $sun^{42\text{-}3.0B}$
$sun^{42\text{-}3.0B}$	Viable	Females are sterile when $sun^{42\text{-}3.0B}$ is trans to lethal *sun* alleles

Table 5.3 Summary of the phenotypes of *sun* alleles

The alleles sun^{EM67} and $sun^{42\text{-}3.0B}$ were isolated by A. Katzen (UCSF). The cause the sterility of sun^{EM67} is not known; it displays the weakest interaction with $sun^{42\text{-}3.0B}$ so it is surprising that it disrupts the females germline. sun^{EM67} may be a double mutant with a second locus causing the female sterility in germline clones.

effect was also partially rescued by growth at 18°C. Neither allele gave rise to *run* like cuticles. sun^{Y6}/*42-3.0B* females were late emerging and sterile (20 females tested). sun^{Y52}/*42-3.0B* females were not viable, suggesting that sun^{Y52} may be a null mutant as *Df(1)sdY#3m/42-3.0B* females were also inviable. A summary of the zygotic and maternal effects of all the *sun* alleles is given in table 5.3.

5.6 The 'neurogenic' maternal effect *stunted* phenotype

All attempts to reproduce the *run* like maternal effect segmentation phenotype of *sun* failed; all embryos lacking maternal *sun* activity showed very little cuticle. A large reduction in the amount of cuticle secreted is a characteristic phenotype of the neurogenic mutations, in which too many epidermal cells choose a neural fate. I was influenced by the finding that the neurogenic gene *groucho* appeared to be playing a dual role in neurogenesis and segmentation (Paroush et al., submitted), and decided to test if the *sun* mutation could also have a dual role.

The *sun* maternal effect was tested for temperature sensitivity, and was found to be partially rescued by growth at 18°C (table 5.4). Only about 20% of the fertilised eggs detailed in table 5.4 had severe reductions in the amount of cuticle, and 20% of the fertilised eggs actually hatched as larvae. Nearly 30% of the eggs showed segmentation defects, suggesting that *sun* plays a role in segmentation, although none of the defects were consistent with a *run* phenotype. This contrasts to growth at 25°C when no larvae hatched and very little cuticle was seen (figure 5.4C). The original phenotype could therefore have been observed at a temperature below 25°C. A systematic attempt to find the temperature at which the *run* like phenotype was observed was unsuccessful.

The temperature sensitivity of the *sun* mutation suggested an approach to separate the segmentation and neurogenic effects of the *sun* maternal

A.

Total number of eggs examined:	2076	
Number judged to be fertilised:	1199	58%
Number judged to be unfertilised:	877	42%

B.

Phenotype of fertilised eggs	Percentage (1199 eggs)
Hatched	19%
Unhatched	81%
Wild type cuticles	23%
Segmentation defects	27%
'Neurogenic' defects	40%

Table 5.4 Maternal effect phenotypes of *sun* at 18°C

The cuticles of eggs laid by chimeric females with germline *sun* clones were examined. A. a total of 1852 unhatched eggs were examined, 548 were brown and the remaining 1304 were white, but nearly 500 of the white eggs were fertilised. It is possible that more white eggs were fertilised, but could not be classified as such by cuticle preparations. B. Distribution of phenotypes amongst the eggs which could be identified as fertilised. Cuticles were classified as having segmentation defects if any of the abdominal denticle belts were missing or fusing. 'Neurogenic' describes cuticles which were noticeably reduced in size. Many of the cuticles showed segmentation defects as well as reduction in the amount of cuticle secreted, and so were classified under both categories.

effect. Segmentation is established shortly after three hours of development at 25°C. The first round of CNS neuroblast delamination is seen just before four hours of development and further rounds continue for approximately five hours. The temporal separation of segmentation and neurogenesis suggested that temperature shift experiments could be used to test if there was an underlying segmentation defect.

An experiment was designed so that embryos would establish segmentation at the restrictive temperature (25°C), and undergo neurogenesis at the permissive temperature (18°C). Females with *sun* germline clones were grown at 25°C. Eggs were collected and shifted to 18°C at different times. The cuticles were of each group of eggs were scored for segmentation or neurogenic disruptions. The graph in figure 5.9 shows the result of this experiment. If eggs are laid over a period of an hour and immediately shifted to 18°C, the number of embryos with wild type cuticles showing neither segmentation for neurogenic defects is almost 60%. This proportion greatly decreases if the eggs are incubated for longer at 25°C, reaching 5% if the shift is delayed 2.3 hours after the egg lay. Comparing with table 5.4 which documents the results of growth at 18°C, this indicates that the temperature sensitive period lies later than the first hour of development. The proportion of neurogenic cuticles greatly increases with delaying the time of the shift to 18°C, reaching over 70% if the shift occurs 2.3 hours after the egg lay. The number of cuticles showing segmentation defects also increases if the shift to 18°C is delayed, but much less dramatically than the percentage of neurogenic cuticles. This suggests that in the context of the *sun* maternal effect, segmentation and the neurogenic effect are temporally close to-gether and cannot be separated. It is unusual that a temperature sensitive period for a neurogenic mutant should be so early.

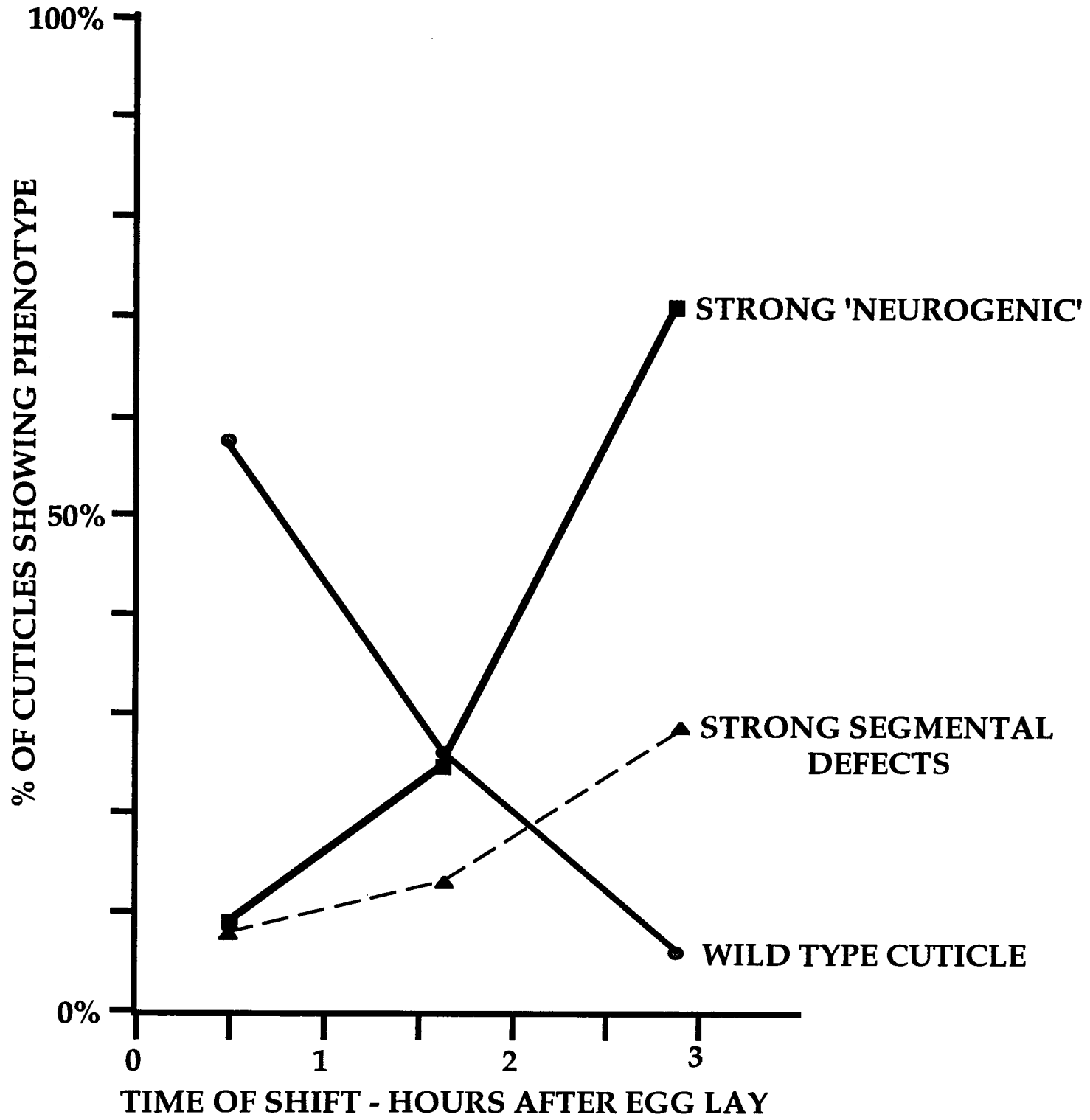

Figure 5.9 Temperature shift experiments on the *sun* maternal effect

To detect an underlying segmentation phenotype of the *sun* maternal effect, females with *sun* germline clones were allowed to lay eggs for one hour at 25°C. The eggs were aged for 0, 1.3 or 2.3 hours and shifted to 18°C for a further 24 hours. The time of shift represented on the graph is the average for each one hour egg lay, eg. shifted to 18°C immediately after the one hour: average time of shift is 0.5 hour. The cuticles of all the unhatched eggs as well as crawling larvae were scored for a wild type pattern, strong neurogenic effects (a substantial reduction in the amount of cuticle secreted) and strong segmentation defects (less than 5 abdominal denticle belts). A proportion of the cuticles showed both segmentation and neurogenic defects. The number of cuticles scored were 88, 81 and 85 for the 0, 1.3 and 2.3 hour shifts respectively.

A second attempt to separate the segmentation and neurogenic phenotypes relied on the observation that expression of the *achaete-scute complex* (AS-C) is required for the development of most neural cells, so removal of the AS-C suppresses a neurogenic phenotype (Brand and Campos-Ortega, 1988). If the *sun* maternal effect was neurogenic, then removal of the AS-C should attenuate the reduction in the amount of cuticle secreted.

A FRT bearing chromosome carrying both a deletion of the AS-C and the *sun* mutation was constructed by meiotic recombination (figure 5.10). In addition the AS-C deletion was recombined onto an FRT bearing chromosome as a control. Both chromosomes were used to generate germline clones. However, the removal of the AS-C failed to alleviate the *sun* maternal effect in all of the lines tested.

The conclusion from these experiments was that embryos lacking maternal *sun* activity display a reduction in cuticle secretion which is perhaps not due to neural hyperplasia. The product of the segmentation gene *hunchback (hb)* is a marker for neuroblasts, and in neurogenic mutants, the expression domains of Hb are greatly expanded. Late Hb expression in sun^{mat-} embryos was essentially random and limited to single cells, or small areas, rather than being expressed in greatly expanded domains (figure 5.11 F). The neural specific enhancer trap lines A37 and A101 were also used to assay for a neurogenic phenotype. X-gal staining of sun^{mat-} embryos carrying the enhancer traps showed less staining than wild type embryos, rather than more as would be expected in a neurogenic mutant.

5.7 Antibody staining of *stunted* maternal effect embryos

The expression patterns of segmentation genes in sun^{mat-} embryos were examined (figure 5.11). Expression of Hb was normal in early embryos, but in cellular blastoderm embryos it had a strange punctate appearance.

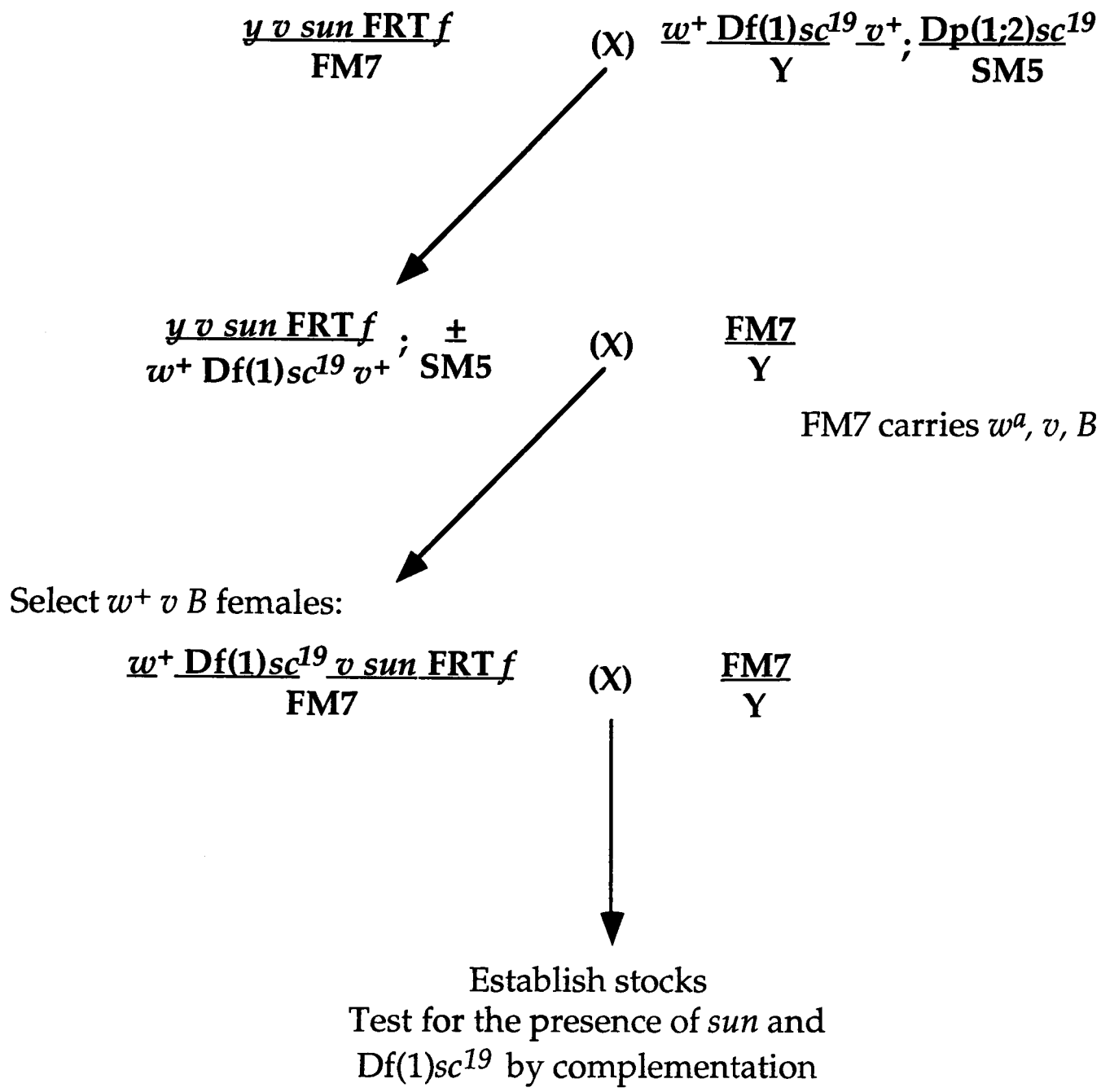

Figure 5.10 Generation of a *Df(1)sc^{19}*, *sun* recombinant chromosome

The breeding scheme combines a deficiency for the *achaete-scute complex* (ASC) and the *sun* mutation with a FRT element to allow generation of germline clones lacking both ASC and *sun* activity. The crosses rely on the w^+ marker carried by the Df(1)sc^{19} chromosome and the *v* marker carried by the *sun* chromosome for selection of the recombinant chromosome. A control stock of Df(1)sc^{19} on an FRT chromosome was constructed in a similar procedure.

Figure 5.11 Expression patterns of segmentation genes in *sun*$^{mat-}$ embryos

Antibody staining of *sun*$^{mat-}$ embryos.

A. Expression of Hunchback (Hb) protein before cellularisation appears to be wild type.

B. At cellularisation, the pattern of Hb staining assumed an unusual disordered, punctate appearance. The same pattern was seen in *sun*$^{mat-}$ embryos stained for the Fushi tarazu (Ftz) or Even-skipped (Eve) proteins, indicating the onset of a global defect at cellularisation, coinciding with the temperature sensitive period of the *sun* maternal effect.

C. Expression pattern of Ftz in the syncytial blastoderm. Stripes 1 and 2, the most leftmost stripes, appear stronger than usual. Stripes 3 and 4 appear weaker than the others, and stripes 5, 6 and 7 are intermediate in strenght of expression. The normal order of Ftz stripe appearance is 1,2,3,5 and 7, followed by 6, and finally 4. The embryo shown has subtle differences in that stripe 6 appears stronger than stripe.

D. Eve expression prior to cellularisation also shows subtle defects. Stripes 1, 2, 3 and 7 appear stronger than 4, 5 and 6.

E. Engrailed (En) expression at 18°C. The embryo is clearly segmented, but the stripes of En expression are disrupted, being broader and more ragged than wild type. At 25°C, no stripes of En expression are seen, and En is limited to seemingly random patches in the embryo.

F. Hb staining after cellularisation. The gap gene expression has disappeared to be replaced by essentially random staining. The embryo shown has a greater level of Hb expression than most *sun*$^{mat-}$ embryos.

A. Hunchback

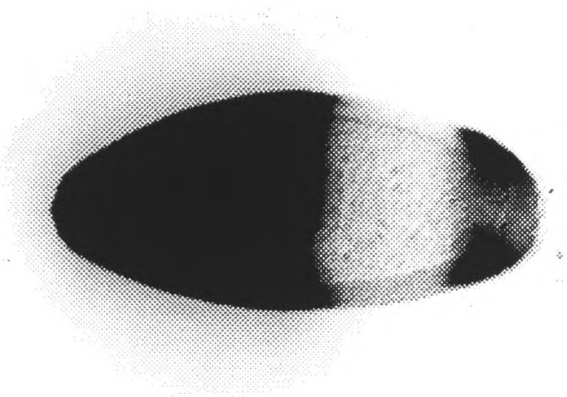

B. Hunchback

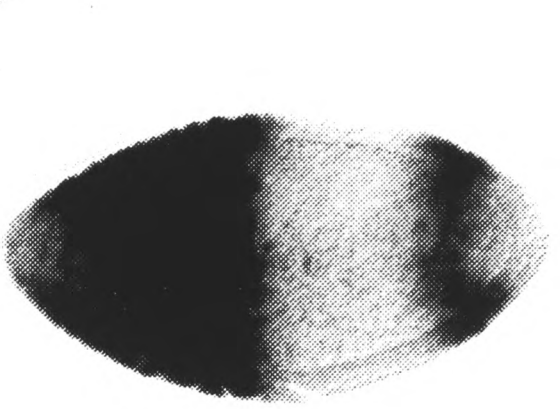

C. Fushi tarazu

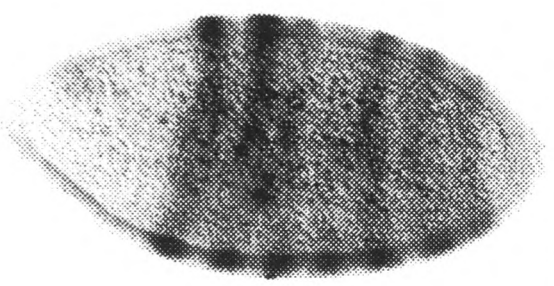

D. Even-skipped

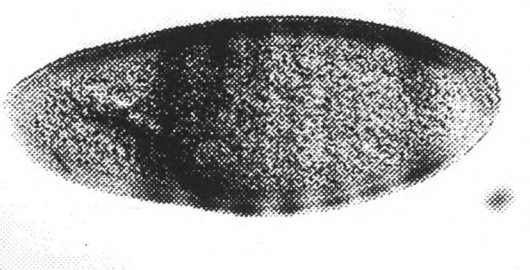

E. Engrailed at 18°C

F. Hunchback

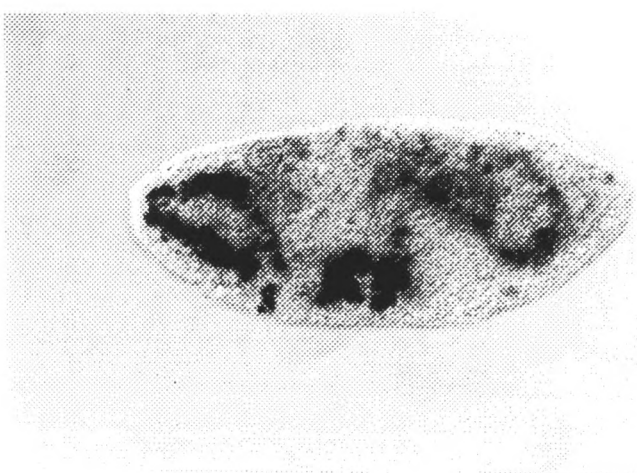

Allele	sun^{1}	sun^{EM67}	sun^{Y6}	sun^{Y52}	shrinkled	$sun^{42\text{-}3.0B}$	$Df(1)sd^{72b}$
sun^{1}	X	X	X	X	wing	sterile	X
sun^{EM67}	-	X	X	X	wing	10% fertile	X
sun^{Y6}	-	-	X	X	wing	sterile	X
sun^{Y52}	-	-	-	X	wing	X	X
shk	-	-	-	-	wing	wing	wing
$sun^{42\text{-}3.0B}$	-	-	-	-	-	fertile	X
$Df(1)sd^{72b}$	-	-	-	-	-	-	X

Table 5.5 Complementation analysis of *stunted* mutations

Complementation table for *sun* alleles; X: lethality, wing: *shk* wing phenotype in a proportion of flies. The mutation sun^{EM67} was not induced on an FRT chromsome, so it was recombined onto a chromosome with an FRT element integrated in region 19 ($FRT^{9\text{-}2}$). No fertilised eggs were recovered so sun^{EM67} either affects female fertility, which seems unlikely as it shows a weaker interaction with $sun^{42\text{-}3.0B}$ than the other lethal *sun* alleles, or it is a double mutant and the second mutation is germline lethal.

Examination of the pair rule genes *fushi tarazu (ftz)* and *even-skipped (eve)* revealed subtle changes in the strength of individual stripes of expression. The changes were not seen in wild type embryos, but it was difficult to attribute a segmentation defect to the alterations. The expression patterns of both Ftz and Eve did not resemble those originally obtained with the recombinant lines which showed greatly reduced or absent stripes. Furthermore at cellular blastoderm, the stripes assumed the same punctate appearance as shown by Hb. Ftz and Eve did not show increased expression at the anterior boundary of each stripe as is seen in wild type. The segment polarity gene *engrailed (en)* is a marker for segmentation and is expressed shortly after cellularisation. The characteristic 14 stripes of En were undetectable in sun^{mat-} embryos at the cellular blastoderm stage. En expression was seemingly random in single cells. The cells were rounded and the entire embryos appeared to lack overall structure, indicating that a global defect becomes apparent at cellularisation in embryos lacking maternal *sun* activity.

No conclusions about segmentation defects in sun^{mat-} embryos could be drawn from the antibody staining experiments. Segmentation gene expression is initially correct, as would be expected by the temperature sensitivity studies showing that the *sun* defect can be partially rescued by transfer to 18°C early in development. Later gene expression appears severely disrupted and it was not possible to establish whether correct segmentation had been established by examining En expression. At 18°C, En is expressed in stripes, but in many embryos these seem wider than usual. In addition, the cells in the stripes of expression do not seem able to adhere to each other and many of the stripes take on a very ragged appearance (figure 18 E).

5.8 Summary of genetic data

Complementation tests between all the mutations and the deficiency which contains *sun* were carried out (table 5.5). The data indicates the pleitropic nature of the *sun* gene with roles in early embryogenesis, female fertility and wing development. It is not possible to say whether *sun* has a role in segmentation or neurogenesis. In the next chapter I describe the underlying defect in the maternal effect of *sun* which accounts for all the observations of early embryogenesis made in this chapter. The cloning of a candidate gene is also described in chapter 6, and its sequence provides clues to the role of *sun* in normal development.

Chapter 6. Characterisation of the *stunted* locus

6.1 Introduction

No common phenotypic theme emerged from studies of the *sun* mutant phenotypes, particularly not with regard to segmentation, the original reason for studying the *sun* maternal effect (chapter 5). The failure to detect significant En or Hb staining after cellularisation of sun^{mat-} embryos suggested they are already abnormal at this stage. In wild type embryos, blastoderm cells form a very regular pattern which is visible by phase microscopy. The surface of sun^{mat-} embryos was examined and the cells found to be highly irregular in shapes and sizes. This phenotype is very similar to that of the *nullo* cellularisation mutant, so prompted a investigation of the early mitotic and morphogenetic events in sun^{mat-} embryos. In this chapter, I present evidence that *sun* is required for cellularisation and encodes a cyclin-related protein.

6.2 Most *sun* embryos show normal nuclear behaviour during cycles 1-14

The early *Drosophila* embryo undergoes very rapid synchronous mitoses without cytokinesis, accompanied by the nuclear migration events of axial expansion and cortical migration (chapter 1.2). Once the nuclei have arrived at the plasma membrane, they undergo a further 4 mitoses prior to cellularisation (the blastoderm mitoses). Nuclear migration and organisation were examined using the nuclear stain DAPI and fluorescent microscopy.

sun^{mat-} embryos were initially checked for gross abnormalities in the pattern of nuclear migration. Both axial expansion and cortical migration appeared normal when compared to wild type controls. However about 17% of *sun* embryos are highly irregular, with fluorescent material of all sizes and morphology scattered throughout the embryo (figure 6.1). These embryos can not be classified according to nuclear cycle but are present in

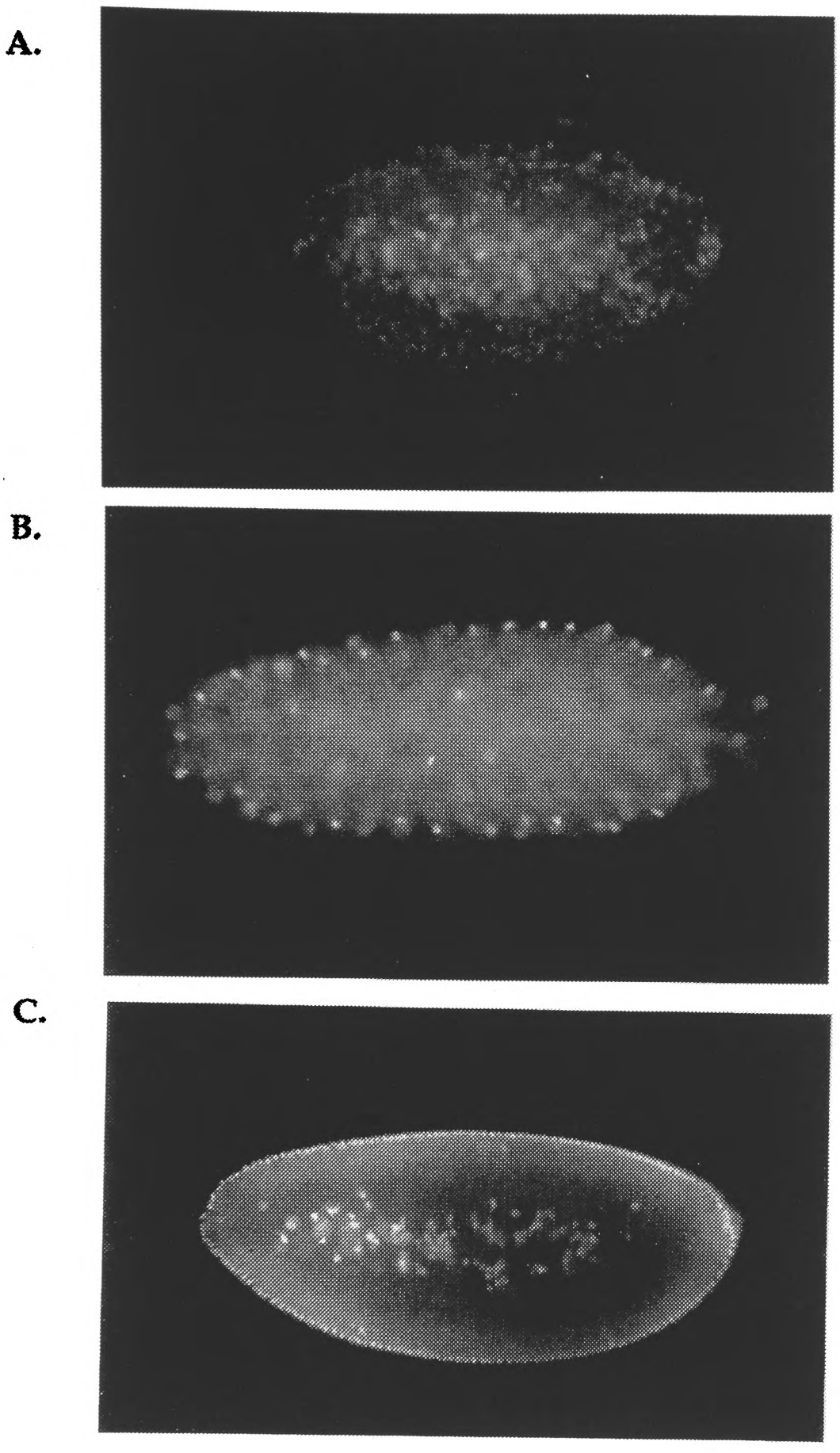

Figure 6.1 DAPI staining of embryos lacking maternal *sun* activity

Fluorescent micrographs of sun^{mat-} embryos stained with DAPI. **A.** About 17% of sun^{mat-} embryos show a very disrupted pattern of nuclear staining. The embryo shown is a mild example and still retains some overall structure. **B.** The remaining embryos complete axial expansion and cortical migration successfully. **C.** During the syncytial mitoses, nuclei fall back into the centre at a slightly higher frequency than wild type.

DAPI stained embryos		Nuclear cycle			Total
		1-6	7-10	11-14	
Wild-type	**Normal**	67	33	28	128
	Abnormal	2 (3%)	2 (6%)	2 (7%)	
stunted	**Normal**	44	28	43	138
	Abnormal	2 (4%)	1 (3%)	7 (16%)	
A further 23 sun embryos were highly abnormal					

Table 6.1 Nuclear behaviour in wild type and *sun* embryos

The nuclei of wild type and *sun* embryos were stained with DAPI and examined for defects in morphology, spacing between nuclei and position relative to the plasma membrane. Rough counts of nuclei established the nuclear cycle of the embryo. 23 sun embryos were highly disorganised containing fluorescent material (DNA) of variable sizes and shapes (see figure 7.1) and could not be assigned to a nuclear cycle.

collections of embryos with an average age of 0.5h, suggesting that the phenotype is the result of a disruption in oogenesis, not embryonic development.

The normal looking *sun* embryos were examined for defects in spacing between nuclei and position relative to the plasma membrane (table 6.1). Wild type embryonic nuclei show approximately equidistant spacing between each other, and nuclei which encounter a division error fall back into the centre of the embryo (figure 6.1). sun^{mat-} embryos show a slight increase in these defects relative to wild type but only during the blastoderm mitoses (cycles 10-13). This result is consistent with the finding that the temperature sensitive period of *sun* does not lie in the first hour of development (see figure 5.6). Nuclei are cellularised during the third hour of development, and as cells in sun^{mat-} embryos are highly irregular in shape, the events of cellularisation were investigated in sun^{mat-} embryos.

6.3 The actin network at cellularisation is abnormal in *sun* embryos

In wild type embryos, actin and myosin are organised into a highly regular hexagonal network at the start of cellularisation (chapter 1.5). In sun^{mat-} embryos the blastoderm cells are highly irregular in size and shape suggesting that the actin-myosin network might also be disrupted. FITC-labelled phalloidin was used to stain for actin and the sun^{mat-} embryos were examined by confocal microscopy. As seen in figure 6.2, the actin network was highly irregular. The actin hexagons were different sizes, and the 'sides' of the hexagons were different lengths and thicknesses. In more severely affected embryos, parts of the actin network were missing, so large cells with several nuclei were formed. Occasionally, the actin network was almost completely absent apart from dense brightly stained small spots (figure 6.2).

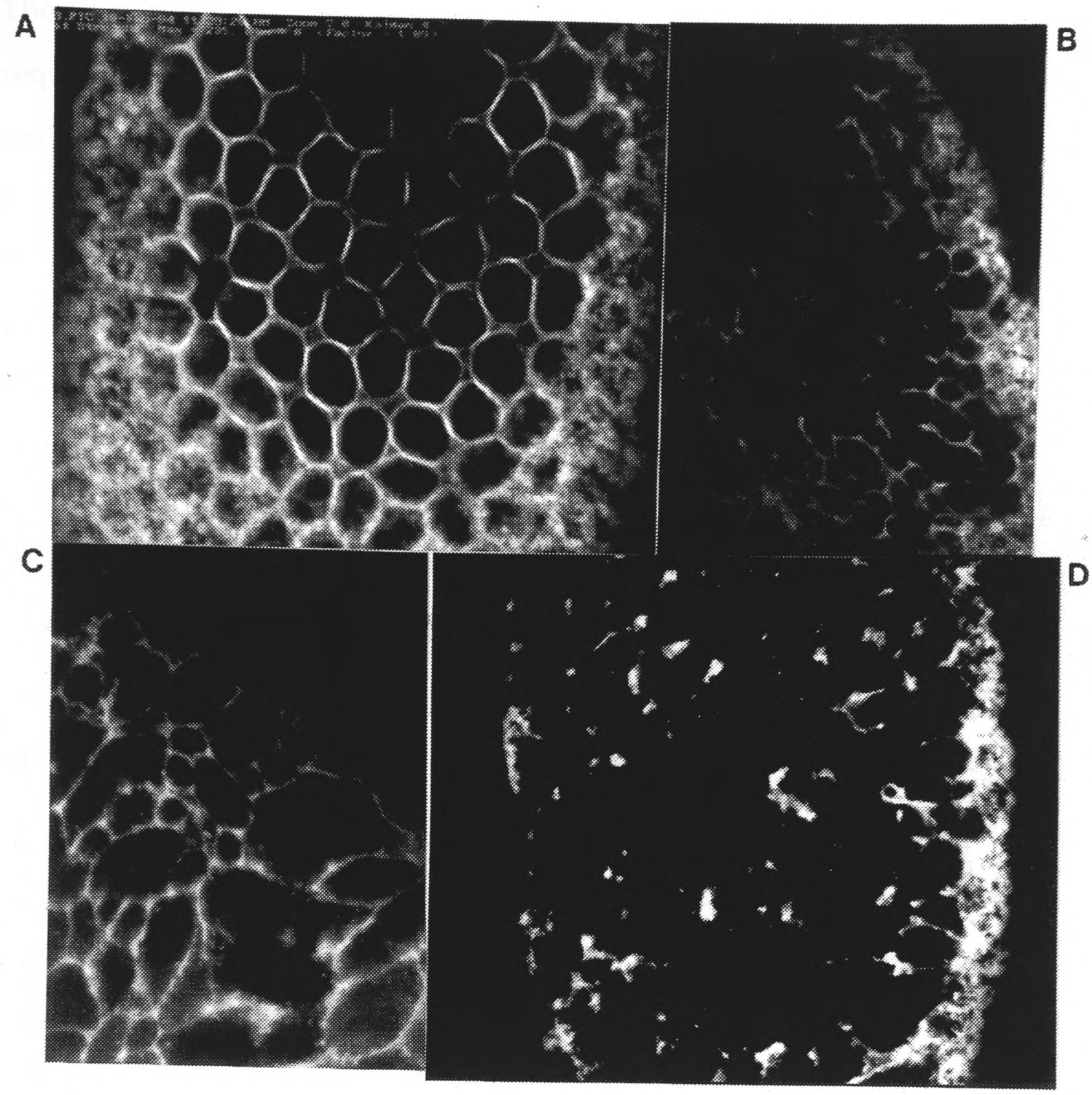

Figure 6.2 Actin distribution in cellularising *sun*$^{mat-}$ embryos

Actin distribution at cellularisation visualised with FITC-phalloidin and confocal microscopy. **A.** Wild type embryo with regular hexagonal actin network. **B, C.** *sun*$^{mat-}$ embryos with irregular actin networks. **D.** *sun*$^{mat-}$ embryo with the actin network almost completely absent.

The zygotically expressed loci *serendipity-alpha (sry-α)* and *nullo* are required for cellularisation; mutations in either lead to defects in the actin network similar to that of sun^{mat-} embryos. The *sry-α* and *nullo* gene products localise to the actin network during cellularisation (Schweisguth et al., 1990; Postner and Wieschaus, in press). Localisation of Sry-α is dependent on *nullo* activity; in *nullo* mutants, Sry-α fails to localise (Postner and Wieschaus, in press). Mislocalisation of either gene product could explain the phenotype of sun^{mat-} embryos. The distribution of Sry-α was examined in sun^{mat-} embryos using an antibody raised against Sry-α and confocal microscopy. Sry-α still localised to the actin network despite the network's irregular nature (figure 6.3). As Sry-α localisation is dependent on *nullo* activity, Nullo must also be expressed and localised. Maternal *sun* activity is therefore not required for the expression or localisation of the *nullo* or *sry-α* gene products.

Cells did form in sun^{mat-} embryos although they were highly irregular in size and shape, because the furrows invaginated in a highly irregular fashion when compared to wild type (figure 6.4). This suggests that the actin-myosin network is functional, but is established incorrectly due to an initial defect earlier in the development of sun^{mat-} embryos. DAPI staining showed a slight increase in the frequency of nuclear defects in sun^{mat-} embryos during the blastoderm mitoses, and so actin distribution was examined in younger sun^{mat-} embryos prior to cellularisation.

6.4 Actin is mislocalised during the syncytial mitoses in *sun* embryos

In wild type embryos, the cortical actin accumulates above the nuclei in 'actin caps' as they arrive at the plasma membrane during nuclear cycle 10. During mitosis, the actin caps reorganise into two 'half crescents' at each end of the mitotic spindle above the centrosomes. Following chromatin separation, the crescents reform into caps above the new nuclei. In sun^{mat-}

Wild type

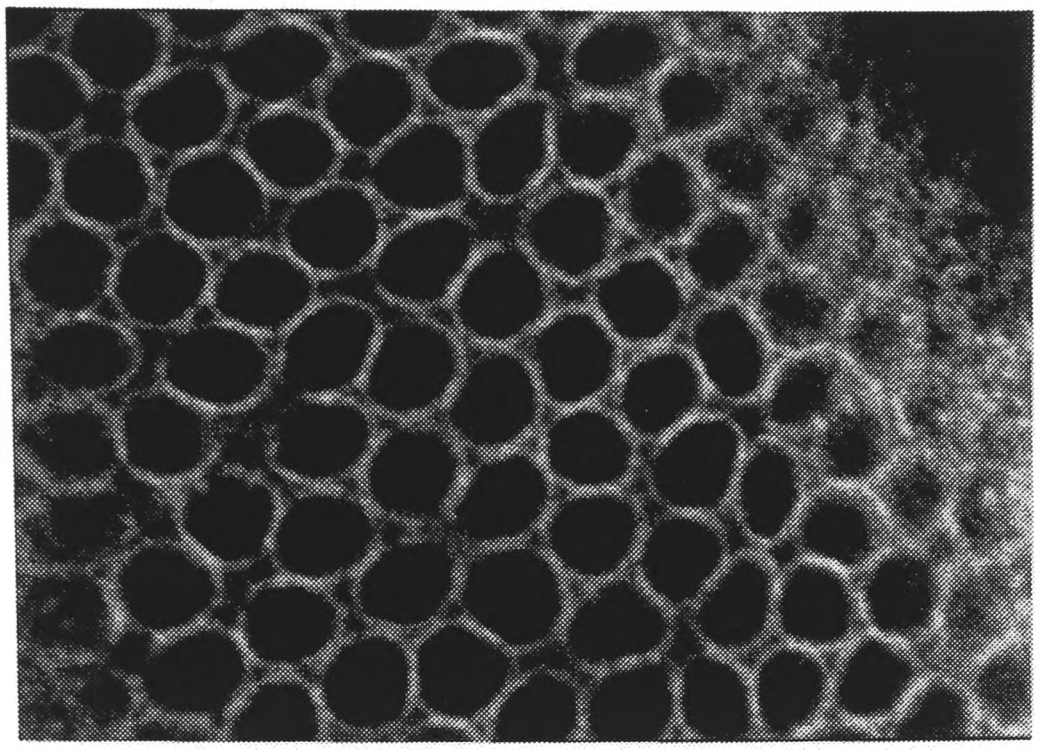

***sun*$^{mat-}$**

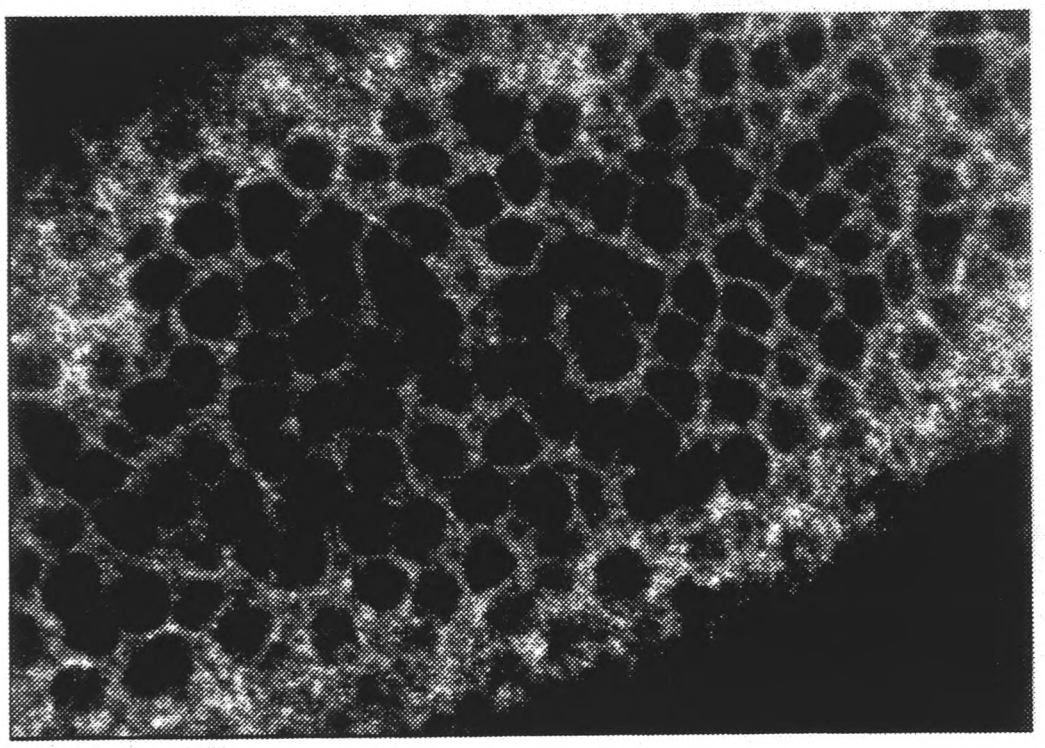

Figure 6.3 Localisation of Sry-α protein in *sun*$^{mat-}$ embryos

The Sry-α protein localises to the actin network during cellularisation both in wild type and *sun*$^{mat-}$ embryos. In the *sun*$^{mat-}$ embryos, the irregular distribution of Sry-α protein reflects the disrupted actin network.

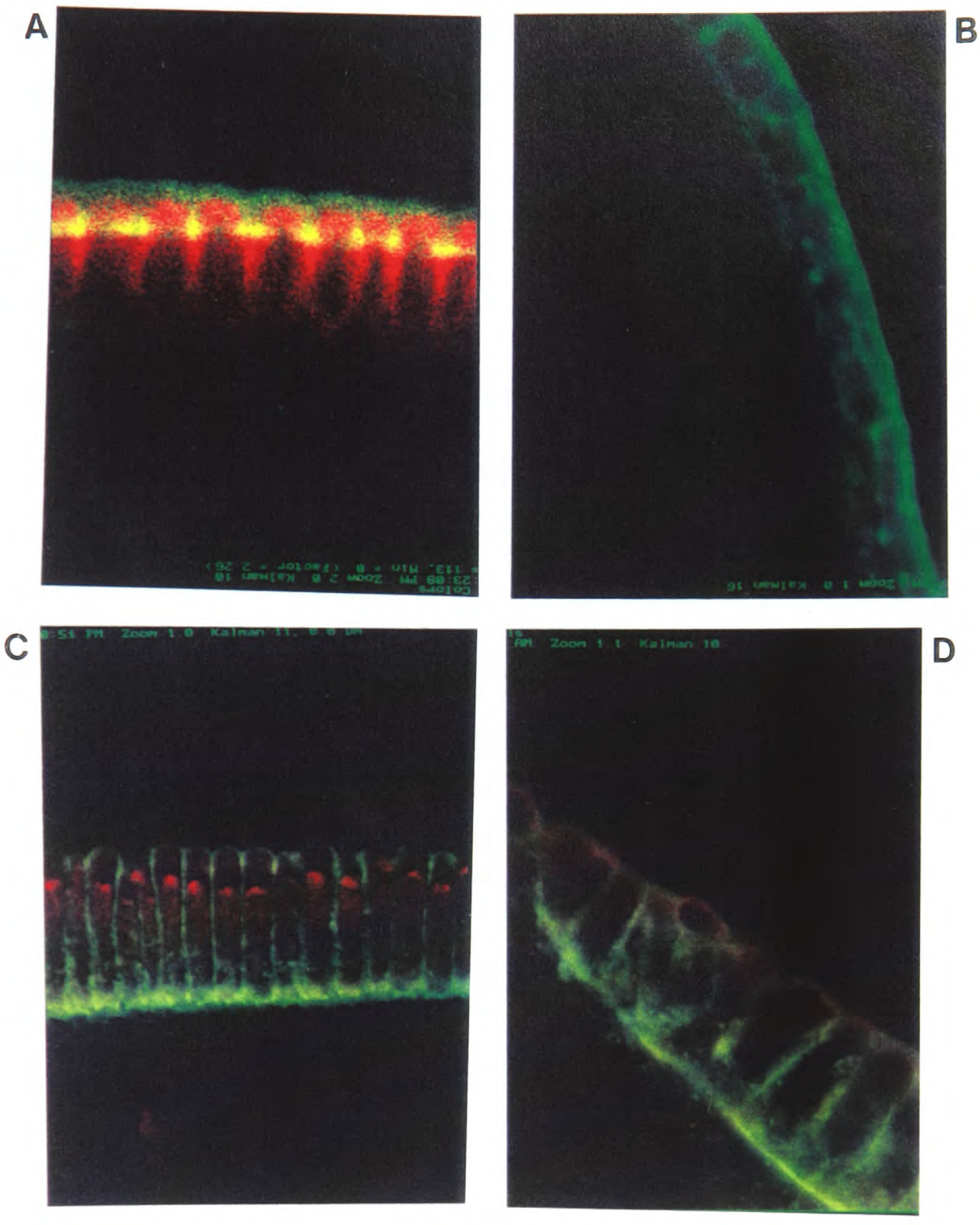

Figure 6.4 Cellularisation occurs in *sun*$^{mat-}$ embryos

Wild type and *sun*$^{mat-}$ embryos stained for actin (green), microtubules (red in A and D) and nuclei (red in C). **A.** In wild type embryos, furrow invagination during cellularisation is a highly regular synchronous process, as indicated by the positions of the membrane fronts (yellow). **B.** In *sun*$^{mat-}$ embryos, the furrows invaginate in a highly irregular manner; the direction of movement is often not perpendicular to the plasma membrane. **C.** A cellularised wild type embryo showing the uniform nature of the cells; cell walls are all perpendicular to the plasma membrane and parallel with adjacent cell walls. **D.** In *sun*$^{mat-}$ embryos, cells do form, but they are of different sizes and shapes, and lack the uniformity seen in wild type embryos.

embryos, actin caps do not form. Instead, actin is excluded from the region above each nucleus, and from above the poles of the mitotic spindle (figure 6.5). The zones of actin depletion may be the result from exclusion of actin by microtubule arrays which are nucleated by the centrosomes. The failure to localise actin correctly is the first visible defect in sun^{mat-} embryos.

This phenotype is very similar to that of the maternal effect mutation *sponge (spg)*. Embryos lacking *spg* activity fail to form actin caps, and zones of actin depletion occur above the nuclei. During the later mitoses *spg* embryos fail to form metaphase furrows, and in strong *spg* alleles very few cells are formed during cellularisation. The absence of metaphase furrows in *spg* embryos leads to the nucleation of mitotic spindles between inappropriate centrosomes. As actin defects lead to microtubule defects in *spg* embryos, sun^{mat-} embryos were examined for microtubule defects.

6.5 Microtubule behaviour in *sun* embryos appears normal

Microtubule patterning appeared normal in sun^{mat-} embryos. β-tubulin was visualised by antibody staining and confocal microscopy. No abnormal nucleation events between inappropriate centrosomes were seen during mitosis (figure 6.6). Therefore, although sun^{mat-} and *spg* embryos share the same defect of failing to localise actin, the *sun* maternal effect does not seem to affect the formation of metaphase furrows.

6.6 Summary of the sun^{mat-} embryonic phenotype

The *sun* maternal-effect gene is required for cellularisation. The first visible disruption in sun^{mat-} embryos was during the syncytial mitoses, when there was a failure to localise actin to caps. Nuclear and microtubule behaviour resembled wild type. At the start of cellularisation, the actin-myosin network formed, but in a highly irregular way. In order to help

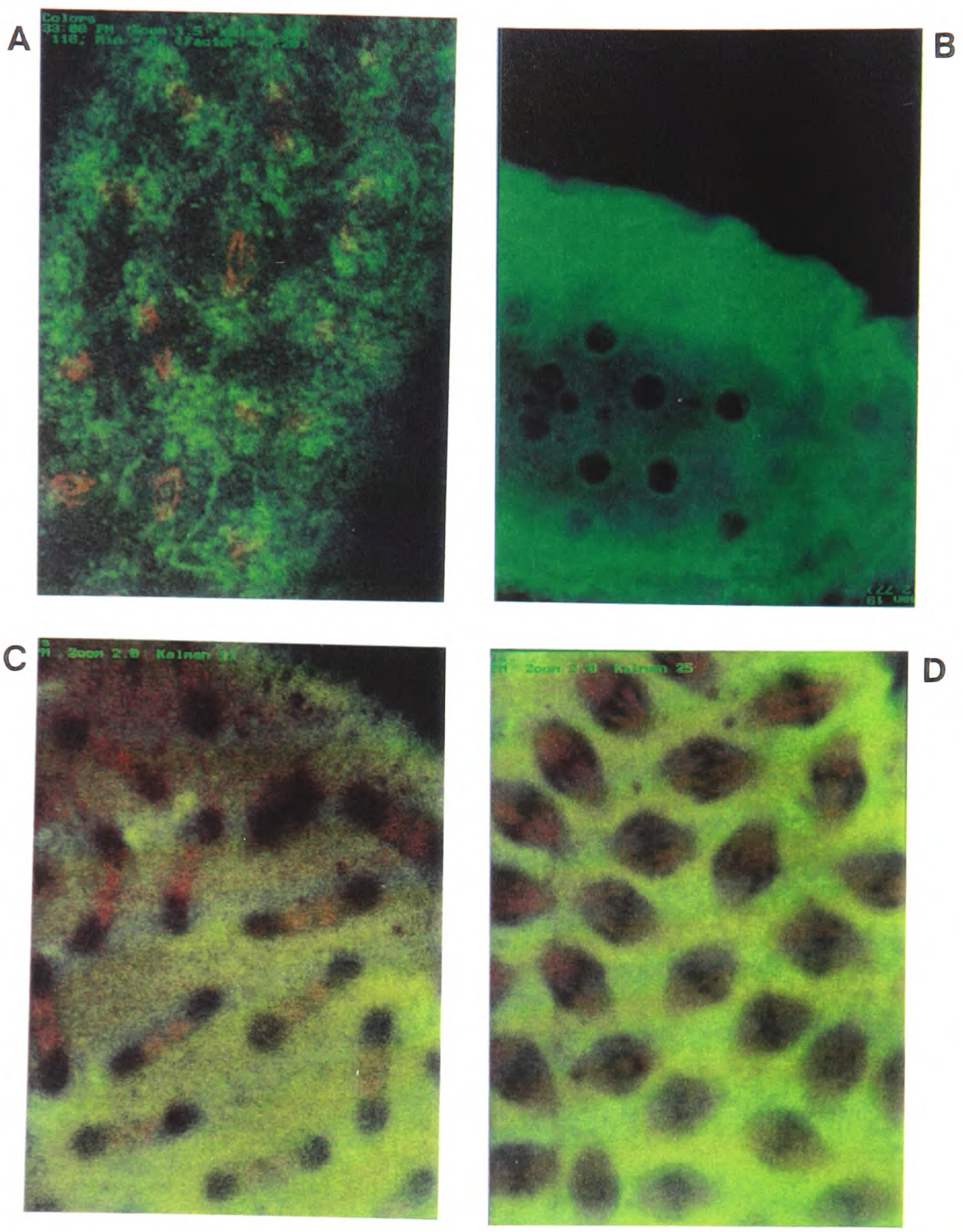

Figure 6.5 Actin localisation in *sun*$^{mat-}$ syncytial blastoderm embryos

Embryos stained for actin (green) and microtubules (red). **A.** A wild type embryo with actin clustering to form caps above the spindle poles. **B. in** *sun*$^{mat-}$ embryos, actin caps do not form. Instead, zones of actin depletion form above nuclei as they arrive in the periplasm. **C.** During mitosis, the zones of actin depletion are located above the spindle poles. **D.** In an older embryo, actin caps still do not form, although actin is no longer excluded from above the poles, perhaps due to the higher nuclear density.

Figure 6.6 Spindle behaviour in *sun*$^{mat-}$ embryos

Spindles were visualised with an antibody against β-tubulin. No evidence of abnormalities was seen in *sun*$^{mat-}$ embryos. Spindles have normal morphologies and are independent of each other.

understand the molecular basis for these phenotypes, I attempted to clone and characterise the *sun* gene.

6.7 Cloning of a candidate gene for *sun*

The zygotic lethality of the *sun* mutation is rescued by a P element construct containing 11.6kb of genomic DNA (chapter 5.3). The fragment of DNA encompasses the *Myb* gene which complements *l(1)EM67*, suggesting *sun* is in the remaining 9.2kb of the fragment (figure 6.7). A Northern blot of maternal RNA was probed with the EcoRI fragment M7-C which is located at the centre of the 9.2kb (figure 6.7). Two bands were seen on the autoradiograph, and when the same blot was reprobed with the flanking EcoRI fragments M7-D and M7-A, no further bands were seen. The two maternal transcripts should therefore be derived from the *sun* locus, and be detectable in a maternal cDNA library using M7-C as a probe.

A random primed maternal cDNA library constructed in λgt11 was screened with the M7-C EcoRI fragment. Ten positive clones were recovered, their inserts amplified by PCR and analysed by restriction enzyme digests. Two clones matched the restriction map of the genomic region when analysed and so were investigated further (figure 6.8).

The cDNAs were recovered as EcoRI fragments from the λ clone digests, which were subcloned into Bluescript. As the two cDNA clones recovered had an internal EcoRI site, each clone consisted of two subclones (figure 6.8). The largest EcoRI subclone contains a polyA tail at the distal end, and stop codons in all three reading frames at the proximal end. Sequencing of both strands revealed an open reading frame (figure 6.9). Sequencing of the 330bp upstream of the EcoRI site did not reveal any open reading frames.

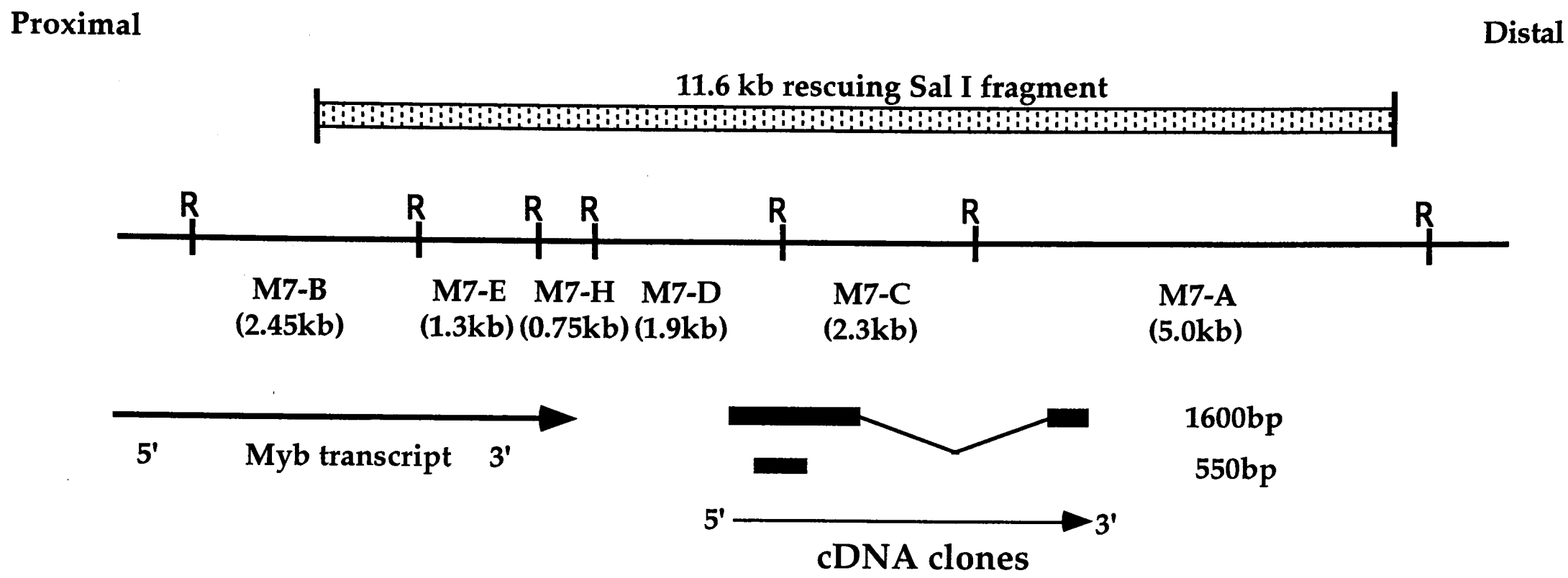

Figure 6.7 Structure of the genomic region distal to the Myb gene

Restriction mapping of the Drosophila Myb gene and downstream regions. EcoRI sites are denoted by R. Each EcoRI fragment is denoted by a letter and the size is indicated underneath. The SalI fragment which rescues *sun* when transformed into the fly is indicated at the top. Below is the Myb transcript and two maternally expressed cDNAs which lie downstream. The position of the second exon of the 1600bp clone is not known; it includes a ClaI site and there are two ClaI sites in M7-A. Restriction map and position of Myb supplied by A. Katzen (UCSF).

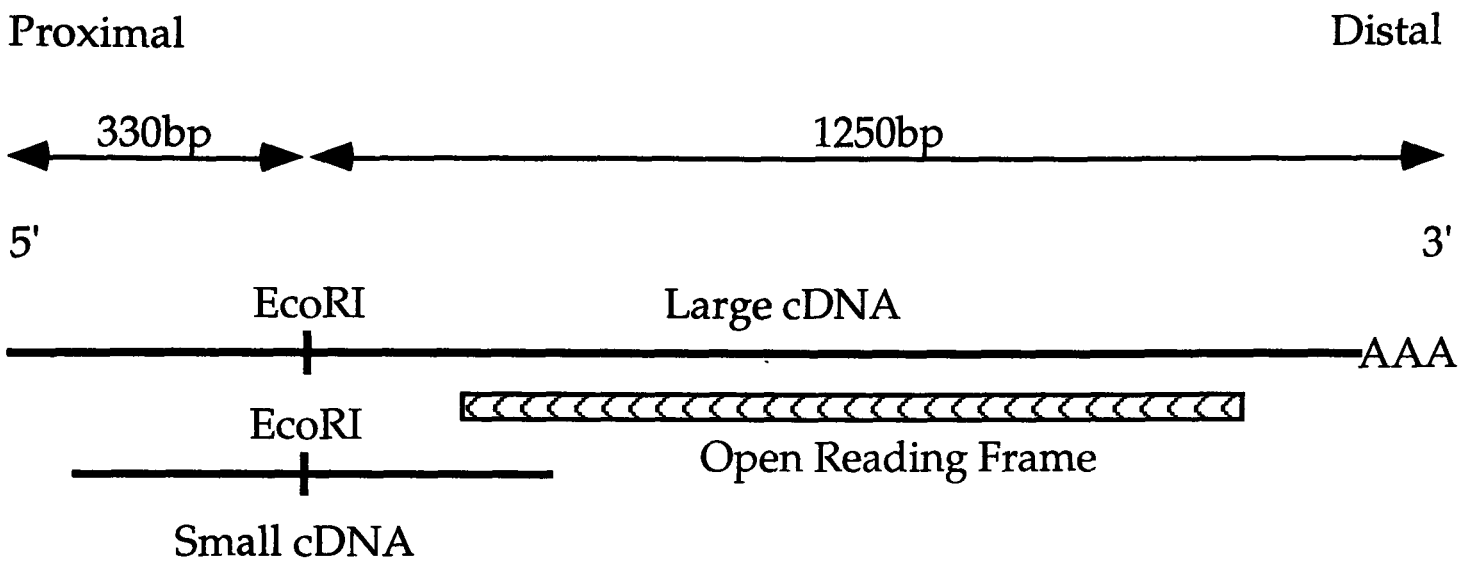

Figure 6.8 Map of the maternal cDNAs recovered

Map of two overlapping cDNAs recovered by screening a λgt11 maternal cDNA library with M7-C (figure 7.7) as a probe. The lines represent the cDNAs and the hatched box the predicted open reading frame in the large EcoRI fragment of the large cDNA.

```
GAATTCGGATGGGCAGTTAAGTCAGTGAATTACTGAATCACTTGAAGACACAAAA        57

AACAAATACGAACTGCAACCCTCTCGCCATGTCGGTAACATCTTCGATTGAGAAG       112
                                    M  S  V  T  S  S  I  E  K
CCAACAACCACAGCAAGTGCAATTCAGCAACAGTATCAGCATCAGCAGCAGCAA        166
P  T  T  T  A  S  A  I  Q  Q  Q  Y  Q  H  Q  Q  Q  Q
CAGCAACAGAAGCCACAACAGCAACAACAGCAGGATAAAAGCAGCACCATCGCA        220
Q  Q  Q  K  P  Q  Q  Q  Q  Q  Q  D  K  S  S  T  I  A
ATCGCAGCAGCAGCAGGACAGCAACAAAAGCGCAAATCCCTGAGTTCCAAGCGC        274
I  A  A  A  A  G  Q  Q  Q  K  R  K  S  L  S  S  K  R
TCGTATTCGCTATCCTCGTCGAGCGCCTCCAGTTCTGGTTCCTTTGGGGCGATA        328
S  Y  S  L  S  S  S  S  A  S  S  S  G  S  F  G  A  I
AGGTCTGCGACATCGCCACTGGTCACCACCGCCGAGAGGGAGAAAGATAAGGAG        382
R  S  A  T  S  P  L  V  T  T  A  E  R  E  K  D  K  E
AAGAGCTCCTCCTCGGCCAGCAATACCCACCATCAACATCATCAGCTTCATCAA        436
K  S  S  S  S  A  S  N  T  H  H  Q  H  H  Q  L  H  Q
CACCAACATCATCATCAGCAGCAGCAGTCGCAGCAGCAGCAGCAATCCTTTTTG       490
H  Q  H  H  H  Q  Q  Q  Q  S  Q  Q  Q  Q  Q  S  F  L
CCGTACTCATATTGCACCGATACCATAGCAGCAGTACATCATCAACGACAGTCG        544
P  Y  S  Y  C  T  D  T  I  A  A  V  H  H  Q  R  Q  S
TACGCGCTGGTCCAGAAGCCCCCATCGTTGCGCTACCAGGGAAAGCCCCATCAT       598
Y  A  L  V  Q  K  P  P  S  L  R  Y  Q  G  K  P  H  H
CAGCTGAGCAACTTCTCGCCCACGATGACCTCCTCGGAACCCTCATCCCCATTG        652
Q  L  S  N  F  S  P  T  M  T  S  S  E  P  S  S  P  L
GCCGCCGATGGTTGCGGATCCGGAATCCTTAGCCCATCGGAGGTCGCCACCCAT       706
A  A  D  G  C  G  S  G  I  L  S  P  S  E  V  A  T  H
TGTTGCGCCAATGTCAAGGCCAATATCACCACCCCATTGGCCACCACCACACAG        760
C  C  A  N  V  K  A  N  I  T  T  P  L  A  T  T  T  Q
AAAATGCACCGAACAATACCATCTGATAAAATTAACCTACGCCTCATTCTTGTT        814
K  M  H  R  T  I  P  S  D  K  I  N  L  R  L  I  L  V
AGTGGTAAAACAAAAGAGTTTATTTTTAGCCCTTCAGATTCCGCAGGTGATATT       868
S  G  K  T  K  E  F  I  F  S  P  S  D  S  A  G  D  I
GCACAAACAGTATTTGATAATTGGCCAGAAGATTGGACCCACGAAACTGTGTCG        922
A  Q  T  V  F  D  N  W  P  E  D  W  T  H  E  T  V  S
AAAGCCGAAATCTTGCGCTTAATTTATCAAGGTCGTTTTCTTCATTGCAATGTA       976
K  A  E  I  L  R  L  I  Y  Q  G  R  F  L  H  C  N  V
ACCTTAGGAGCACTGGGACTTCCATTAGGCAAAACGACTGTTATGCATTTAGTG       1030
T  L  G  A  L  G  L  P  L  G  K  T  T  V  M  H  L  V
CCACGTGATAATTTGCCAGAGCCCAATTCACAAGATCAAAGACAAAATAGTAAA       1084
P  R  D  N  L  P  E  P  N  S  Q  D  Q  R  Q  N  S  K
GGCGGTTCTGGACGATGCTGTTCGACAAATTGCTCTATTTTGTAACTAAATTAT       1138
G  G  S  G  R  C  C  S  T  N  C  S  I  L  .

TATATAATAGCGTAATATTTAAACTAATTTGCATTAAAAGAAAAAAGAAAAAAA       1192
AAAACACCCACAACCGAAAAAAAAAAAAAAAAAAAAAAAAAAAAAAAAAAAAA        1246
AAAAAAAAAAAAA
```

Figure 6.9 Sequence of cDNA clone and predicted open reading frame

Partial sequence of large cDNA clone from the internal EcoRI site to the polyA tail. The predicted open reading frame is shown.

6.8 Sequence analysis of the candidate Sun protein

The large EcoRI fragment contained an open reading frame (ORF) coding for a 347 amino acid protein (figure 6.9). The predicted protein was basic with a pI of 9.73 and a molecular weight of 38kD. The amino terminus is composed of a glutamine rich region, a serine rich region and a second glutamine rich region. At the carboxy terminus was a putative prenyl group binding site. Hydropathy analysis did not reveal any potential transmembrane domains (figure 6.10).

Glutamine rich regions are found in a variety of proteins, mainly transcription factors in which they are associated with transcriptional activation, but also cytoplasmic proteins, eg. Notch. The cellularisation specific proteins, Nullo and Bottleneck (Bnk) are also small basic proteins and are both cytoplasmic. As *sun* is not required for expression of *sry-α* or *nullo*, it is unlikely to be a transcription factor and have a nuclear location.

Homology searching revealed a distant homology to the CyclinA family of cell cycle proteins (figure 6.11). The predicted Sun protein shows similarity to the amino terminal two-thirds of the most conserved region of the cyclin sequences, the cyclin box, which is responsible for kinase binding.

The cyclins have a weak but significant homology with Ras proteins (Leopold and O'Farrell 1991). The small Ras related GTPase proteins rac and rho mediate changes in the actin cytoskeleton (Ridley and Hall, 1992; Ridley et al., 1992). Like other members of the Ras superfamily, both are localised to the membrane by attachment of prenyl groups. Direct comparisons between the predicted Sun protein and members of the Ras family did not reveal any significant homologies.

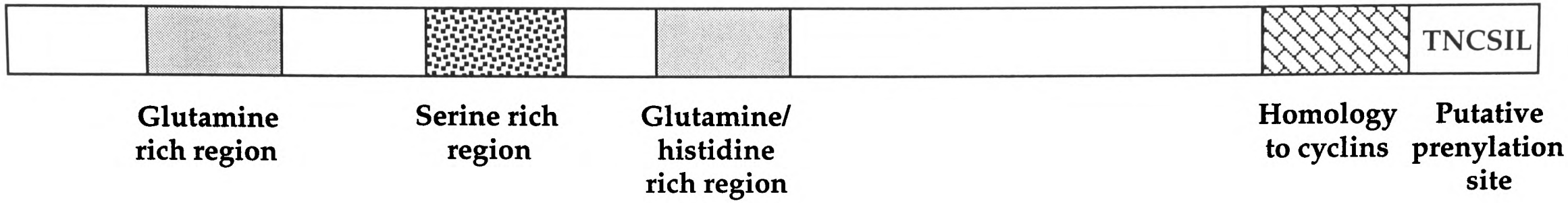

Predicted:

347 amino acids

Molecular Weight 38kD

pI 9.73

15% glutamine

12% serine

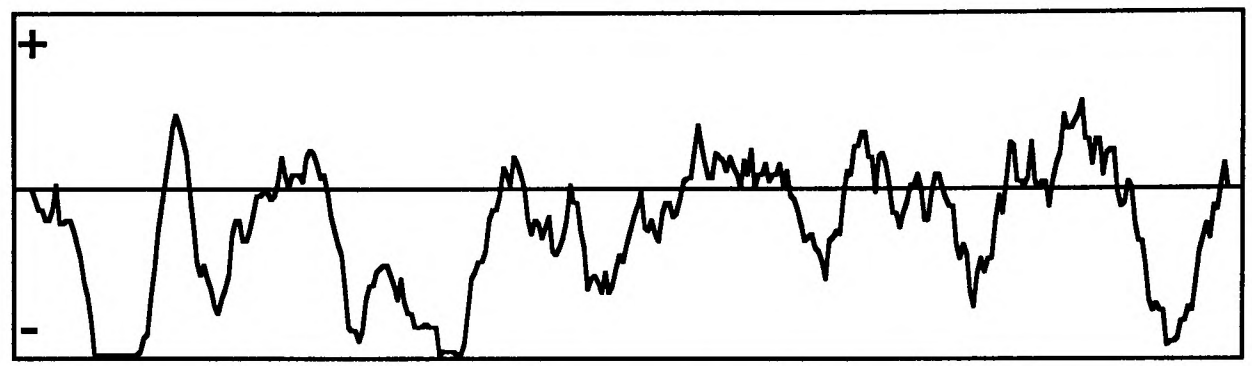

Hydropathy analysis reveals no transmembrane domains

Figure 6.10 Features of the candidate Sun protein

The candidate Sun protein is a small, basic protein, with two amino terminal glutamine rich regions, a feature normally found in transcription factors, but also some cytoplasmic proteins. There is a putative prenylation site at the carboxy terminus which could serve as a membrane anchor. No likely transmembrane regions are seen in the hydropathy plot. There is also a carboxy terminal domain with homology to the cyclins (see figure 6.11).

(i)

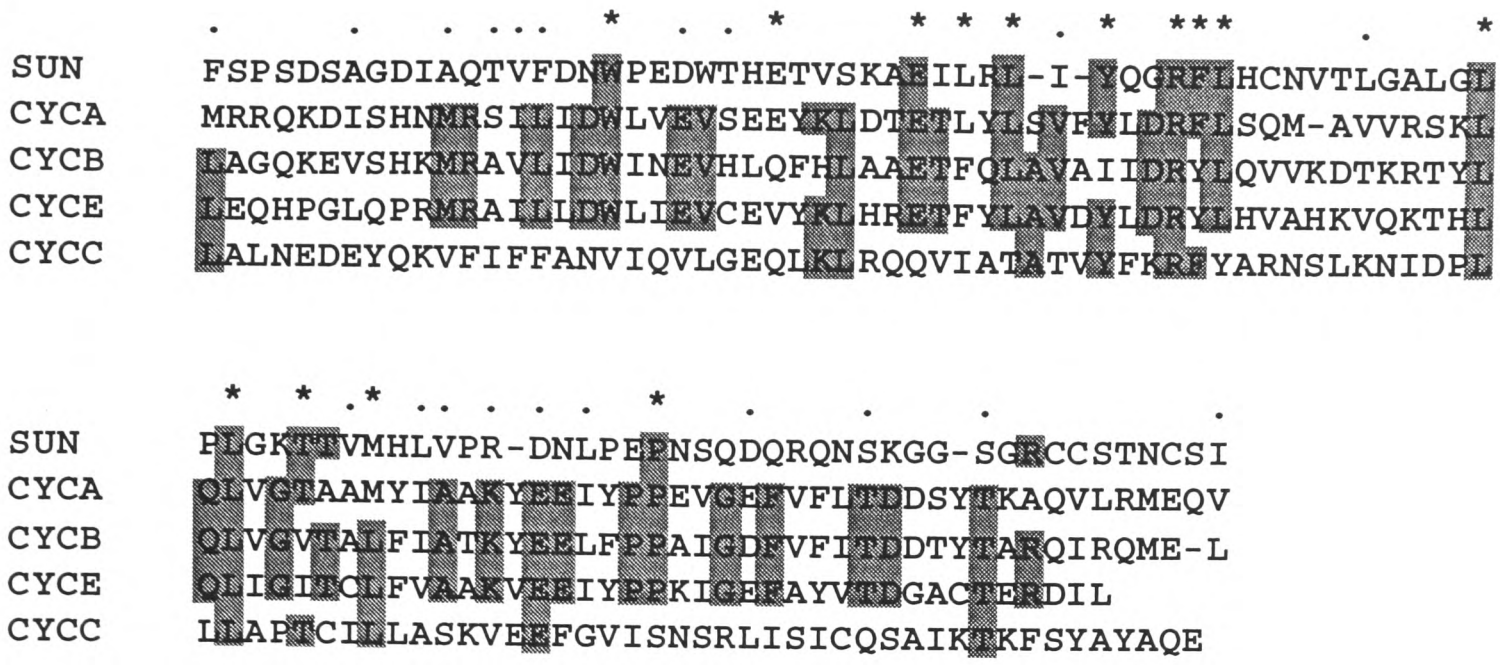

(ii)

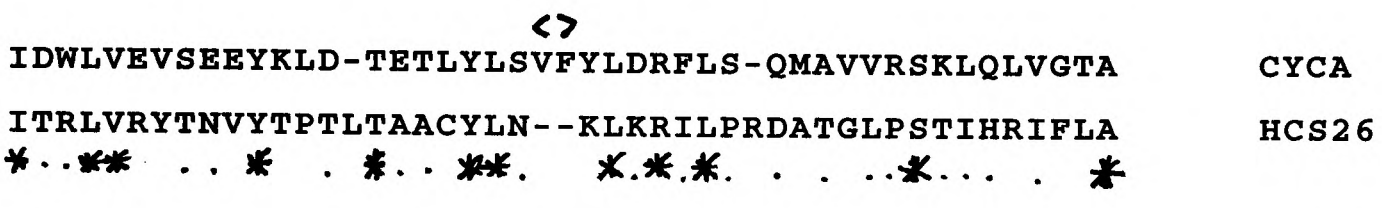

Figure 6.11 Similarity of predicted Sun protein to cyclins

(i) Comparison of the predicted Sun protein with Drosophila cyclins A, B, E and C. Above each sequence, matches between Sun and cyclin A are indicated by '*', conservative substitutions by '.'; **(ii)** To make the alignment between the predicted Sun protein and the cyclins, two insertions have to be introduced. Spacing is crucial to cyclin activity and very minor insertions and deletions can abolish activity (T.Hunt, pers. comm.). However, alignment of the distantly related cyclin HCS26 and cyclin A requires the introduction of two spaces (<>) in the same place as the two insertions made in the candidate Sun protein. The homology to cyclinA was discovered using PROSRCH6 (J.F. Collins and A.F.W. Coulson), running on a distributed array processor (DAP). Multiple sequence alignments were generated using the CLUSTAL program (D. Higgins and P.M. Sharp)

6.9 Discussion

Although early *sun* stocks showed a *run*-like phenotype, current stocks show the cellularisation phenotype described above. The reason for the early results is unclear, but the above results suggest that the effects of maternal *sun* on segmentation are indirect. This chapter shows that *sun* is required for actin localisation in the syncytial blastoderm and for cellularisation. The segmentation defects seen in the cuticles of sun^{mat-} embryos grown at 18°C may result from localised defects in cellularisation affecting segmental patterning.

The phenotypic analyses of *sun* suggest it is defective in cell division. A large number of zygotic lethal mutations affecting cell cycle functions have been shown to complete embryogenesis using maternally supplied components, and only begin to die when proliferation of the imaginal tissues begins in the larvae (Gatti and Baker, 1989). The *sun* zygotic component is indispensable for the larval/pupal stages (chapter 5.3), coinciding with imaginal proliferation. Maternal effect mutants which exhibit extensive mitotic division errors, such as *nuclear fallout (nuf)*, display initial defects in cytoskeletal structures which are followed by abnormal cellularisation, a pattern seen in sun^{mat-} embryos. Mitotic mutants can also affect adult fertility, eg. *abnormal spindle* (Ripoll et al., 1985). Sterility is associated with $sun^{42\text{-}3.0B}$, and possibly *shk* (chapter 5.3 & 5.4).

One model to explain the *sun* phenotype is that sun^{+} is required for cytokinesis, despite the first major disruptions in sun^{mat-} embryos occurring at cellularisation. Although cellularisation occurs during interphase, it resembles normal cytokinesis in several respects and has been described as 'monopolar cytokinesis', ie. standard cytokinesis without centrosome separation (Foe et al., 1993). Actin is critical for normal

cytokinesis; the yeast *cdc3* mutant is specifically defective in cytokinesis, and the *cdc3* gene codes for a profilin, an actin binding protein (Balasubramanian et al., 1994). Actin organisation is disrupted in *sun* embryos. As *sun* has roles throughout development, it would not be surprising to find it playing a role in normal mitoses. The imaginal discs and neuroblasts of zygotically deficient *sun* larvae have not yet been examined, but could provide further clues to the *sun* phenotype, particularly whether cells stall at a specific point in the cell cycle. The model predicts that in *sun* larvae, neuroblasts would be polyploid due to continuing DNA replication in the absence of cell divison, as is seen for the *spaghetti-squash* mutant in which cytokinesis is disrupted (Karess et al., 1991).

The *peanut (pnut)* gene is also required for cytokinesis, and mutations lead to polyploid neuroblasts and death during the larval pupal stages (Neufeld and Rubin, 1994). The Pnut protein has homology to yeast proteins which localise to the bud neck during cell division. Pnut localises to the cleavage furrow of dividing cells, and to the front of the invaginating membranes during cellularisation. The localisation suggests that $pnut^{mat-}$ embryos will show cellularisation defects. Females rescued by a construct allowing heat shock induced expression of *pnut* are sterile unless kept at an inducing temperature. Clearly, *pnut* has phenotypic similarities to *sun* supporting the model that *sun* is required for cytokinesis.

The zygotically acting *pebble (pbl)* locus is required for cytokinesis during mitoses 14, 15 and 16 (Hime and Saint, 1992; Lehner, 1992). Mutations lead to multinucleate cells with multiple spindles. However, embryos homozygous for *pbl* display morphogenetic movements and tissue differentiation, whereas sun^{mat-} embryos appear to lack any overall structure. This suggests that the defect in sun^{mat-} embryos may be more

severe than merely blocking cytokinesis. Embryos mutant for the *string* gene which blocks all mitotic activity beyond the G2 phase of cycle 14, can still respond to patterning information (Hartenstein and Posakony, 1990).

sun^{mat-} embryos are composed of rounded cells after cellularisation, whereas wild type cells have a columnar morphology. Gene expression is also clearly interrupted in cellularised sun^{mat-} embryos (Hb, En; chapter 6.7). The cells may be unable to complete cellularisation, or alternatively may be stalled in the next mitosis, when the cells 'round up', losing their columnar structure. Future experiments, such as time lapse microscopy of living embryos and BrdU labelling to test for DNA synthesis, will determine whether sun^{mat-} embryos undergo further cell divisions after cellularisation.

The cells in sun^{mat-} embryos may be failing to re-establish the morphology after the mitosis following cellularisation. Screens for morphological mutants in yeast uncovered the *orb* phenotype in which cells are unable to re-establish the wild type rod-like morphology after cytokinesis (Snell and Nurse, 1994). The yeast cells show defects in actin distribution and the consequence is that cells stall in a rounded morphology. A recent screen for *Drosophila* polarity mutants was based on the overexpression of *Drosophila* cDNAs in yeast (Edwards et al., 1994). The screen recovered several known cytoskeletal proteins which affected yeast morphology, implying the cellular machinery is conserved between *Drosophila* and yeast. Overexpression of the *sun* cDNA in yeast will determine whether *sun* has a similar effect.

The three sun alleles recovered which show maternal effects on cellularisation, sun^{1}, sun^{Y6} and sun^{Y52} are all temperature sensitive. This suggests that the process they are affecting is temperature sensitive, rather

than the mutant protein recovering activity at lower temperatures. The requirement for *sun*$^{+}$ may only be completely rate limiting at 25°C.

The candidate *sun* cDNA is maternally expressed. Northern analysis revealed that there are two maternal transcripts emanating from the region encompassed by the cDNA clone. As the cDNA is subject to splicing, the two transcripts may be splice variants, which can be easily tested by Northern analysis. Adult viable alleles often reflect genomic rearrangements, so a Southern blot of mutant alleles to look for disruptions in the coding region, or upstream of it would link the cDNA to the *sun* phenotypes. Rescue of *sun*$^{mat-}$ embryos by injection of RNA coding for the ORF will provide a definitive test of function.

Perhaps most exciting is the cyclin homology in the predicted Sun protein. Cyclins control transitions between phases of the cell cycle by binding to, and activating p34 and cdk2 kinases. Although the ORF does not contain the complete 100 amino acids of similarity shared by most cyclins, and the similarity is poor (28% over 46 amino acids), an expanding family of proteins have been shown to physically interact with p34/cdk2 kinases despite poor homologies to cyclins. To prove that the predicted Sun protein is a functional cyclin, it could be shown to rescue a cyclin deficiency in yeast (Lahue et al., 1991), or to physically interact with a kinase activity using a two hybrid system (Gyuris et al., 1993), or an in vitro assay (Ewen et al., 1992).

No cyclins are known to be involved in the control of the actin cytoskeleton. Nevertheless, such activities would explain several aspects of cell cycle regulated morphogenesis. During cytokinesis, an actin-myosin ring pinches off the two daughter cells like a purse string. Activation of the contractile machinery is dependent on inactivation of the MPF (maturation promoting factor) cyclinB-cdc2 kinase complex. The

contractile machinery could be additionally regulated by other cyclin-kinase complexes, and not just by MPF inactivation.

Regulation by cyclins is not limited to cell cycle control. *PHO80-PHO85*, a cyclin-cdc2 kinase complex has been shown to regulate the transcription of the yeast *PHO5* gene in response to phosphate levels. *PHO5* is repressed under conditions of high phosphate by *PHO80-PHO85* phosphorylation of the *PHO4* transcriptional activator (Kaffman et al., 1994). The predicted Sun protein could potentially have a role outside the cell cycle too.

The carboxy terminus of the ORF contains a putative prenyl group binding site. Attachment of a farnesyl or geranyl-geranyl group mediates membrane localisation for a number of eukaryotic proteins, eg. Ras (Lowy and Willumsen, 1989). No cyclins are currently known to be prenylated, but given the role of *sun* in cellularisation, localisation of the Sun protein to the membrane would suggest it is prenylated. Antibodies against the predicted protein will allow the protein's cellular location to be determined.

The protein encoded by the ORF may not be a cyclin. It could still be playing a regulatory role during cellularisation, modifying proteins required for actin cap assembly. The possible membrane localisation also suggests that the protein has a structural role, in which case it could be found to localise to actin caps. A collection of actin binding proteins isolated from syncytial embryos have been shown to localise with actin structures, including caps (Miller et al., 1985; Miller et al., 1989). Immunolocalisation of these actin binding proteins in sun^{mat-} embryos will allow the role of *sun* in the localisation of the proteins to be determined. For example, the 13D2 antigen is localised normally in *spg* embryos to above the nuclei, even though actin is not localised. This

suggests *spg*$^{+}$ is required, directly or indirectly, for actin association with the 13D2 antigen (Postner et al., 1992).

Clearly there are many experiments to investigate the *sun* maternal effect, and the candidate Sun protein. The phenotypic and molecular characterisation of the *sun* maternal effect presents an opportunity to learn more about cellularisation and organisation of the cytoskeleton in the early embryo.

The identification of *odd Oz* and *sno* highlights limitations to the arguments that there are no further zygotic genes affecting segmentation or early morphogenesis. The use of different mutagens, and more sensitive screening procedures, such as antibody based screens, may lead to the discovery of further zygotic mutations, but they will probably be limited in number.

7.2 Future directions

The use of germline clones allows recessive lethals that are not germline lethals to be examined for maternal effects. Many genes are reused during development, and it is reasonable to expect that a large proportion will be required for germline development. Based on the screens carried out in the Perrimon laboratory and my screen, between 30-50% of lethals will be required for germline development. Alternative procedures must be employed for their recovery if genetics is to be used.

Trans-heterozygote screens are based on the dosage sensitivity often displayed by genes acting in the same pathway. If the level of two components is reduced by half, a severe phenotype can be produced if the two components are functionally linked, although neither locus produces a phenotype when heterozygous alone. Trans-heterozygote screens allow recessive lethal mutations to be recovered. The approach is often modified to look for mutations which enhance or suppress a phenotype. The role of the Ras pathway in signal transduction by the *sevenless* receptor tyrosine kinase in the *Drosophila* eye was successfully elucidated by using such an approach (Simon et al., 1991).

Tricoire showed that maternally acting genes can be detected in trans-heterozygote screens (Tricoire, 1988). The approach would allow recovery of genes required for germline development, but it is not clear that such an approach is widely applicable. A large quantity of maternal product is laid

Chapter 7. Conclusions

7.1 Novel zygotic genes acting in segmentation and cellularisation

Screening for zygotic and strict maternal effect mutations has reached saturation, and aneuploid screens indicate that there are no further zygotic genes affecting segmentation or early morphogenesis. Zygotic lethals with maternal effects are a focus of attention for uncovering further genes required during early embryogenesis. Yet, two novel zygotic mutations have recently been isolated with effects on segmentation and morphogenesis.

The saturating screens of Nüsslein-Volhard and colleagues used EMS as a mutagen. However, there is evidence that some parts of the genome are refractile to EMS mutagenesis, so some patterning loci could have been missed. For example, no mutations in the *nullo* gene have been recovered and the phenotypic effects of the gene needed to be examined using deficiencies. Recently, a novel zygotic pair-rule gene, *odd Oz*, was isolated (Levine et al., 1994). The gene is represented only by P element insertion alleles and does not correspond to any known EMS mutations, suggesting that it too lies in a region of the genome refractile to EMS mutagenesis. As *odd Oz* is not expressed until cellular blastoderm, it would not have been detected in the aneuploid screens, which were designed to test for the presence of novel gap genes and early acting pair-rule genes.

Other zygotic mutations may have been missed because their phenotypes were too subtle to detect or were masked by other effects. The aneuploid screens failed to detect the *strawberry-notch (sno)* X-linked locus which gives rise to disruptions of the hexagonal actin network at cellularisation (Coyle-Thompson and Banerjee, 1993). The aneuploid screen relied on light microscopy, and embryos lacking zygotic *sno* might resemble wild type embryos when examined without staining for actin.

The identification of *odd Oz* and *sno* highlights limitations to the arguments that there are no further zygotic genes affecting segmentation or early morphogenesis. The use of different mutagens, and more sensitive screening procedures, such as antibody based screens, may lead to the discovery of further zygotic mutations, but they will probably be limited in number.

7.2 Future directions

The use of germline clones allows recessive lethals that are not germline lethals to be examined for maternal effects. Many genes are reused during development, and it is reasonable to expect that a large proportion will be required for germline development. Based on the screens carried out in the Perrimon laboratory and my screen, between 30-50% of lethals will be required for germline development. Alternative procedures must be employed for their recovery if genetics is to be used.

Trans-heterozygote screens are based on the dosage sensitivity often displayed by genes acting in the same pathway. If the level of two components is reduced by half, a severe phenotype can be produced if the two components are functionally linked, although neither locus produces a phenotype when heterozygous alone. Trans-heterozygote screens allow recessive lethal mutations to be recovered. The approach is often modified to look for mutations which enhance or suppress a phenotype. The role of the Ras pathway in signal transduction by the *sevenless* receptor tyrosine kinase in the *Drosophila* eye was successfully elucidated by using such an approach (Simon et al., 1991).

Tricoire showed that maternally acting genes can be detected in trans-heterozygote screens (Tricoire, 1988). The approach would allow recovery of genes required for germline development, but it is not clear that such an approach is widely applicable. A large quantity of maternal product is laid

down in the egg weakening the effect of reducing the amount of a gene product by half. To reliably detect an interaction, large numbers of embryos might have to be examined which is not feasible for large scale screening (see (Paroush et al., submitted)). The approach is undoubtedly useful for providing evidence if a candidate gene is suspected to be involved in a process, particularly if different alleles of the mutations being examined are available.

Genes involved in early embryogenesis may be recovered in screens for disruptions in non-embryonic tissues. A good example is the screen of Gatti and Baker, which examined larval pupal lethals for effects on the cell cycle (Gatti and Baker, 1989). Early embryogenesis is supported by maternally supplied components, and cell cycle defects only occur when the imaginal tissues begin to proliferate. Mutations isolated by screening larval-pupal lethals can subsequently be examined for maternal effects on early development. Many adult tissues are patterned in part by reusing embryonic genes. For example, the segment polarity genes were first identified by their effects on limb patterning, e.g.. *wingless*. Screens can be conducted for mutations which enhance or suppress the phenotypes of mutations in these genes in adult tissues. Candidate mutations can then be tested for embryonic effects. The FLP-FRT system can also be used to generate clones of cells homozygous for lethal mutations in adult tissues such as the wing or eye, allowing rapid screening (Xu and Rubin, 1993). For example, mutations leading to neurogenic defects in the peripheral nervous system could be subsequently tested for effects on the CNS.

Although the approaches described present alternative ways of recovering mutations affecting early development, only the X chromosome has been thoroughly screened for zygotic lethals with maternal effects. The extension of the FLP-DFS technique to the autosomes has altered this

situation (Chou et al., 1993; Xu and Rubin, 1993). Autosomal screens are currently underway, and as the autosomes represent approximately 80% of the genome, it is to expected that many mutants will be recovered with maternal effects on embryogenesis. Even small scale screens of the X chromosome, such as the one described in this thesis, yield collections of interesting mutations, so systematic screens will produce many more mutants.

References

Amati, B., Brooks, M. W., Levy, N., Littlewood, T. D., Evan, G. I. and Land, H. (1993). Oncogenic activity of the c-Myc protein requires dimerization with Max. Cell *72*, 233-245.

Amati, B., Dalton, S., Brooks, M. W., Littlewood, T. D., Evan, G. I. and Land, H. (1992). Transcriptional activation by the human c-Myc oncoprotein in yeast requires interaction with MAX. Nature *359*, 423-426.

Ashburner, M. (1989). "*Drosophila*: a laboratory handbook". (Cold Spring Harbour Press, NY).

Baker, J., Theurkauf, W. E. and Schubiger, G. (1993). Dynamic changes in microtubule configuration correlate with nuclear migration in the preblastoderm *Drosophila* embryo. J. Cell. Biol. *122*, 113-121.

Balasubramanian, M. K., Hirani, B. R., Burke, J. D. and Gould, K. L. (1994). The Schizosaccharomyces pombe cdc3+ gene encodes a profilin essential for cytokinesis. J. Cell Biol. *125*, 1289-1301.

Benedyk, M. J., Mullen, J. R. and DiNardo, S. (1994). odd-paired: a zinc finger pair-rule protein required for the timely activation of engrailed and wingless in *Drosophila* embryos. Genes Dev. *8*, 105-117.

Bengal, E., Ransone, L., Scharfmann, R., Dwarki, V. J., Tapscott, S. J., Weintraub, H. and Verma, I. M. (1992). Functional antagonism between c-jun and MyoD proteins - a direct physical association. Cell *68*, 507-519.

Binari, R. and Perrimon, N. (1994). Stripe-specific regulation of pair-rule genes by hopscotch, a putative Jak family tyrosine kinase in *Drosophila*. Genes Dev. *8*, 300-312.

Botas, J., Moscoso del Prado, J. and García-Bellido, A. (1982). Gene dose titration analysis in the search for trans-regulatory genes in *Drosophila*. EMBO J. *1*, 307-310.

Brand, M. and Campos-Ortega, J. A. (1988). Two groups of interrelated genes regulate early neurogenesis in *Drosophila* melanogaster. Roux's Arch. Dev. Biol. *197*, 457-470.

Brosseau, G. E., Nicoletti, B., Grell, E. H. and Lindsley, D. L. (1961). Production of altered Y chromosomes bearing specific sections of the X chromosome in *Drosophila*. Genetics *46*, 330-346.

Cabrera, C. V. and Alonso, M. C. (1991). Transcriptional activation by heterodimers of the *achaete-scute* and *daughterless* gene products of *Drosophila*. EMBO J. *10*, 2965-2973.

Cabrera, C. V., Martinez-Arías, A. and Bate, M. (1987). The expression of three members of the *achaete-scute* gene complex correlates with neuroblast segregation in *Drosophila*. Cell *50*, 425-433.

Campos-Ortega, J.A. and Hartenstein V. (1985) "The embryonic development of *Drosophila* melanogaster" (Springer-Verlag).

Carroll, S. B. and Scott, M. P. (1986). Zygotically active genes that affect the spatial expression of the *fushi tarazu* segmentation gene during early *Drosophila* embryogenesis. Cell *45*, 113-26.

Chen, M. S., Obar, R. A., Schroeder, C. C., Austin, T. W., Poodry, C. A., Wadsworth, S. C. and Vallee, R. B. (1991). Multiple forms of dynamin are encoded by *shibire*, a *Drosophila* gene involved in endocytosis. Nature *351*, 583-586.

Chou, T.-B. and Perrimon, N. (1992). Use of a yeast site-specific recombinase to produce female germline chimers in *Drosophila*. Genetics *131*, 643-653.

Chou, T. B., Noll, E. and Perrimon, N. (1993). Autosomal p[ovo(d1)] dominant female-sterile insertions in *Drosophila* and their use in generating germ-line chimeras. Development *119*, 1359-1369.

Clark, I., Giniger, E., Ruoholabaker, H., Jan, L. Y. and Jan, Y. N. (1994). Transient posterior localization of a kinesin fusion protein reflects anteroposterior polaritty of the oocyte. Curr. Biol. *4*, 289-300.

Corbin, V., Michelson, A. M., Abmayr, S. M., Neel, V., Alcamo, E., Maniatis, T. and Young, M. W. (1991). A role for the *Drosophila* neurogenic genes in mesoderm differentiation. Cell *67*, 311-323.

Coyle-Thompson, C. and Banerjee, U. (1993). The strawberry notch gene functions with Notch in common developmental pathways. Development *119*, 377-395.

de la Concha, A., Dietrich, U., Weigel, D. and Campos-Ortega, J. A. (1988). Functional interactions of neurogenic genes of *Drosophila* melanogaster. Genetics *118*, 499-508.

Driever, W. (1993). Maternal control of anterior development in the *Drosophila* embryo. In "The development of *Drosophila* melanogaster". (M. Bate and Martinez-Arias, A., ed.), *1*, 301-363, (Cold Spring Harbor Laboratory Press,

Driever, W. and Nüsslein-Volhard, C. (1988a). The *bicoid* protein determines position in the *Drosophila* embryo in a concentration-dependent manner. Cell *54*, 95-104.

Driever, W. and Nüsslein-Volhard, C. (1988b). A gradient of *bicoid* protein in *Drosophila* embryos. Cell *54*, 83-93.

Driever, W., Thoma, G. and Nüsslein-Volhard, C. (1989). Determination of spatial domains of zygotic gene expression in the *Drosophila* embryo by the affinity of binding sites for the *bicoid* morphogen. Nature *340*, 363-367.

Drysdale, R., Warmke, J., Kreber, R. and Ganetzy, B. (1991). Molecular characterisation of eag: a gene affecting potassium channels in *Drosophila* melanogaster. Genetics *127*, 497-505.

Edgar, B. A., Kiehle, C. P. and Schubiger, G. (1986a). Cell cycle control by the nucleo-cytoplasmic ratio in early *Drosophila* development. Cell *44*, 365-72.

Edgar, B. A., Weir, M. P., Schubiger, G. and Kornberg, T. (1986b). Repression and turnover pattern *fushi tarazu* RNA in the early *Drosophila* embryo. Cell *47*, 747-54.

Edwards, K. A., Montague, R. A., Shepard, S., Edgar, B. A., Erikson, R. L. and Kiehart, D. P. (1994). Identification of *Drosophila* cytoskeletal proteins by induction of abnormal cell shape in fission yeast. PNAS *91*, 4589-4593.

Ellis, H. M., Spann, D. R. and Posakony, J. W. (1990). *extramacrochaete*, a negative regulator of sensory organ development in *Drosophila*, defines a new class of helix-loop-helix proteins. Cell *61*, 27-38.

Ewen, M. E., Faha, B., E., H. and Livingston, D. M. (1992). Interaction of p107 with cyclin-a independent of complex-formation with viral oncoproteins. Science *255*, 85-87.

Fields, S. and Song, O. (1989). A novel genetic system to detect protein-protein interactions. Nature *340*, 245-246.

Finkelstein, R. and Perrimon, N. (1990). The orthodenticle gene is regulated by bicoid and torso and specifies *Drosophila* head development. Nature *346*, 485-488.

Foe, V. A. and Alberts, B. M. (1983). Studies of nuclear and cytoplasmic behaviour during the five mitotic cycles that precede gastrulation in *Drosophila* embryogenesis. J. Cell Sci. *61*, 31-70.

Foe, V. E., Odell, G. M. and Edgar, B. E. (1993). Mitosis and morphogenesis in the *Drosophila* embryo. In "The Development of *Drosophila*

melanogaster". (M. Bate and Martinez-Arias, A., ed.), *1*, 149-300, (Cold Spring Harbor Laboratory Press,

Frasch, M., Warrior, R., Tugwood, J. and Levine, M. (1988). Molecular analysis of *even-skipped* mutants in *Drosophila* development. Genes Dev. *2*, 1824-1838.

Freeman, M., Nüsslein-Volhard, C. and Glover, D. M. (1986). The dissociation of nuclear and centrosomal division in gnu, a mutation causing giant nuclei in *Drosophila*. Cell *46*, 457-68.

Garrell, J. and Modolell, J. (1990). The *Drosophila extramacrochaete* locus, an antagonist of proneural genes that, like these genes, encodes a helix-loop-helix protein. Cell *61*, 39-48.

Gatti, M. and Baker, B. S. (1989). Genes controlling essential cell-cycle functions in *Drosophila* melanogaster. Genes Dev. *3*, 438-453.

Gavis, E. R. and Lehmann, R. (1994). Translational regulation of nanos by RNA localisation. Nature *369*, 315-318.

Golic, K. G. (1991). Site-specific recombination between homologous chromosomes in *Drosophila*. Science *252*, 958-961.

Golic, K. G. and Lindquist, S. (1989). The FLP recombinase of yeast catalyzes site-specific recombination in the *Drosophila* genome. Cell *59*, 499-509.

Goto, T., Macdonald, P. M. and Maniatis, T. (1989). Early and late periodic patterns of *even-skipped* expression are controlled by distinct regulatory elements that respond to different spatial cues. Cell *57*, 413-422.

Greenspan, R. J. (1992). Initial determination of the neuroectoderm in *Drosophila*. In "Determinants of neuronal identity". (M. Shankland, ed.), 155-188, (Academic Press,

Grigliatti, T. (1986). Mutagenesis. In "*Drosophila*, a practical approach". (D.B. Roberts, ed.), 39-58, (IRL Press, Oxford).

Grossniklaus, U., Pearson, R. K. and Gehring, W. J. (1992). The *Drosophila* sloppy paired locus encodes two proteins involved in segmentation that show homology to mammalian transcription factors. Genes Dev *6*, 1030-51.

Gyuris, J., Golemis, E., Chertkov, H. and Brent, R. (1993). Cdi1, a human G1-phase and S-phase protein phosphatase that associates with cdk2. Cell *75*, 791-803.

Harding, K., Hoey, T., Warrior, R. and Levine, M. (1989). Autoregulatory and gap gene response elements of the *even-skipped* promoter of *Drosophila*. EMBO J. *8*, 1205-1212.

Hardy, R. W., Lindsley, D. L., Livak, K. J., Lewis, B., Siversten, A. L., Joslyn, G. L., Edwards, J. and Bonaccorse, S. (1984). Cytogenetic analysis of a segment of the Y chromosome of *Drosophila* melanogaster. Genetics *107*, 591-610.

Hartenstein, A. Y., Rugendorff, A., Tepass, U. and Hartenstein, V. (1992). The function of the neurogenic genes during epithelial development in the *Drosophila* embryo. Development *116*, 1203-1220.

Hartenstein, V. and Campos-Ortega, J. A. (1984). Early neurogenesis in wild-type *Drosophila* melanogaster. Roux's Arch Dev Biol *193*, 308-325.

Hartenstein, V. and Posakony, J. W. (1990). Sensillum development in the absence of cell division: the sensillum phenotype of the *Drosophila* mutant string. Dev. Biol. *138*, 147-58.

Hartley, D. A., Preiss, A. and Artavanis-Tsakonas, S. (1988). A deduced gene product from the *Drosophila* neurogenic locus, enhancer of split, shows homology to mammalian G-protein beta subunit. Cell *55*, 785-95.

Hatanaka, K. and Okada, M. (1991). Retarded nuclear migration in *Drosophila* embryos with aberrant f-actin reorganization caused by maternal mutations and by cytochalasin treatment. Development *111*, 909-920.

Heitzler, P. and Simpson, P. (1991). The choice of cell fate in the epidermis of *Drosophila*. Cell *64*, 1083-1092.

Higashijima, S., Michiue, T., Emori, Y. and Saigo, K. (1992). Subtype determination of *Drosophila* embryonic external sensory organs by redundant homeo box genes BarH1 and BarH2. Genes Dev *6*, 1005-18.

Hime, G. and Saint, R. (1992). Zygotic expression of the pebble locus is required for cytokinesis during the postblastoderm mitoses of *Drosophila*. Development *114*, 165-71.

Hiromi, Y. and Gehring, W. J. (1987). Regulation and function of the *Drosophila* segmentation gene *fushi tarazu*. Cell *50*, 963-974.

Hiromi, Y., Kuroiwa, A. and Gehring, W. J. (1985). Control elements of the *Drosophila* segmentation gene *fushi tarazu*. Cell *43*, 603-613.

Howard, K. and Ingham, P. (1986). Regulatory interactions between the segmentation genes *fushi tarazu, hairy* and *engrailed* in the *Drosophila* blastoderm. Cell *44*, 949-957.

Howard, K. R. and Struhl, G. (1990). Decoding positional information: regulation of the pair-rule gene *hairy*. Development *110*, 1223-1231.

Hülskamp, M., Pfeifle, C. and Tautz, D. (1990). A morphogenetic gradient of *hunchback* protein organizes the expression of the gap genes *Krüppel* and *knirps* in the early *Drosophila* embryo. Nature *346*, 577-580.

Hülskamp, M., Schröder, C., Pfeifle, C., Jäckle, H. and Tautz, D. (1989). Posterior segmentation of the *Drosophila* embryo in the absence of a maternal posterior organizer gene. Nature *338*, 629-632.

Ingham, P., Martinez-Arias, A., Lawrence, P. A. and Howard, K. (1985). Expression of engrailed in the parasegment of *Drosophila*. Nature *317*, 634-636.

Ingham, P. W. and Gergen, J. P. (1988). Interactions between the pair-rule genes *runt*, *hairy*, *even-skipped* and *fushi tarazu* and the establishment of periodic pattern in the *Drosophila* embryo. In "Mechanisms of Segmentation". (V. French, Ingham, P.W., Cooke, J. and J., S., ed.), Development *s104*, 51-60,

Ingham, P. W. and Martinez, A. A. (1992). Boundaries and fields in early embryos. Cell *68*, 221-35.

Irish, V. F., Lehmann, R. and Akam, M. (1989). The *Drosophila* posterior-group gene *nanos* functions by repressing *hunchback* activity. Nature *338*, 646-648.

Ish-Horowicz, D. and Pinchin, S. M. (1987). Pattern abnormalities induced by ectopic expression of the *Drosophila* gene *hairy* are associated with repression of *fushi tarazu* transcription. Cell *51*, 405-415.

Jan, Y. N. and Jan, L. Y. (1993). Functional gene cassettes in development. Proc. Natl. Acad. Sci. USA *90*, 8305-8307.

Jürgens, G., Wieschaus, E., Nüsslein-Volhard, C. and Kluding, H. (1984). Mutations affecting the pattern of the larval cuticle in *Drosophila* melanogaster. II. Zygotic Loci on the third chromosome. Roux's Arch. Dev. Biol. *193*, 283-295.

Kaelin, W. G. J., Pallas, D. C., DeCaprio, J. A., Kaye, F. J. and Livingston, D. M. (1991). Identification of cellular proteins that can interact specifically with the T/E1A-binding region of the retinoblastoma gene product. Cell *64*, 521-532.

Kaffman, A., Herskowitz, I., Tijan, R. and O'Shea, E. K. (1994). Phosphorylation of the transcription factor PHO4 by a cyclin-CDK complex, PHO80-PHO85. Science *263*, 1153-1156.

Kagoshima, H., Shigesada, K., Satake, M., Ito, Y., Miyoshi, H., Ohki, M., Pepling, M. and Gergen, P. (1993). The runt domain identifies a new family of heteromeric transcriptional regulators. TIGS *9*, 338-341.

Kania, M. A., Bonner, A. S., Duffy, J. B. and Gergen, J. P. (1990). The *Drosophila* segmentation gene *runt* encodes a novel nuclear regulatory protein that is also expressed in the developing nervous system. Genes Dev. *4*, 1701-1713.

Karess, R. E., Chang, X. J., Edwards, K. A., Kulkarni, S., Aguilera, I. and Kiehart, D. P. (1991). The regulatory light chain of nonmuscle myosin is encoded by *spaghetti-squash*, a gene required for cytokinesis in *Drosophila*. Cell *65*, 1177-1189.

Karr, T. L. and Alberts, B. M. (1986). Organisation of the cytoskeleton in early *Drosophila* embryos. J. Cell Biol. *102*, 1494-1509.

Kellogg, D. R., Mitchison, T. J. and Alberts, B. M. (1988). Behaviour of microtubules and actin filaments in living *Drosophila* embryos. Development *103*, 675-686.

Kidd, S., Kelley, M. R. and Young, M. W. (1986). Sequence of the Notch locus of *Drosophila* : relationship of the encoded protein to mammalian clotting and growth factors. Mol. Cell. Biol. *6*, 3094-3108.

Kaffman, A., Herskowitz, I., Tijan, R. and O'Shea, E. K. (1994). Phosphorylation of the transcription factor PHO4 by a cyclin-CDK complex, PHO80-PHO85. Science *263*, 1153-1156.

Kagoshima, H., Shigesada, K., Satake, M., Ito, Y., Miyoshi, H., Ohki, M., Pepling, M. and Gergen, P. (1993). The runt domain identifies a new family of heteromeric transcriptional regulators. TIGS *9*, 338-341.

Kania, M. A., Bonner, A. S., Duffy, J. B. and Gergen, J. P. (1990). The *Drosophila* segmentation gene *runt* encodes a novel nuclear regulatory protein that is also expressed in the developing nervous system. Genes Dev. *4*, 1701-1713.

Karess, R. E., Chang, X. J., Edwards, K. A., Kulkarni, S., Aguilera, I. and Kiehart, D. P. (1991). The regulatory light chain of nonmuscle myosin is encoded by *spaghetti-squash*, a gene required for cytokinesis in *Drosophila*. Cell *65*, 1177-1189.

Karr, T. L. and Alberts, B. M. (1986). Organisation of the cytoskeleton in early *Drosophila* embryos. J. Cell Biol. *102*, 1494-1509.

Kellogg, D. R., Mitchison, T. J. and Alberts, B. M. (1988). Behaviour of microtubules and actin filaments in living *Drosophila* embryos. Development *103*, 675-686.

Kidd, S., Kelley, M. R. and Young, M. W. (1986). Sequence of the Notch locus of *Drosophila* : relationship of the encoded protein to mammalian clotting and growth factors. Mol. Cell. Biol. *6*, 3094-3108.

Klämbt, C., Knust, E., Tietze, K. and Campos-Ortega, J. A. (1989). Closely related transcripts encoded by the neurogenic gene complex *Enhancer of split* of *Drosophila melanogaster*. EMBO J. *8*, 203-210.

Knust, E., Bremer, K. A., Vässin, H., Ziemer, A., Tepass, U. and Campos-Ortega, J. A. (1987). The *Enhancer of split* locus and neurogenesis in *Drosophila melanogaster*. Dev. Biol. *122*, 262-73.

LaBonne, S. G., Sunitha, I. and Mahowald, A. P. (1989). Molecular genetics of pecanex, a maternal-effect neurogenic locus of *Drosophila* melanogaster that potentially encodes a large transmembrane protein. Dev. Biol. *136*, 1-16.

Lahue, E. E., Smith, A. V. and Orr-Weaver, T. L. (1991). A novel cyclin gene from *Drosophila* complements CLN function in yeast. Genes Dev. *5*, 2166-2175.

Lawrence, P. A. and Johnston, P. (1989). Pattern formation in the *Drosophila* embryo: allocation of cells to parasegments by *even-skipped* and *fushi tarazu*. Development *105*, 761-767.

Lawrence, P. A., Johnston, P., Macdonald, P. and Struhl, G. (1987). Borders of parasegments in *Drosophila* embryos are delimited by the *fushi tarazu* and *even-skipped* genes. Nature *328*, 440-442.

Lehner, C. F. (1992). The pebble gene is required for cytokinesis in *Drosophila*. J. Cell Sci. *103*, 1021-1030.

Leopold, P. and O, F. P. H. (1991). An evolutionarily conserved cyclin homolog from *Drosophila* rescues yeast deficient in G1 cyclins. Cell *66*, 1207-16.

Levine, A., Bashan-Ahrend, A., Budai-Hadrian, O., Gartenberg, D., Menasherow, S. and Wides, R. (1994). odd Oz: a novel *Drosophila* pair rule gene. Cell *77*, 587-598.

Li, X. L. and Noll, M. (1994). Evolution of distinct developmental functions of 3 *Drosophila* gene by acquisition of different cis-regulatory regions. Nature *367*, 83-87.

Lindsley, D.L. and Zimm, G.G. (1992) "The genome of *Drosophila* melanogaster" (Academic Press Inc.)

Lowy, D. R. and Willumsen, B. M. (1989). New clue to Ras lipid glue. Nature *341*, 384-385.

Martinez-Arías, A. and Lawrence, P. A. (1985). Parasegments and compartments in the *Drosophila* embryo. Nature *313*, 639-642.

Merrill, P. T., Sweeton, D. and Wieschaus, E. (1988). Requirements for autosomal gene activity during precellular stages of *Drosophila melanogaster*. Development *104*, 495-509.

Miller, K. G., Field, C. M. and Alberts, B. M. (1989). Actin-binding proteins from *Drosophila* embryos: a complex network of interacting proteins detected by F-actin affinity chromatography. J. Cell. Biol. *109*,

Miller, K. G., Karr, T. L., Kellogg, D. R., Mohr, I. J., Walter, M. and Alberts, B. M. (1985). Studies on the cytoplasmic organization of early *Drosophila* embryos. Cold Spring Harb. Symp. Quant. Biol. *50*,

Mortin, M. A., Zuerner, R., Berger, S. and Hamilton, B. J. (1992). Mutations in the second-largest subunit of *Drosophila* RNA polymerase II interact with Ubx. Genetics *131*, 895-903.

Murre, C., Schonleber McCaw, P. and Baltimore, D. (1989a). A new DNA Binding and dimerisation motif in immunoglobulin enhancer binding, *daughterless*, *MyoD*, and *myc* proteins. Cell *56*, 777-783.

Murre, C., Schonleber McCaw, P., Vässin, H., Caudy, M., Jan, L. Y., Jan, Y. N., Cabrera, C. V., Buskin, J. N., Hauschka, S. D., Lassar, A. B., Weintraub, H. and Baltimore, D. (1989b). Interactions between heterologous Helix-Loop-Helix proteins generate complexes that bind specifically to a common DNA sequence. Cell *58*, 537-544.

Neufeld, T. P. and Rubin, G. M. (1994). The *Drosophila* peanut gene is required for cytokinesis and encodes a protein similar to yeast putative bud neck filament proteins. Cell *77*, 371-379.

Nüsslein-Volhard, C. and Wieschaus, E. (1980). Mutations affecting segment number and polarity in *Drosophila*. Nature *287*, 795-801.

Nüsslein-Volhard, C., Wieschaus, E. and Kluding, H. (1984). Mutations affecting the pattern of the larval cuticle in *Drosophila* melanogaster I. Zygotic loci on the second chromosome. Roux's Arch. Devl. Biol. *193*, 267-282.

Ogawa, E., Inuzuka, M., Maruyama, M., Satake, M., Naito-Fujimoto, M., Ito, Y. and Shigesada, K. (1993a). Molecular cloning and characterisation of PEBP-beta, the heterodimeric partner of a novel *Drosophila* runt-related DNA binding protein PEBP-alpha. *194*, 314-331.

Ogawa, E., Maruyama, M., Kagoshima, H., Inuzuka, M., Lu, J., Satake, M., Shigesada, K. and Ito, Y. (1993b). PEBP2/PEA2 represents a family of transcription factors homologous to the products of the *Drosophila* runt gene and the human AML1 gene. PNAS *90*, 6859-6863.

Pankratz, M. J. and Jäckle, H. (1993). Blastoderm segmentation. In "The development of *Drosophila* melanogaster". (M. Bate and Martinez-Arias, A., ed.), *1*, 467-516, (Cold Spring Harbor Laboratory Press,

Pankratz, M. J., Seifert, E., Gerwin, N., Billi, B., Nauber, U. and Jäckle, H. (1990). Gradients of *Krüppel* and *knirps* gene products direct pair-rule gene stripe patterning in the posterior region of the *Drosophila* embryo. Cell *61*, 309-317.

Parkhurst, S. M., Bopp, D. and Ish-Horowicz, D. (1990). X:A ratio, the primary sex determining signal in *Drosophila*, is transduced by helix-loop-helix proteins. Cell *63*, 1179-1191.

Parkhurst, S. M. and Ish-Horowicz, D. (1991). *wimp*, a dominant maternal-effect mutation, reduces transcription of a specific subset of segmentation genes in *Drosophila*. Genes. Dev. *5*, 341-357.

Paroush, Z., Finley, R. L. J., Kidd, T., Wainwright, S. M., Ingham, P. W., Brent, R. and Ish-Horowicz, D. (submitted). Groucho is required for *Drosophila* neurogenesis, segmentation and sex-determination, and interacts directly with Hairy-related bHLH proteins that mediate these processes.

Perrimon, N., Engstrom, L. and Mahowald, A. (1989). Zygotic lethals with specific maternal effect phenotypes in *Drosophila melanogaster*. I. Loci on the X chromosome. Genetics *121*, 333-352.

Perrimon, N., Engstrom, L. and Mahowald, A. P. (1984). The effects of zygotic lethal mutations on female germ-line functions in *Drosophila*. Dev. Bio. *105*, 404-414.

Perrimon, N. and Gans, M. (1983). Clonal analysis of the tissue specificity of recessive female sterile mutations of *Drosophila* melanogaster using a dominant female sterile mutation. Fs(1)K1237. Dev. Biol. *100*, 365-373.

Perrimon, N. and Mahowald, A. P. (1986). *l(1)hopscotch*, a larval-pupal zygotic lethal with a specific maternal effect on segmentation in *Drosophila*. Dev Biol *118*, 28-41.

Poodry, C. A. (1990). *shibire*, a neurogenic mutant of *Drosophila*. Dev. Biol. *138*, 464-72.

Postner, M. A., Miller, K. G. and Wieschaus, E. F. (1992). Maternal effect mutations of the sponge locus affect actin cytoskeletal rearrangements in *Drosophila* melanogaster embryos. J. Cell Biol. *119*, 1205-1218.

Postner, M. A. and Wieschaus, E. F. (in press). The nullo protein is a component of the actin-myosin network that mediates cellularization in *Drosophila* melanogaster embryos. J. Cell Sci.

Preat, T., Therond, P., Lamourisnard, C., Limbourgbouchon, B., Tricoire, H., Erk, I., Mariol, M. C. and Busson, D. (1990). A putative serine threonine protein-kinase encoded by the segment-polarity fused gene of *Drosophila*. Nature *347*, 87-89.

Raff, J. W. and Glover, D. M. (1989). Centrosomes, not nuclei, initiate pole cell formation in *Drosophila* embryos. Cell *57*, 611-619.

Rao, Y., Jan, L. Y. and Jan, Y. N. (1990). Similarity of the product of the *Drosophila* neurogenic gene *big brain* to transmembrane channel proteins. Nature *345*, 163-167.

Riddihough, G. and Ish-Horowicz, D. (1991). Individual stripe regulatory elements in the *Drosophila hairy* promoter respond to maternal, gap and pair-rule genes. Genes Dev. *5*, 840-854.

Ridley, A. J. and Hall, A. (1992). The small GTP-binding protein rho regulates the assembly of focal adhesions and actin stress fibers in response to growth-factors. Cell *70*, 389-399.

Ridley, A. J., Paterson, H. F., Johnston, C. L., Diekmann, D. and Hall, A. (1992). The small GTP-binding protein rac regulates growth-factor induced membrane ruffling. Cell *70*, 401-410.

Ripoll, P., Pimpinelli, S., Valdivia, M. and Avila, J. (1985). A cell division mutant of *Drosophila* with a functionally abnormal spindle. Cell *41*, 907-912.

Roberts, D.B. (1986). Basic *Drosophila* care and techniques. In "*Drosophila*, a practical approach". (D.B. Roberts, ed.), 39-58, (IRL Press, Oxford).

Romani, S., Campuzano, S. and Modolell, J. (1987). The *achaete-scute* complex is expressed in neurogenic regions of *Drosophila* embryos. EMBO J. *6*, 2085-2092.

Rose, L. S. and Wieschaus, E. (1992). The *Drosophila* cellularization gene nullo produces a blastoderm-specific transcript whose levels respond to the nucleocytoplasmic ratio. Genes Dev *6*, 1255-68.

Ruohola, H., Bremer, K. A., Baker, D., Swedlow, J. R., Jan, L.-Y. and Jan, Y.-N. (1991). Role of neurogenic genes in establishment of follicle cell fate and oocyte polarity during oogenesis in *Drosophila*. Cell *66*, 433-449.

Rushlow, C. A., Hogan, A., Pinchin, S. M., Howe, K. R., Lardelli, M. T. and Ish-Horowicz, D. (1989). The *Drosophila hairy* protein acts in both segmentation and bristle patterning and shows homology to *N-myc*. EMBO. J. *8*, 3095-3103.

Sasai, Y., Kageyama, R., Tagawa, Y., Shigemoto, R. and Nakanishi, S. (1992). Two mammalian helix-loop-helix factors structurally related to *Drosophila hairy* and *Enhancer of split*. Genes Dev. *6*, 2620-2634.

Sauer, F. and Jäckle, H. (1991). Concentration-dependent transcriptional activation or repression by Kruppel from a single binding site. Nature *353*, 563-6.

Schejter, E. D. and Wieschaus, E. (1993a). Bottleneck acts as a regulator of the microfilament network governing cellularization of the *Drosophila* embryo. Cell *75*, 373-385.

Schejter, E. D. and Wieschaus, E. (1993b). Functional elements of the cytoskeleton in the early *Drosophila* embryo. Ann. Rev. Cell Biol. *9*, 67-99.

Schrons, H., Knust, E. and Campos-Ortega, J. A. (1992). The Enhancer of split complex and adjacent genes in the 96F region of *Drosophila* melanogaster are required for segregation of neural and epidermal progenitor cells. Genetics *132*, 481-503.

Schweisguth, F. C., Lepesant, J.-A. and Vincent, A. (1990). The *serendipity alpha* gene encodes a membrane associated protein required for the cellularization of the *Drosophila* embryo. Genes Dev. *4*, 922-931.

Shamanski, F. L. and Orr, W. T. (1991). The *Drosophila* plutonium and pan gu genes regulate entry into s-phase at fertilization. Cell *66*, 1289-1300.

Simon, M. A., Bowtell, D. D., Dodson, G. S., Laverty, T. R. and Rubin, G. M. (1991). Ras1 and a putative guanine nucleotide exchange factor perform crucial steps in signaling by the sevenless protein tyrosine kinase. Cell *67*, 701-16.

Simpson, L. and Wieschaus, E. (1990). Zygotic activity of the *nullo* locus is required to stabilize the actin myosin network during cellularization in *Drosophila*. Development *110*, 851-863.

Small, S., Kraut, R., Hoey, T., Warrior, R. and Levine, M. (1991). Transcriptional regulation of a pair-rule stripe in *Drosophila*. Genes Dev. *5*, 827-839.

Smith, D. B. and Johnson, K. S. (1988). Single-step purification of polypepetides expressed in *Escherichia coli* as fustions with glutathione S-transferase. Gene *67*, 31-40.

Smoller, D., Friedel, C., Schmid, A., Bettler, D., Lam, L. and Yedvobnick, B. (1990). The *Drosophila* neurogenic locus *mastermind* encodes a nuclear-protein unusually rich in amino-acid homopolymers. Genes Dev. *4*, 1688-1700.

Snell, V. and Nurse, P. (1994). Genetic analysis of cell morphogenesis in fission yeast - a role for casein kinase II in the establishment of polarized growth. EMBO J. *13*, 2066-2074.

St. Johnston, D. and Nüsslein-Volhard, C. (1992). The origin of pattern and polarity in the *Drosophila* embryo. Cell *68*, 201-19.

Stanojevic, D., Hoey, T. and Levine, M. (1989). Sequence specific DNA-binding activities of the gap proteins encoded by *hunchback* and *Krüppel* in *Drosophila*. Nature *341*, 331-335.

Stanojevic, D., Small, S. and Levine, M. (1991). Regulation of a segmentation stripe by overlapping activators and repressors in the *Drosophila* embryo. Science *254*, 1385-1387.

Stewart, B. and Merriam, J. R. (1973). Segmental aneuploidy of the X-chromosome. DIS *50*, 167-179.

Struhl, G. (1989). Differing strategies for organising anterior and posterior body patterns in *Drosophila* enbryos. Nature *338*, 741-744.

Struhl, G., Johnston, P. and Lawrence, P. A. (1992). Control of *Drosophila* body pattern by the hunchback morphogen gradient. Cell *69*, 237-249.

Struhl, G., Struhl, K. and Macdonald, P. M. (1989). The gradient morphogen *bicoid* is a concentration-dependent transcriptional activator. Cell *57*, 1259-1273.

Sullivan, W., Fogarty, P. and Theurkauf, W. (1993). Mutations affecting the cytoskeletal organization of syncytial *Drosophila* embryos. Development *118*, 1245-1254.

Tautz, D. (1988). Regulation of the *Drosophila* segmentation gene hunchback by two maternal morphogenetic centres. Nature *332*, 281-284.

Tietze, K., Oellers, N. and Knust, E. (1992). Enhancer of splitD, a dominant mutation of *Drosophila*, and its use in the study of functional domains of a helix-loop-helix protein. Proc Natl Acad Sci U S A *89*, 6152-6.

Tricoire, H. (1988). Dominant maternal interactions with *Drosophila* segmentation genes. Roux's Arch Dev. Biol. *197*, 115-123.

Van Doren, M., Ellis, H. M. and Posakony, J. W. (1991). The *Drosophila extramacrochaetae* protein antagonizes sequence-speicific DNA binding by *daughterless/achaete-scute* protein complexes. Development *113*, 245-255.

Vanderbliek, A. M. and Meyerowitz, E. M. (1991). Dynamin-like protein encoded by the *Drosophila shibire* gene associated with vesicular traffic. Nature *351*, 411-414.

Vässin, H., Bremer, K. A., Knust, E. and Campos-Ortega, J. A. (1987). The neurogenic gene *Delta* of *Drosoophila melanogaster* is expressed in neurogenic territories and encodes a putative transmembrane protein with EGF-like repeats. EMBO J. *6*, 3431-3440.

Vavra, S. and Carroll, S. (1989). The zygotic control of *Drosophila* pair-rule expression: I. a search for new pair-rule regulatory loci. Development *107*, 663-672.

Wainwright, S. M. and Ish-Horowicz, D. (1992). Point mutations in the *Drosophila hairy* gene demonstrate *in vivo* requirements for basic, helix-loop-helix, and WRPW domains. Mol. Cell Biol. *12*, 2475-2483.

Wang, C. and Lehmann, R. (1991). *nanos* is the localized posterior determinant in *Drosophila*. Cell *66*, 637-647.

Warn, R. M., Magrath, R. and Webb, S. (1984). Distribution of f-actin during cleavage of the *Drosophila* syncytial blastoderm. J. Cell Biol. *98*, 156-162.

Warn, R. M. and Robert-Nicoud, M. (1990). F-actin organization during the cellularization of the *Drosophila* embryos as revealed with a confocal laser scanning microscope. J. Cell Sci. *96*, 35-42.

Wharton, K. A., Johansen, K. M., Xu, T. and Artavanis-Tsakonas, S. (1985). Nucleotide sequence from the neurogenic locus notch implies a gene product that shares homology with proteins containing EGF-like repeats. Cell *43*,

Wieschaus, E., Nüsslein-Volhard, C. and Jürgens, G. (1984). Mutations affecting the pattern of the larval cuticle in *Drosophila* melanogaster. III. Zygotic loci on the X chromosome and the fourth chromosome. Roux's Arch. Dev. Biol. *193*, 296-307.

Wieschaus, E. and Sweeton, D. (1988). Requirements for X-linked zygotic gene activity during cellularization of early *Drosophila* embryos. Development *104*, 483-493.

Xu, T. and Rubin, G. M. (1993). Analysis of genetic mosaics in developing and adult *Drosophila* tissues. Development *117*, 1223-1237.

Yasuda, G. K., Baker, J. and Schubiger, G. (1991). Independent roles of centrosomes and dna in organizing the *Drosophila* cytoskeleton. Development *111*, 379-391.

Young, P. E., Pesacreta, T. C. and Kiehart, D. P. (1991). Dynamic changes in the distribution of cytoplasmic myosin during *Drosophila* embryogenesis. Development *111*, 1-14.

Zalokar, M., Audit, C. and Erk, I. (1975). Developmental defects of female-sterile mutants of *Drosophila* melanogaster. Dev. Biol. *47*, 419-432.

Appendix: Materials and Methods

Materials

Standard laboratory supplies were obtained from either Sigma or BDH. All other supplies are either noted below or in the methods section.

Agarose for gel electrophoresis of nucleic acids- Pharmacia

Low melting point agarose - BRL Life Technologies

Ultra Pure Urea - BRL Life Technologies

Bacterial Strains

E.coli XL1 Blue. Genotype: recA1, endA1, gyrA96, thi-1, hsdR17, supE44, relA1, lac, [F' proAB, lacI^{q}ZΔM15, Tn10 (tet^r)]. Standard laboratory strain for the production of competent cells, the lacI^{q}ZΔM15 mutation provides a-complementation of the lacZ gene allowing blue/white colour selection. The presence of the lacI^q repressor gene helps prevent leaky expression from IPTG inducible vectors.

E.coli SRP84. Genotype: F-, ilv, his, pro, supo, strA, glaOP::IS1, Δbio, Δlon, htpR165::Tn10, [l ΔBam, N+, cI857, ΔH1 cro RAJ bio uvrB]. This is an expression strain which contains mutations in the La protease and heat shock sigma factor s32 which controls the transcription of a number of gene products implicated in protein turnover. It was built by S. R. Pearce in the laboratory of C. Higgins and was obtained from S. Hyde/C. Higgins. The strain is unstable and was grown at 30°C. It was stored as 1ml of an overnight culture grown in LB tetracycline, mixed with 77µl of DMSO and frozen at -80°C. These cells should keep for at least two years.

E. coli Y1090. Genotype: hsd ($r_k^-m_k^+$), lacU169, ProA$^+$, lon$^-$, araD 139, Str A, Sup F, trp C22:Tn10 (pMC9). This strain is used for the as a host for lambda phage, and is employed when lytic phage growth and plaque formation are required (λgt11 plaques are grown at 43°C). The absence of the Eco K

restriction enzyme prevents loss of clones which contain sites for this enzyme.

Drosophila stocks

Details of the mutations used can be found in Lindsley and Zimm, 1992. Stocks were reared according to standard conditions (Roberts, 1986).

Genotype of stock	**Origin**
y w v FRT^{101}	T.-B. Chou & N. Perrimon
y ovo^{D1} FRT^{101}/*Y; C(1)DX f*	T.-B. Chou & N. Perrimon
Df(1)runt^{B102}/*FM7* y^{+} *Y* mal^{+}	DIH
upd/FM7	DIH
FG2	DIH
sc cv ct v g f /FM3	DIH
y^{2} m^{74f} wy^{74i} *sd* os^{s}	Bloomington #1261
C(1;Y)Y^{S}*X.*Y^{L}*, In(1)EN, y* g^{2} *na/ FM3 /Dp(1;f)LJ8,* y^{+} g^{+} na^{+} Ste^{+}	Bloomington #2870
C(1;Y)Y^{S}X.Y^{L}*, In(1)EN, Df(1)g, y f B/ C(1)A, y/ Dp(1;f)LJ9,* y^{+} g^{+} na^{+} Ste^{+}	Bloomington #3219
C(1)m3/Y; Sb/Tm6	DIH
C(1)DX y w f / T(1;Y)B51, y y^{+} B^{S}	Bowling Green #492
C(1)A, y / T(1;Y)S29, y y^{+} *w f* B^{S}	Bowling Green #201
C(1)DX, y w f / T(1;Y)B117, y y^{+} B^{S}	Bowling Green #531
C(1;Y)P2, XY^{S}.$Y^{L}B^{S}$*, Dp(1;3)P115, y pn* sn^{3}*/O/C(1)M4, In(1)*w^{m4}*+AB (y), In(1)FM7* (y^{31d} w^{a} v^{Of})	Bloomington #1396

C(1;Y)P3, $XY^S.Y^LB^S$, Dp(1;3)P115, y pn sn^3/O/C(1)M4, In(1)w^{m4}+AB (y), In(1)FM7 (y^{31d} w^a v^{Of})	Bloomington #1397
w sd^{58}	A. Chovnick
C(1)DX f/ Df(1)sd^{72b}/ Dp(1)sd Y #3m	A. Chovnick
Df(1)D15 v f/C(1)DX y f; Dp(1;4)SHORT v^+ f^+/+	A. Katzen
Df(1)D15 v f/C(1)DX y f; Dp(1;4)MEDIUM v^+ f^+/+	A. Katzen
Df(1)l9 f/ X^X y w f; Dp(1;4)LONG r^+ f^+/+	A. Katzen
Df(1)l9 f/C(1)RM y shi^{ts} f /Dp(1) y^+ shi^+ Y #3 (Dp probably same as Dp(1)sd Y #3m)	A. Katzen
Tp(1;2)sc19	DIH
A37	A. Ghysen
A101	P. Simpson
y w FRT^{9-2}	T.-B. Chou & N. Perrimon
Fs(1)K1103 FRT^{9-2}/C(1)DX f/Y	T.-B. Chou & N. Perrimon

DIH - laboratory of David Ish-Horowicz

The following collection of recessive lethal mutations located in Df(1)sd^{72b} were obtained as FM7 stocks from Alisa Katzen: EM63, EM16, EM60, EM8, EM26, EM34, EM24, EM45, EM32, EM22, EM29, EM17, EM23, EM2, EM19m, EM49, EM1, EM6, EM67.

Drosophila maternal cDNA library

A *Drosophila* stage 10 library was obtained from John Tower. The cDNAs were made using a mixture of random and oligo dT priming and were cloned into the EcoRI site of λgt11.

Antibodies

Specificity	Raised in	Dilution	Origin	Type
Engrailed	Rat	1:100	P. Ingham	Polyclonal
Fushi tarazu	Rabbit	1:600	H. Krause	Polyclonal
Even-skipped	Rat	1:200	P. Ingham	Polyclonal
Hunchback	Rat	1:400	K. Howard	Polyclonal
Sex-lethal	Mouse	1:10	D. Bopp	Monoclonal
Sry-α	Mouse	1:25	E.Schejter	Monoclonal
β-tubulin	Mouse	1:1000	Jackson Lab	Monoclonal
Secondary Antibodies				
mouse-AP	Mouse	1:3000	Jackson Lab	Monoclonal
mouse-TR	Mouse	1:200	Jackson Lab	Monoclonal

AP - conjugated to alkaline phosphatase; TR - conjugated to Texas red

Methods

Ethyl methanesulfonate mutagenesis

All operations were carried out in a fume hood. A denaturing solution (4g NaOH, 0.5ml thioglycolic acid per 100ml water) was made up fresh each day. Using a 1ml syringe, 0.26ml of EMS was added to 100ml of a 1% sucrose solution. The EMS was dispersed by stirring. Male flies (3-5 days

old) were placed in a split bottle into the bottom of which two circles of Whatman No. 1 filter paper had been placed. The flies were etherised and stored in the bottle for three hours to dessicate them and encourage them to drink. 1.1ml of ethyl methanesulfonate (EMS) sucrose solution was dripped onto the filter paper with a syringe and needle passed through the cotton wool plug of the bottle. The flies were allowed to drink for 24 hours, and then allowed to recover for a further 24 hours in a yeasted bottle of food prior to mating. All items that came into contact with the EMS were stored in the decontamination solution for 24 hours.

Diepoxybutane mutagenesis

Diepoxybutane (DEB) mutagenesis was carried out essentially as for EMS by administering as a 1% sucrose solution to 3-5 day males. The decontaminating solution was 5N NaOH. A typical concentration of DEB was 5mM (see chapter 4).

X-ray induced mutagenesis

Males were aged for 3-5 days, exposed to a ^{60}Co source and immediately mated. To induce chromosomal aberrations, doses of 4000 rads were used, although this was lowered to 3,500 rads after high levels of sterility were encounted (see chapter 5). For mitotic recombination, doses of 1000 rads were used.

Germline clone production by FLP/DFS induced mitotic recombination

To assess the optimal heat shock regime for induction of the FLP recombinase and generation of germline mosaics, FRT^{101}/FRT^{101} females mated to ovo^{D1} FRT^{101}/Y; F38/F38 males were allowed to lay eggs in bottles for 48 hours. After 72 or 48 hours ageing, the bottles were placed in a 37°C incubator for 3, 4 or 5 hours. F1 females were assessed for viable offspring, indicating that a mitotic recombination event had occurred in

their germline. The results are shown in table below. A 4 hour heat shock after a 48 hour ageing period was selected as the most suitable regime. The control bottle, which received no heat shock displays a spontaneous mitotic exchange, a very rare event normally, suggesting that there could be a basal level of FLP recombinase expression from the heat shock promoter. Six bottles were established and the flies were allowed to lay eggs for 48 hours. After a further 24 or 48 hours, the bottles were placed in an incubator at 37°C and heat shocked for 3, 4 or 5 hours. Single females were individually mated with 3-4 wild type males The females were scored for the presence of hatching larvae (table 4.2). The optimal heat shock regime was chosen as a 48 hour egg lay, 48 hour ageing, and a 4 hour heat shock.

Time of heat shock	**72 hours**			**48 hours**			**No heat**
Duration	**3hr**	**4hr**	**5hr**	**3hr**	**4hr**	**5hr**	**shock**
% mosaics	31%	48%	38%	62%	69%	55%	3%
Total tested	29	29	29	29	29	29	29

Cuticle Preparations

Eggs were collected on apple juice agar plates and aged as necessary. Excess yeast was washed off before removing the eggs with a paint brush into small sieves. Embryos were dechorionated for 2-3 minutes in small sieves. After washing, they were transferred to a slide with a drop of lacto-Hoyer's medium. Dechorionation was also carried out regularly when dealing with small numbers of embryos, by transferring the embryos using forceps between drops of bleach and water on a siliconised slide, before mounting. After lining up the embryos in the lacto-Hoyer's medium to aid subsequent microscopic examination, a cover slip was placed on top and pressure applied until the vitelline membranes of the embryos burst.

Alternatively, the embryos were popped by hand under water prior to transfer to lacto-Hoyer's medium. Slides were baked for 2 hours at 80°C.

Fertility experiments

Single females were mated to 5-6 males and allowed to mate for one week. The tubes were scored for evidence of larvae or pupae after a further 2 weeks at 25°C.

Fixation of embryos

Embryos were dechorionated with bleach for 2-3 minutes in small sieves. The embryos were rinsed with ddH2O and blotted dry on kitchen towels. The sieve was emptied into a universal containing 5ml heptane, and 5ml of FIX (4% formaldehyde, 1*PBS). Fixing was in shaking incubator at room temperature for 15 minutes. The FIX (bottom layer) was removed and replaced with 5ml methanol. The universal was immediately shaken by hand for 30 seconds. The universal was allowed to stand so that devitellinised embryos could fall from the interphase to the bottom of the tube. The devitellinised embryos were transferred to an eppendorf tube and washed with 1ml methanol.

When staining for microtubules, the embryos were washed into heptane and left for 30 seconds. Neat 37% formaldehyde was added without any buffer and the embryos were rocked very gently (important not to shake the embryos at this stage). After 5-7 minutes in the fix, the aqueous phase was removed , the tube filled to the top with methanol and shaken vigourously to pop the vitelline membranes.

Antibody Staining of Embryos

Blocking was with PAT (1*PBS, 0.1% BSA, 0.1% triton, 0.2% azide) for two hours at room temperature. Incubation with the antibody in PAT was overnight at 4°C. Embryos were washed in PAT + 2% FCS for 30 minutes.

Two further washes were carried out in PbT (1*PBS, 0.1% BSA, 0.1% triton, 2% FCS). Incubation with the secondary antibody was in PbT (no FCS) for 2-4 hours at room temperature. One 10 minute wash in PbT (no FCS), and two 10 minute washes in PTW (1*PBS, 0.1% Tween-20) followed. The embryos were washed in alkaline phosphatase staining solution (4M NaCl, 1M MgCl2, 1M Tris pH9.5, 0.1% Tween-20). The embryos were transferred to a transparent multiwell dish in 1ml staining buffer (4.5µl of NBT, 3.5µl BCIP). The reaction was stopped with PTW when stained was completed. (Protocol of Anita Taylor).

Mounting of embryos for microscopy

Stained embryos were briefly washed with ethanol in a microfuge tube, and infused with ~150µl of cold JB-4 methacrylate mount (component A + 0.9% catalyst; Polysciences) until the embryos settled. 1ml of cold component A + catalyst was mixed with 40µl of JB-4 component B. The JB-4 above the settled embryos was replaced with 100-150µl of the complete mix. Using a Gilson with the end cut off a tip, the embryos were transferred from the eppendorf tube to a slide in 35µl of mix. After 15 seconds the embryos were stirred towards the centre of the liquid, and a cover-slip lowered slowly onto them. If necessary, more JB-4 was added to fill the cover slip. The slides were inverted and polymerisation took place under CO2 for 2 hours at room temperature.

X-gal staining of enhancer trap lines

Embryos were dechorionated in bleach, washed in water, blotted dry by placing the sieve on top of kitchen towel and transferred to a mix of 5ml heptane and 5ml fixative (1 volume of 37% formaldehyde solution (BDH), 10 volumes of phospho-citrate buffer (pH7.6: 9 volumes of a fresh solution of Na2HPO4 0.2M (0.89g Na2HPO4.2H2O in 25ml water), 1 volume of citric acid 0.1M, 10 volumes of water)). The embryos were shaken vigourously

every 5 minutes for 15 minutes. The bulk of the heptane was discarded (upper phase) and the fixative was replaced twice with phospho-citrate buffer. The embryos were transferred to a 24 well clear plastic plate, as much liquid as possible removed and the remaining heptane evaporated by blowing gently. 200µl of incubation buffer (phospho-citrate buffer containing 5mM each of potassium ferri- and ferro-cyanides and 0.02% triton (33mg K3Fe(CN6), 42mg K4Fe(CN6), 200µl triton X-100 in 20ml freshly prepared phospho-citrate buffer)). A few crystals of X-gal powder were then added to the well, and the plate covered and incubated at 30°C for 1-2 days and examined periodically for staining. For mounting, the incubation buffer was replaced with a 1:2 mixture of fresh incubation buffer and glycerol. The embryos shrink, but recover their normal shape after a few minutes. The embryos were transferred to mounting medium (7g of gelatin swelled in 42ml of water, and then dissolved by boiling, after which 63g of glycerol and a crystal of phenol as a bacteriocide were added. The medium is kept at 4°C and used at 45°C. The medium was transferred to a warm slide, embryos positioned, a cover slip placed on top and the medium allowed to set. (Protocol of A. Ghysen and C. O'Kane).

DAPI staining of embryos

Fixed embryos were washed in PTW. A 5µg/ml stock solution of DAPI was diluted 1:5 prior to adding to the washed embryos. Incubation was for four minutes at room temperature. The embryos were washed in PTW for overnight, changing the washing solution at least four times.

Phalloidin staining of embryos

Eggs were collected and dechorionated in bleach as above. They were fixed in 5ml heptane saturated with 37% formaldehyde solution for 30 minutes. The embryos were transferred to a slide and the heptane allowed to evaporate, after which the embryos were placed on double sided tape on a

slide. The embryos were submerged in PTW and devitellinised by hand using a 25 gauge hypodermic needle. 20µl aliquots of FITC conjugated phalloidin (Sigma) (50µg/ml) were diluted 1:20 in PBS, or 25µl aliquots of Texas-Red conjugated phalloidin (Sigma) (50µg/ml) were diluted 1:50 in PBS. Embryos were stained for 5 minutes, and rinsed four times in PBS.

Daunomycin staining of embryos

Dechorionated and devitellinised embryos were incubated in PTX (1*PBS, 0.1% triton X100, 1% serum) for 1 hour and transferred to 5µg/ml daunomycin (Sigma, 1:1000 dilution of 5mg/ml stock) diluted in PTX. The embryos were washed four times in PBS before mounting. For double staining with phalloidin-FITC, daunomycin was used at 25µg/ml and phalloidin-FITC at 1µg/ml.

Mounting embryos for fluorescent or confocal microscopy

A slide was prepared by placing a square of insulation tape on it, and cutting a smaller square out of the centre with a razor blade. Embryos were suspended in Citifluor (UKC) and transferred to the square in the middle of the insulation tape. A coverslip was placed on top and the arrangement sealed with nail varnish (Boots). (Protocol of H. Francis-Lang).

Image Analysis

An MRC-600 (Bio-Rad) confocal microscope with the standard fluorescence filter set was used. For FITC visualisation, the BHS filter was used, and for double labelling the A1 and A2 filters.

Molecular Biology Techniques

Preparation of DNA from bacteria

DNA was prepared using Magic or Wizard mini- and maxi-prep columns (Promega) following the manufacturer's instructions. If the DNA was to be used for sequencing it was prepared differently (below), due to poor sequencing results obtained either from manual or automated sequencing

(despite modifying the manufacturer's protocol to include a second RNaseA step).

Boiling DNA miniprep

This method was used to prepare DNA for manual sequencing. 1.5ml of cells grown overnight were spun down in an eppendorf tube, and resuspended in 200µl STET buffer (0.1M NaCl, 10mM Tris·Cl pH 8.0, 1mM EDTA, 5% triton X-100). 20µl of lysozyme (10mg/ml - in water frozen aliquots, thawed only once) was added to each cell suspension. After 2 minutes at room temperature, the cells were boiled in a water bath for 1 minute, and then placed on ice for 2 minutes. The lysate was spun in a microfuge (13,000rpm, 4°C, 15 minutes), and the resulting pellet removed with a yellow tip. The supernatant was mixed with 200µl of isopropanol and incubated at room temperature for 5 minutes. The DNA was precipitated in a microfuge (13,000rpm, 4°C, 15 minutes), washed with 70% ethanol and resuspended in 50µl of TE (10mM Tris·Cl pH8.0, 1mM EDTA pH8.0). 10µl was used for each sequencing reaction. (Protocol of U. Strähle).

PEG precipitation DNA minipreps

This was one of two methods found to yield good results in automated sequencing. 1.5ml of an overnight culture of cells were spun down in an eppendorf tube for one minute and resuspended in 200µl of GTE buffer (50mM glucose, 25mM Tris pH8.0, 10mM EDTA pH8.0). The cells were lysed by adding 300µl of freshly prepared 0.2N NaOH / 1% SDS, mixing by inversion and incubation on ice for 5 minutes. The solution was neutralised by adding of 300µl of 3.)M potassium acetate pH4.8, mixing by inversion and incubation on ice for 5 minutes. Cellular debris was removed by centrifuging for 10 minutes at room temperature. RNaseA was added to a final concentration of 20µg/µl, and the DNA was incubated at 37°C for 30 minutes. The mixture was extracted twice with 300µl

chloroform, (mixing by hand for 30 seconds, and centrifuging for one minute). The DNA was precipitated with 1 volume of isopropanol and centrifuging for 10 minutes at room temperature. The pellet was washed with 500µl 70% ethanol, and dried under vacuum for three minutes. The pellet was resuspended in 35µl of water. 3µl was run on a gel to check the yield and quality of DNA. The remaining 32µl was precipitated by adding 8µl of 4M NaCl, and 40µl of autoclaved 13% PEG8000. After thorough mixing, the sample was incubated on ice for 20 minutes, and then pelleted in a microfuge (13,000rpm, 4°C, 15 minutes). The pellet was washed with 500µl of 70% ethanol, dried under vacuum for 3 minutes, and resuspended in 20µl water. (Modified from an Applied Biosystems Inc. protocol by D.Henrique).

Qiagen columns / second RNaseA digestion DNA minipreps

Contaminating RNA was found to be a problem in obtaining good automated sequence data, hence the inclusion of an extra RNaseA step in this protocol. A 1.5ml overnight culture was spun down, and the cells subjected to alkaline lysis using the solutions (containing RNaseA) and instructions supplied by the manufacturer (Qiagen). The supernatant was applied to an equilibrated Qiagen minicolumn, and the eluate mixed with 0.7 volumes of isopropanol. Precipitation of the DNA was in a microfuge (13,000rpm, 4°C, 15 minutes). The pellet was air dried for 5 minutes and resuspended in 300µl of water. RNaseA was added to a final concentration of 20µg/µl, and the DNA was incubated at 37°C for 30 minutes. The mixture was extracted twice with 300µl chloroform. 30µl of 3M Na·acetate pH5.2, and 750µl of absolute alcohol was added to the aqueous phase. After mixing, and incubation on ice for 5 minutes, the DNA was precipitated in a microfuge (13,000rpm, 4°C, 20 minutes). The pellet was washed with 70%

ethanol, briefly vacuum dried and resuspended in 10-20µl water. The yield was estimated by running on an agarose gel. (Protocol of M. Tomlinson).

Manual sequencing with Sequenase

Manual sequencing was carried out using Sequenase version 2.0 (United States Biochemical). Approximately 2µg in 10µl was denatured by adding 10µl of 0.4M NaOH and incubating for five minutes at room temperature. The DNA was precipitated by adding 10µl 4M ammonium acetate pH7.5, 150µl of absolute ethanol, incubating at -20°C for 30 minutes, and centrifuging (13,000rpm, 4°C, 15 minutes). The pellet was washed with 80% ethanol and dried under vacuum. 10ng of primer in 10µl 1X Sequenase reaction buffer was annealed to the denatured DNA during a 15 minute incubation at 37°C. The final reactions were not performed on more than five samples simultaneously. The labelling reaction was initiated by adding to the 10µl of template/primer mix: 1µl DTT (0.1M), 2µl labelling mix (diluted 1:5 in water), 0.5µl 35S-ATP, and 2µl Sequenase (diluted 1:8 in enzyme dilution buffer). The mix was incubated for 5 minutes at 37°C. Termination reactions were performed in a microtitre plate: 2.5µl of ddA, ddG, ddC and ddT were aliquoted into adjacent wells for each sample. 3.5µl of the labelling reaction was added to each well, and the plare incubated for 15-20 minutes. 4µl of stop buffer was added to each well. The samples were preheated to 75°C for 10 minutes before loading. Sequencing gels were 5% Long Ranger concentrate (AT Biochem), 1.2X TBE buffer (10X: 108g Tris base, 55g boric acid, 40ml 0.5M EDTA pH8.0 in 1 litre), 42% (w/v) urea. Polymerisation was initiated with 25µl TEMED (N, N, N', N' - tetramethylethylenediamine) and 250µl fresh 10% ammonium persulfate solution per 50ml of gel solution. Narrow gels (16 x 46.5cm) were run in 0.6X TBE at 36W constant power. One glass plate was treated with Acrylease non stick plate coating (Stratagene), and sharkstooth combs

were used to form wells. When the run was complete, the glass plates were separated and the gel allowed to cool for 2-3 minutes. The gel was transferred to Whatman 3 MM paper by firmly pressing onto the gel surface and carefully peeling the paper and gel from the plate. The gel was covered with cling-film and dried under vacuum at 80°C for 1 hour. The dried gel was exposed to X-omat film (Kodak) for autoradiography.

Automated Sequencing with fluorescent terminators

This protocol relies on the Taq DyeDeoxy terminator cycle sequencing kit (Applied Biosystems). The following premix was prepared: 4µl 5X TACS buffer, 1µl dNTP mix, 1µl of each DyeDeoxy terminator, 0.5µl AmpliTaq DNA polymerase. This is a 1X premix - the volume was adjusted according to the number of samples. In a 0.6ml microcentrifuge tube, 9.5µl of premix was added to 10.5µl template DNA in water (~1µg). The reaction was covered with mineral oil. The tubes were placed in a Perkin Elmer model 480 thermal cycler preheated to 96°C. The following program was followed: 96°C for 30 seconds, 50°C for 15 seconds, 60°C for 4 minutes. 25 cycles in total with rapid ramping. Final hold temperature: 4°C. At the end of the thermal cycling, 80µl of water was added to the reaction mixture, and 100µl of chloroform to dissolve the mineral oil. The unincorporated terminators were extracted with 100µl phenol : water : chloroform (68:18:14) (Applied Biosystems). The sample was vortexed, centrifuged and the lower, organic phase discarded before re-extraction with a second 100µl aliquot of phenol : water : chloroform. The extension products in the aqueous phase were precipitated with 15µl 2M Na·acetate pH4.5, and 300µl 100% ethanol. The sample was centrifuged for 15 minutes at room temperature and the pellet washed with 70% ethanol and dried under vacuum. The sample was resuspended in 4-6µl of 5:1 deionised formamide

/ 50mM EDTA pH8.0 and loaded onto an Applied Biosystems 373A DNA sequencing system.

Automated Sequencing with fluorescent labelled primers

This protocol relies on the Pyroseq cycle sequencing kit (Genpak Ltd.). Reagents were thawed out and maintained at 4°C prior to use. Pyroseq DNA polymerase was diluted as follows: 0.5µl pyroseq, 1µl 5X cycle sequencing buffer, 5.5µl water. Template DNA was reacted with four different termination mixes, each with the same primer conjugated to a different fluorescent label. Reagents were added to labelled tubes in the following order:

	A	C	G	T
d/ddNTPs	1µl	1µl	1µl	1µl
JOE primer	1µl			
FAM primer		1µl		
TAMRA primer			2µl	
ROX primer				2µl
5X cycle sequencing buffer	1µl	1µl	2µl	2µl
DNA template	1µl	1µl	2µl	2µl
Diluted pyroseq	1µl	1µl	2µl	2µl

Thermal cycling was in a Perkin-Elmer model 480 with maximum ramping: 15 cycles of 95°C 30 seconds, 55°C 30 seconds, 70°C 1 minute, followed by 15 cycles of 95°C 30 seconds, 70°C 1 minute. Samples were overlaid with mineral oil. After cycling the four reactions were combined

and oil was removed. Precipitation was with 3µl 3M Na·acetate and 80µl 95% ethanol. After 15 minutes on ice, the tubes were spun at 4°C for 15-30 minutes. The pellet was rinsed with ice cold 70% ethanol, spun for 5 minutes and dried under vacuum for 3 minutes. The sample was resuspended in 4-6µl of 5:1 deionised formamide / 50mM EDTA pH8.0 and loaded onto an Applied Biosystems 373A DNA sequencing system. (Genpak Ltd. protocol modified by A. Williams).

Sequence analysis

Sequencing projects were managed using Geneworks (Intelligenetics) on the Apple Macintosh. The GCG program CODONPREFERENCE was used to check for frameshift errors. The GCG MOTIFS program was usedto search for recognised protein motifs and domains. Protein homology searches used the PROSRCH6 program (J.F. Collins and A.F.W. Coulson) on the Active Memory Technology DAP, with the VAX front end SHARQ (ICRF biocomputing unit). The GCG program FASTA was also used. Multiple sequence alignments were performed with the CLUSTAL program (D. Higgins and P.M. Sharp).

DNA probe preparation

The probe was prepared by restriction enzyme digestion, and purified by electrophoresis onto DEAE-cellulose paper. Labelling was with a Prime-It II random primer kit (Stratagene). The manufacturer's instructions were altered as follows: 50ng of DNA was used instead of 25ng; the mixture of DNA and random primers were denatured at 80°C, not 100°C; and after adding the Klenow enzyme, the reaction was incubated for 30 minutes at 37°C, not 2-10 minutes. After adding 2µl of stop solution, the reaction was immediately transferred to a G50 Sephadex spin column, and spun at 1500rpm in a bench top centrifuge for 5 minutes. 1µl of the eluate was diluted 1:5 in water, and 1µl of the dilution was added to 6ml Aquasol (Du

Pont), and counts per minute (cpm) determined in a scintillation counter (Packard). A further test occasionally employed to check the incorporation was to spot 1µl of probe onto 2 discs of DEAE-cellulose paper. Both discs were air dried, so that any DNA is bound irreversibly. One disc was put aside, and the other washed 5 times in 20mM Na_2HPO_4 pH7.2 for 5 minutes per wash. The disc was rinsed in water, and then twice in ethanol. Both discs were immersed in 6ml of Aquasol and counted. The ratio of cpm between the washed disc (removing unincorporated radionucleotides) and the unwashed disc reveals how much of the cpm measured for the probe is actually incorporated into the probe.

Hybridisation of Northern blots

The Northern blots used were a gift from Gerardo Jimenez. The filters were prepared by wetting with 20x SSC. 100µl of ssDNA (10µg/ml) was boiled and added to 10ml of hybridisation solution (0.5M Na_2HPO4, adjusted to ph7.2 with H_3PO_4, 1mM EDTA, 7% SDS), and this pre-hybridisation solution was added to the filter in a glass tube and incubated at 65°C in an air oven (Hybaid). Hybridisation was carried out overnight at 65°C in 5ml of hybridisation buffer (containing $1x10^7$ cpm of probe, which had been boiled with 50µl ssDNA (10µg/ml) and cooled on ice before adding to the hybridisation buffer). The filters were rinsed three times in high stringency buffer (40mM Na_2HPO4, adjusted to ph7.2 with H_3PO_4, 1% SDS) preheated to 65°C. The filters were washed three times, at 30 minutes pre wash in 0.1x SSC, 0.01% SDS at 65°C, and sealed in a plastic bag. A pre-flashed film was placed exposed side down on an intensifying screen, with the filters on top. A second intensifying screen was placed above the filters, and the sandwich placed in an autoradiography cassette.

λ Library plating

Large square LB plates were prepared in advance. E.coli Y1090 was streaked on an LB amp plate, grown overnight, and a colony used to innoculate an LBM overnight culture (LB 0.4% maltose, 10mM $MgSO_4$). The λ library was diluted in SM buffer (Per litre: 5.8g NaCl, 2g $MgSO_4.7H_2O$, 6.05g Tris base, 5ml 2% gelatin) to give 250,000 plaques per large plate. 5µl of the dilution was mixed with 1ml of the Y1090 overnight culture and incubated in a 37°C water bath for 1hr. 40ml of top agarose (LB, 0.8% agarose, 0.4% maltose, 10mM $MgSO_4$, autoclaved and kept at 48°C before use) was added, the tube inverted twice and immediately poured onto the centre of one of the large square LB plates. The top agarose was allowed to harden 10' at RT, and the plate incubated at 37°C for 5.5hr. The plate was cooled rapidly on ice and left overnight at 4°C.

Filter lifts of λ phage

Four baths were prepared, 1 of denaturing solution (0.5N NaOH, 1.5M NaCl), 2 of neutralising solution (1.5M NaCl, 0.5M Tris.Cl pH7.4), and 1 bath of 2xSSC. Each bath was a plastic box with 2 sheets of 3MM paper on the bottom; the solutions poured in and the excess subsequently drained off and the paper smoothed by rolling with a test tube. Hybond-N^+ was placed on the λ plate, taking care not to trap air bubbles and left for 1'. Needle holes were made in the filter and LB agar and marked on the plate. The filter was placed DNA side up in the denaturing bath for 5', 2x5' in the neutralising baths and rinsed in 2xSSC. The filter was dried on 3MM paper in air. Duplicate filters were done for each plate. The filter was fixed by placing on 3MM paper soaked in 0.4M NaOH for 20', and rinsed in 5xSSC for 1'.

Hybridisation of filters and colony selection

The fixed filter was placed in pre-hyb buffer (Church and Gilbert: 0.5M Na_2HPO_4, adjusted to pH7.2 with H_3PO_4, 1mM EDTA, 7% SDS) at 65°C for several hours. The filter was then incubated overnight in 40ml of hybridisation buffer (Church and Gilbert with 10^6cpm DNA probe per ml) at 65°C. The filters were washed in 4x1 litre 20mM Na_2HPO_4 pH7.2, 5% SDS in a water bath at 65°C. Each wash was 30'-1hr. The filters were sealed in plastic bags; each bag was asymmetrically marked with dots of radioactive ink. The filters were exposed to pre-flashed film overnight. The radioactive ink dots on the filter and autorad were lined up and the needle holes marked on the autorad. The LB plate and the autorad were lined up to pick colonies with a pasteur pipette or an innoculating loop. Plaques were placed in 0.5ml SM buffer with 1 drop of chloroform and left overnight at 4°C. Serial dilutions of the picked phage were made and plated onto small plates: 10µl phage + 100µl Y1090 were mixed, grown for 15' at 37°C, mixed with 4ml top agarose and poured immediately. The plates were kept at 37°C for 1hr before pouring. The phage were incubated for 5hr at 37°C. Second round colony selection used nitrocellulose filters, the differences in protocol being a longer time on the phage plate for the duplicate filter, the use of Maniatis hybridisation buffer (6xSSC, 0.05% Blotto)instead of Church and Gilbert and fixation by baking at 80°C for 2hr. The filters were washed as before and exposed to film. For isolation of the candidate *sun* gene, a third round of screening was carried out to isolate single colonies.

Isolation of λ clone DNA

Phage were mixed with Y1090 and plated. After incubation, the plates with the highest density of plaques were selected, 4ml SM buffer was added and the plates left shaking gently at 4°C for 2-3hr. The SM buffer was removed

to a test tube, the plate washed with a further 1ml SM buffer which was added to the tube. A drop of $CHCl_3$ was added, and the SM vortexed briefly. Spin: 4000rpm, 10', 4°C. The supernatant was removed (can be stored at 4°C). 4ml of lysate was mixed with 4ml of sterile 20% PEG/NaCl solution, mixed and incubated on ice for 1hr. Spin: 3000rpm, 20'. The pellet was drained, the walls of the tube dried with a tissue, and the pellet resuspended in 750µl of LB. The suspension was transferred to a microfuge tube, and 750µl of DE52 in LB added. Spin: 5', microfuge. The supernatant was transferred to a fresh tube and 750µl DE52 added. Spin: 5', microfuge. 17.5µl of a 20mg/ml solution of proteinase K and 42.5µl of 10% SDS were added to the supernatant, the solutions mixed and left at RT for 5'. 190µl 3M KAc added and the tube incubated at 88°C for 20'. Ice, 10' (precipitate forms). 10', microfuge. The supernatant was transferred to two eppendorf tubes, and an equal volume of cold isopropanol added. -70°C, 10'. The tubes were allowed to warm to RT, then spun for 10' in a microfuge. The pellets were dried and resuspended in a combined volume of 40µl TE.

Oligonucleotides

Oligonucleotides were ordered from the ICRF oligonucleotide service at Clare Hall, or from the Institute of Molecular Medicine, Oxford. Where required, oligo elution and deprotection was performed as follows. A 1ml syringe was filled with 1ml of ammonia solution, and attached to one end of the oligonucleotide column. A second 1ml syringe was attached to the other side of the column, and the ammonia solution pushed/pulled through the column every 5 minutes for 30 minutes. The arrangement was chilled at -20°C for 2 minutes, and the ammonia solution transferred to a tight sealing eppendorf tube. Deprotection was at 50°C for five hours or overnight. The 1ml of ammonia solution was then split between three eppendorf tubes and Na·acetate added to 0.3-0.5M (pH5.5). The

oligonucleotide was precipitated with 3-5 volumes of ethanol, and centrifugation (13,000rpm, 4°C, 15 minutes). The pellet was washed with 70% ethanol and dissolved in 200µl T(1/10)E (10mM Tris·Cl pH8.0, 0.1mM EDTA pH8.0). After measuring the OD260 (oligonucleotides: OD260 of 1 = 20µg/ml), the oligonucleotide was diluted to 1mg/ml with T(1/10)E.

PCR

Typical parameters for the polymerase chain reaction were an annealing temperature of 56-58°C for 1', extension: 2' at 72°C, denaturing 94°C 30"-1'. Phage colonies stocks (SM buffer) were diluted 1:4 to 50µl and boiled for 3'. Bacterial colonies were picked and used to innoculate 50µl water; 5µl was used in the reaction mix and the remainder to innoculate an agar plate. 50µl reaction mix: 5µl 10x buffer, 1µl 10mM dNTPs, 1µl each primer at 250ng/µl, 0.5µl Taq, water and template to 50µl. Hot start, addition of Taq during the first round of denaturing, was routinely used.

SDS polyacrylamide gel electrophoresis (PAGE)

A BioRad minigel apparatus was used. The separating gel was made according to the following table:

Component	8.5%	10%	12.5%	15%	17.5%
Water	3.5ml	3.1ml	2.5ml	1.8ml	1.2ml
Acrylamide solution	2.0ml	2.4ml	3.0ml	3.7ml	4.3ml
Separating gel buffer	1.9ml	1.9ml	1.9ml	1.9ml	1.9ml
10% ammonium persulfate	112µl	112µl	112µl	112µl	112µl
TEMED	5µl	5µl	5µl	5µl	5µl

Acrylamide solution (30%): 30g acrylamide, 0.8g bisacrylamide to a final volume with water. Separating gel buffer: 18.17g Tris base, 4ml 10% SDS, pH to 8.8 with 12N HCl and to a final volume of 100ml with water. The ammonium sulfate was kept at 4°C for a maximum of a week. In general, for the size range of proteins that I dealt with, 12.5% acrylamide gels were used. After pouring the separating gel mixture between the glass plates, the liquid was overlaid with water and allowed to polymerise. The water was removed prior to pouring the stacking gel which consisted of: 1ml water, 444µl stacking gel buffer, 300µl acrylamide solution, 28µl 10% ammonium persulfate solution, and 5µl TEMED. The well forming comb was positioned and the gel allowed to set. (Stacking gel buffer: 6.06g Tris base, 4ml 10% SDS, pH to 6.8 with 12N HCl and to a final volume of 100ml with water). Samples were prepared in SDS sample buffer (1ml glycerol, 2ml 10% SDS, 2mg bromophenol blue, 1.25ml stacking gel buffer to a final volume of 10ml; add 1µl of ß-mercaptoethanol to 20µl of sample buffer immediately prior to use), boiled for 1 minute and spun for 1 minute before loading. Gels were run at 30mA in running buffer (3g Tris base, 14.4g glycine, 10ml 10% SDS to a final volume of 1 litre with water). If proteins were required to be visualised by staining with Coomassie blue dye, the gel was immersed in stain solution (500ml 95% ethanol, 100ml glacial acetic acid, 400ml water, 2g Coomassie brilliant blue R250) for 2 hours-overnight at room temperature. Background staining was removed by washing in destain solution (500ml methanol, 75ml glacial acetic acid, 425ml water) in the presence of Dowex. The gel was swelled to its original size in swelling solution (70ml glacial acetic acid, 20ml glycerol, 910ml water). Gels were placed on damp 3MM paper, covered with clingfilm and dried on a BioRad gel drier for 30 minutes at 80°C. For autoradiography, Kodak X-omat film was exposed to the dried gel.

pET vector constructs

pET-Hairy, -T3, -T4, -T5 and -Da were present in the Ish-Horowicz laboratory. pET-Groucho, -$Hairy_{mhx1}$ were constructed by Z. Paroush.

Construction of pGEX constructs

A hairy PCR fragment was amplified from a *h* cDNA cloned into a pET vector using the following primers: AAA CAA TAT CTG ACC GAA ATG GTT ACC GGC (HALT) and ATG CAT ATG CAG GAA TTC TCT ACC AGG GC (HGST3'). The fragment was gel purified, cut with EcoRI and cloned into the EcoRI site of pGEX-2T producing an in frame fusion of the GST and hairy genes, called pGEX-Hairy (pGH). A carboxy terminus truncation of the fusion protein was produced by digesting the construct with NotI, filling in with Klenow, kinasing and religating (pGEX-Hairy-NotI (pGHN)). pGHN encodes amino acids 1-246 of Hairy and has 12 additional amino acids at the carboxy terminus. All other pGEX constructs were made by Z. Paroush, except GST-T4, GST-T5 and GST-Da which were obtained from M. Van Doren and J. Posakony.

Miniprotein preps for screening candidate constructs

To select the required construct, mini-protein preps were used to check for expression of a fusion protein in the expected size range. 277ul of an overnight culture of a selected colony grown in LB ampicillin and 0.4% glucose was used to innoculate 2.5ml of LB amp (tetracyclin if strain was XL1 blue, no glucose). This gives a 1:10 dilution. The culture was grown for 1-1.5 hours, before induction with 27ul freshly made IPTG (~0.6mg per ml). The culture was grown for a further three hours, and the bacteria harvested by centrifugation for one minute in a 2.2ml eppendorf tube. The cells were resuspended in 1ml MTPBS (150mM NaCl, 16mM Na2HPO4, 4mM NaH2PO4, pH7.3). The cells were sonicated for 10 seconds and 100µl 10% triton added prior to a 10 minute spin in a microfuge at 4°C. The

supernatant was transferred to 100-300ul of a 50:50 slurry of glutathione-agarose beads (Sigma/Pharmacia) pre-swelled in MTPBS with 0.1% beta-mercaptoethanol. The tube was rolled for 5' at room temperature to allow absorption of the fusion protein to the beads. The beads were washed once with 1ml MTPBS. 100µl SDS sample buffer was added and 10-40µl of the supernatant loaded onto an SDS polyacrylamide gel.

Expression of GST fusion proteins in bacteria

E.coli SRP84 cells containing the appropriate pGEX construct were used to innoculate a 10ml overnight culture of LB containing ampicillin, tetracycline and 0.4% glucose. This was grown at 30°C with 225rpm shaking. The OD550 of the culture was measured in the morning (about 12-15 hours of growth) and was usually in the range 2.0-2.5. Sufficient of the culture (usually about 5ml) was diluted into 100ml of LB containing ampicillin and tetracyclin to give an OD550 of about 0.5. This culture was incubated at 30°C with shaking, in a 1 litre flask for 1-1.5 hours. Expression of fusion proteins was induced with 40mg IPTG per 100ml culture (isopropyl-ß-D-thiogalactopyranoside (1.7mM), Sigma/Biosynth AG). If desired, an uninduced control was also established or a 1ml sample of cells removed before adding the IPTG. The culture was further incubated for 3 hours at 30°C. Longer incubation did not significantly increase the yield of expressed protein. The cells were harvested by spinning at 4000rpm in a Sorval GSA rotor at 4°C for 10 minutes. The cells were resuspended in 10ml MTPBS supplemented with 1mM PMSF (phenylmethyl-sulfonyl fluoride, 100mM stock in 100% isopropanol, Sigma), 2mM EDTA, 5µg/ml aprotinin (Boehringer Mannheim, 5mg/ml stock in water), 0.5µg/ml leupeptin (Boehringer Mannheim, 5mg/ml stock in water), 0.7µg/ml pepstatin (Boehringer Mannheim, 1mg/ml stock in methanol) and 0.1% ß-mercaptoethanol. A sample was removed at this point to check the level of

induction prior to purification (the cells spun down and resuspended in SDS sample buffer). The resuspended bacteria were transferred to an Oakridge tube on ice. The cells were sonciated in a Soniprep 150 for 1 minute, cooled and sonicated for a further 30 seconds. The probe was also cooled during the interval. Sonication was typically at 12-14 microns amplitude, as judged by a 'frying egg'noise. 1ml of 10% triton was added and insoluble material removed by centifuging in a Sorvall SS-34 at 13,000 rpm at 4 °C for 10 minutes. A sample of the supernatant was kept for SDS-PAGE analysis, and the rest mixed with 1ml of glutathione-Sepharose 4B beads (Pharmacia; 2ml of 1:1 MTPBS slurry) in a 15ml Falcon tube. The beads were prepared by pre-swelling and washing in MTPBS with 0.1% ß-mercaptoethanol three hours before use. The beads and supernatant were rolled at 4°C for 15 minutes, before pouring into a disposable plastic column (BioRad). A sample of the eluate was retained for SDS-PAGE analysis. The column was washed with 30ml of MTPBS supplemented with the protease inhibitors and 1% triton as above. The final wash was performed without the triton, but still in the presence of the protease inhibitors. The beads were recovered from the column and stored as a 50:50 slurry with MTPBS supplemented with protease inhibitors. A sample of beads was suspended in SDS sample buffer and analysed along with other samples collected on SDS-PAGE to examine the purification and estimate the amount of fusion protein recovered by comparison with a series of bovine serum albumin standards. Different amounts of different fusion proteins were found to be present on the glutathione agarose beads, and relative quantities were noted.

In vitro translation

In vitro translated proteins were produced using the TNT coupled reticulocyte lysate system (Promega), which has the advantage of coupling

transcription and translation in the same reaction. The manufacturer's instructions were followed; a rabbit reticulocyte lysate and T7 RNA polymerase were used for all constructs. DNA was prepared using Magic Midipreps (Promega) and was typically used at a concentration of 1µg per 50µl final reaction volume. High grade ^{35}S-methione (Amersham #SJ1015) was used to label the translation products, and RNasin ribonuclease inhibitor (Promega) was included at a final concentration of 0.8U/µl. Translation products were visualised by SDS-PAGE and autoradiography.

pGEX protein-protein interaction assay

In each experiment, the amounts of fusion protein used were normalised to 30µl of beads of the least concentrated fusion protein, as judged by Coomassie staining of SDS-PAGE gels. Blank glutathione beads blocked with a blank bacterial extract were used to bring the volume of beads in all tubes to 30µl. To each tube 180µl of binding buffer (20mM HEPES-KOH (pH7.9), 50mM KCl, 2.5mM $MgCl_2$, 10% glycerol, 1mM DTT, 0.2% NP40, 3µl rabbit serum and 3µl 100mM PMSF) was added and the tube rolled at 4°C for 1 hour. 20-30µl of programmed reticulocyte lysate containing the required labelled protein was added to the tube. The beads and in vitro translated protein were rolled overnight at 4°C. The beads were washed four times in RIPA buffer (10mM Tris-HCl (pH7.5), 150mM NaCl, 1mM EDTA and 0.2% NP-40): 1ml of RIPA buffer was added to the beads, the tube inverted several times, briefly spun at 1000rpm, and the supernatant removed with a Gilson and a 25 gauge needle taking care not to suck up any of the beads. 100µl of SDS sample buffer was added to the beads and equal amounts of each sample loaded onto an SDS-PAGE gel after boiling to release the bound protein.

Western blots

Proteins separated by SDS-PAGE were transferred to nitrocellulose using a semi-day electroblotter (Ancos). Four sheets of 17mm paper exactly the same size as the separating gel were soaked in buffer (39mM glycine, 48mM Tris, 0.0375% v/v SDS, 20% methanol); two sheets were placed on the bottom graphite plate of the electroblotter, after it had been rinsed with deionised water. A piece of nitrocellulose the same size as the separating gel was rinsed in deionised water and laid on top of the two sheets of 17mm paper. The separating gel, from which the stacking gel had been removed, was placed on top of the nitrocellulose; bubbles were removed by smoothing out with a finger wetted with buffer. The remaining two sheets of 17mm were placed on top, and the sandwich rolled over with a pipette. The top plate of the electroblotter was placed on top, and the apparatus run at 0.8mA/cm^2 for 1-2 hours. The filter was blocked overnight at 4°C with PBS/10% fetal calf serum (FCS)/0.05% azide. The filter was rinsed in PBS, incubated with the primary antibody diluted in 5ml PBS/10% FCS for two hours, with shaking, at room temperature. Three 15 minute washes with PBS/0.1% NP40, and a rinse in PBS. The secondary antibody was added in 3ml PBS/10% FCS, and incubated at 37°C for 30 minutes or for 2 hours at room temperature. Three 15 minute washes in PBS/0.1%NP40, and the filter was rinsed in substrate buffer (0.1M Tris.Cl pH9.5, 0.1M NaCl, 50mM $MgCl_2$). Substrate (4.4µl NBT and 3.3µl BCIP per ml of substrate buffer) was added and the blot developed. The reaction was stopped with PBS.